UNIVERSITY
OF TURKU

Exploring the Cosmic History of Star Formation, Metallicity Evolution, and Core-Collapse Supernova Rates

MSc Thesis
University of Turku
Department of Physics and Astronomy
Astronomy

April 2023
BSc Christian Vassallo

Supervisor:
prof. Seppo Mattila
Examiner:
prof. Seppo Mattila
Docent Rubina Kotak

UNIVERSITY OF TURKU
Department of Physics and Astronomy
VASSALLO, CHRISTIAN: Exploring the Cosmic History of Star Formation, Metallicity Evolution, and Core-Collapse Supernova Rates
MSc Thesis, 86 pages (+ 19 pages of appendix)
Astronomy
April 2023

Research on star formation is essential for understanding galaxy evolution and the universe's evolution. Astronomers can learn about star formation over time by observing core-collapse supernovae and determining their occurrence rate. Core-collapse supernovae are a valuable resource in the investigation of star formation due to the period between the birth of a massive star and the supernova being so brief compared to the cosmic timescale.

This thesis explores various aspects related to star formation and core-collapse supernovae rates and their connection to host galaxies. The characteristics of host galaxies are also examined using the core-collapse supernova sample. The study also discusses different models of star formation rate, such as Madau & Dickinson (2014), and compares them. The thesis also addresses highly active galaxies and their star formation and investigates the relationship between metallicity evolution and star formation history across cosmic time. It is observed that metallicity increases over cosmic time and reaches its highest value at present day.

This study looks at the rate of nearby core-collapse supernovae, considering both the cumulative and shell volume rates. It also examines the significance of any decrease in this rate using statistical methods, as well as the impact of galaxy orientation and extinction in host galaxies. Additionally, the study calculates the absolute magnitudes of these supernovae.

The findings indicate that the rate of core-collapse supernovae decreases at a distance of 16 Mpc. the study also concludes that observed rates of these supernovae need to be adjusted to account for different missing supernova fractions at different redshifts to fit the rates derived from star formation rate models.

Keywords: supernovae, core-collapse supernova rate, star formation rate, metallicity

Contents

1 Introduction

Before delving into the thesis, it is essential to define the key terms and concepts used throughout.

The cosmic star formation history studies the rate of star formation in the universe over time, which is generally measured in terms of star formation rate (SFR). SFR is expressed as stars born per year per cubic megaparsec (Mpc) volume. Redshift is the phenomenon where the wavelength of light emitted from a distant object is shifted towards the red end of the spectrum due to the expansion of space, which stretches the wavelength of light over greater distances. This redshift is used not only to measure the distance to other galaxies but also to infer the age of the universe.

Metallicity measures the abundance of elements heavier than helium in a star or galaxy. It is typically measured in terms of the fraction of the total mass that is composed of elements heavier than helium, expressed as a fraction of the total mass. Metallicity is an important measure because it affects the evolution of stars. Metallicity also affects the formation of planets and the evolution of galaxies.

Core-collapse supernovae (CCSNe) are some of the most energetic and powerful phenomena in the Universe. CCSNe are generated when a massive star (more than 8 masses of the sun) runs out of nuclear fuel, resulting in the core collapsing and releasing an immense amount of energy that causes the star's outer layers to shoot into space, creating a spectacular explosion that can outshine an entire galaxy for weeks. These events can be observed across the whole electromagnetic spectrum, from radio waves to gamma rays, and they have an important role in the formation of new elements and the evolution of galaxies. The rate of CCSNe is closely connected to the SFR, as the timescale of the massive stars (few million to tens of million years) leading up to a CCSN is much shorter than the cosmic timescale. Therefore, the rate of CCSN can be estimated using the SFR. Conversely, the SFR can also be estimated by measuring the CCSN rate.

Various statistical methods were also used in the thesis to analyze the data, such as the cumulative distribution function (CDF) and the Kolmogorov-Smirnov test (KS-test), which are explained in more detail later on in the thesis.

This thesis aims to explore the relationship between the evolution of star formation and metallicity with redshift, the CCSN rate at 0-30 Mpc, and the connection between CCSN rate and SFR in both our local neighborhood and at larger distances.

It is important and relevant to understand the evolution of SFR, metallicity, and CCSN rate with redshift to understand the universe's evolution. By studying these phenomena, we can gain insight into the formation of galaxies and the structure of the universe. This is especially true in light of the recent observations of distant galaxies. My thesis provides a comprehensive analysis of several topics related to the formation and evolution of stars and galaxies. The study includes an exploration of SFR, the evolution of metallicity with redshift, and the rate of CCSN within 0-30 Mpc. The analysis also includes cumulative and co-moving CCSN rates, the significance of decrease analysis using statistics, and the inclinations of galaxies hosting CCSN. Additionally, the thesis examines the effects of host galaxy extinction, the absolute magnitudes of CCSN, the faintest and failed supernovae, and a comparison of observed CCSN rates with calculated CCSN rates. The topics of this thesis are important and relevant to gain a better understanding of the universe and its evolution. I primarily reviewed the relevant literature in the sections on SFR and metallicity. However, I produced my own results when examining the topic of CCSN rate, which I compared with other studies.

1.1 Tracking the Cosmic History of Star Formation

In the last few decades, advancements in observational techniques, such as multi-wavelength imaging with the Hubble Space Telescope and spectroscopic studies, have enhanced our understanding of the origin and evolution of galaxies. It is now believed that the peak of cosmic star formation occurred at a redshift of z = 1.9 or around 3.5 Gyr after the Big Bang. This is mainly because the available gas supply for star formation is used up over time. This SFR was approximately nine times higher than the current rate we observe today, indicating that the Universe was much more active in the past [1]. Further research into the history of star formation is a key objective of astrophysics and astronomy.

1.1.1 Calibrating the Cosmic Star Formation Rate Evolution with Redshift: A Comparison of Models

Madau & Dickinson (2014) present a function that is fitted to observational data in order to describe the cosmic SFR evolution with redshift [1]:

$$\mathrm{SFR}(z) = \frac{a(1+z)^b}{1+((1+z)/c)^d} \tag{1}$$

Parameters a,b,c and d used in Madau & Dickinson (2014) [1] are $a = 0.015$, $b = 2.7$, $c = 2.9$ and $d = 5.6$.

Wilkins et al. (2019) [2] proposed a new study to recalibrate the parameters of the function used in Madau & Dickinson. Wilkins (2019) [2] used two different models for the parameters: one that was calculated using a study from Murphy et al. (2011) and one using a v2.2.1 of the Binary Population and Spectral Synthesis (BPASS) model. The results of the fitted function are represented in the graphs of Figure 1. The parameters for each study, in terms of ultraviolet (UV), thermal infrared (TIR), and UV + TIR, are presented in Table I. In Figure 1, a substantial difference can be observed between the BPASS SFR curve and the other SFR curves. These differences can be attributed to three distinct choices: a different initial mass function (IMF) that extends to 300 $M_\odot$, the incorporation of binary pathways in the stellar population synthesis model, and the selection of their metallicity [2].

Table I: Cosmic star formation function parameters.

	a [$M_\odot$ yr^{-1} Mpc^{-3}]	b	c	d
	Madau & Dickinson et al. (2014) [1]			
UV+IR	0.015	2.7	2.9	5.6
	Murphy et al. (2011) [2]			
UV	0.0107	2.70	3.22	7.22
TIR	0.0124	3.43	2.37	5.38
UV+TIR	0.0149	2.52	3.07	6.27
	BPASS [2]			
UV	0.0087	2.70	3.22	7.22
TIR	0.0082	3.43	2.37	5.38
UV+TIR	0.0103	2.48	3.10	6.26

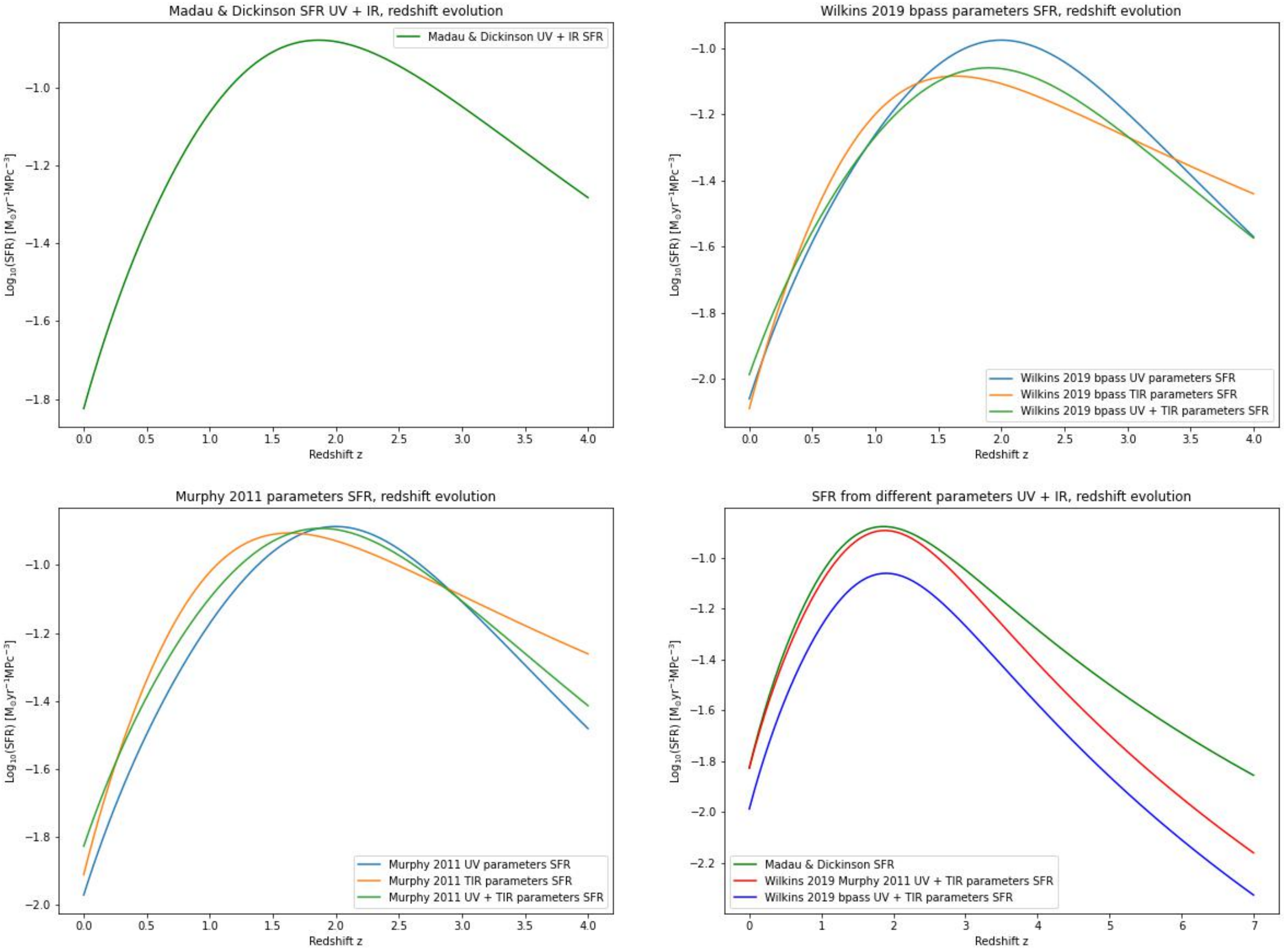

Figure 1: SFR as a function of redshift. The panels represent results from three different studies, each with UV and TIR Top left: Madau & Dickinson [1] , top right: Wilkins et al. 2019 [2], bottom left: Murphy et al. 2011 [2], bottom right: Combined results from all three studies.

1.1.2 Active Galaxies: Star Formation

The luminous and ultraluminous infrared galaxies (LIRGs and ULIRGs, respectively) are bright in the infrared region ($L_{\mathrm{IR}} > 10^{11} L_{\odot}$ [3]) compared to other wavelengths. At the center of these galaxies are extremely powerful supernova factories because of their ability to create a high-density environment. These galaxies usually form when two large gas-rich galaxies merge together, which triggers a burst of star formation that heats up dust within the galaxies and causes them to emit a lot of infrared light. The most extreme examples of these galaxies are ones that emit even more infrared light (greater than the brightness of 1 trillion suns!). These very bright galaxies are usually the result of even larger mergers and can be powered by both intense star formation and active black holes in the center of the galaxy [4].

The starburst produces a large number of massive stars that eventually go supernova, leaving behind a powerful and bright supernova factory. Dust extinction in the optical region obscures star formation, active galactic nuclei and supernovae, making them difficult to detect. LIRGs tend to have large amounts of molecular gas, which can sustain vigorous star formation. The rare type of galaxies in our local universe have been found to exist more frequently at higher redshifts between $z \approx 1$ - 2 [5].

Star Forming Dwarf Galaxies (SFDGs) are incredibly prevalent, with estimates of their population comprising more than 80% of all galaxies in the local universe [6]. Despite this, few SFDGs have been identified due to their low mass and luminosity [7] and thus contribute little to the overall SFR density. The mass-metallicity relation (MZR) further supports this, as it suggests that SFDGs typically have very low metallicity, likely due to their lack of sufficient gravity to hold gas within their borders.

Garrison-Kimmel (2019) [8] investigated the star formation of dwarf galaxies in a simulation of 500 dwarf galaxies. They found a large scattering of star formation in SFDGs and a lack of a universal trend in star forming with a given mass and environment as a function of redshift. However, they did observe a trend with mass, with the fraction of stars formed at late times increasing with the stellar mass of the dwarf galaxy.

1.2 Metallicity Evolution Across Cosmic Time

Studies have revealed a correlation between stellar and gas phase metallicities and galaxy mass, referred to as the MZR. This suggests that as the stellar mass of a galaxy increases, so does its metallicity. It is believed that this is due to the increased gravitational pull of more massive galaxies, which allows them to better resist processes such as supernova driven winds that may otherwise eject gas from the galaxy [9]. Conversely, the weaker gravitation of lower mass galaxies makes them more susceptible to such ejective mechanisms.

This is also supported by the effects of galaxies evolving and increasing their metallicities through stars evolving and supernovae (SNe). As stars evolve and eventually die, they return their metals to the interstellar medium, enriching the gas and increasing the overall metallicity of a galaxy. Similarly, SNe also release metals into the gas, further increasing the metallicity of a galaxy.

The MZR has been observed to evolve with increasing redshift, with a decrease in metallicity. This rate of decrease varies depending on the mass of the galaxy, where lower mass galaxies have a higher rate of metallicity decrease when redshift is increasing.

In addition to the MZR, there is a secondary effect of gas metallicity known as the Fundamental Metallicity Relation (FMR). This describes the reverse correlation between gas metallicity and SFR, and states that there is no or very small amount of evolution with redshift up to $z \approx 2.5$. Nevertheless, the transformation of the FMR at higher redshifts is still a mystery because of adjustments in other galactic and intergalactic characteristics. [10].

Genzel et al. 2015 [11] reported a fitting function for metallicity as a function of redshift:

$$12 + \log(\mathrm{O/H})_{\mathrm{PPO4}} = a - 0.087 \times (\log M_* - b)^2$$

$$\mathrm{a} = 8.74(0.06),$$

$$\mathrm{b} = 10.4(0.05) + 4.46(0.3) \times \log(1+\mathrm{z}) - 1.78(0.4) \times (\log(1+z))^2$$

Where $12+\log(\mathrm{O/H})_{\mathrm{PPO4}}$ is a measure of the relative abundance between oxygen and hydrogen atoms and the paranthesis are the uncertainties associated with the values. The equation is used as a measure of metallicity because oxygen is one of the most abundant elements in the Universe, and its abundance is related to the overall metallicity. The measure expresses the abundance of oxygen as a logarithmic ratio, making it easy to compare the metallicity. M_* is defined as the stellar mass ($M_* = 10^{10}\mathrm{M}_\odot$). The graph in Figure 2 shows the trend of decreasing metallicity as redshift (z) increases. The linearity of the graph suggests that metallicity decreases with increasing redshift.

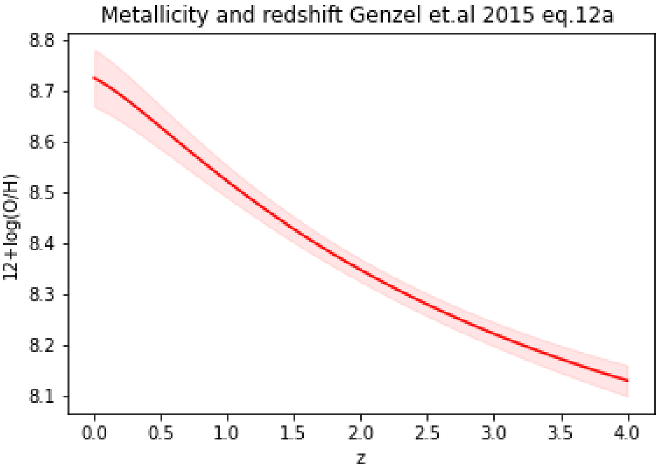

Figure 2: Graph of the fitting function for metallicity as a function of the redshift from Genzel et al. 2015 [11].

The evolution of the metallicity of galaxies over time has an effect on the number of produced gravitational wave transients.

Gravitational wave transients are a fascinating and a brand new field of study within astronomy and cosmology. These are events that generate gravitational waves, which are ripples in the fabric of space-time. These events can provide insights into a multiple astronomical phenomena, such as the formation of black holes and neutron stars, and supernovae.

In Briel et al. (2022) [12], the predicted rates of both electromagnetic and gravitational wave transients were reported, based on the results of BPASS and four different star formation histories: Empirical star formation history [1] and three cosmological simulations (Millennium, EAGLE, and IllustrisTNG). Cosmological simulation is a simulation of the evolution of the large-scale structure of the universe. The simulation typically models the expansion of the universe, the growth of structure within it, and the effects of dark matter and dark energy. The empirical star formation history was combined with the cosmic metallicity evolution from Langer and Norman (2006) [13], resulting in the mean metallicity evolution shown in Figure 3. The figure shows the evolution of metallicity of the three cosmological simulations, in addition to the empirical results. The empirical metallicity appears to increase over cosmic time, reaching its highest value at present day (lowest redshift). The cosmological simulations show different metallicity evolutions; for example, the Millennium simulation seems to have a relatively constant metallicity evolution for most of cosmic time.

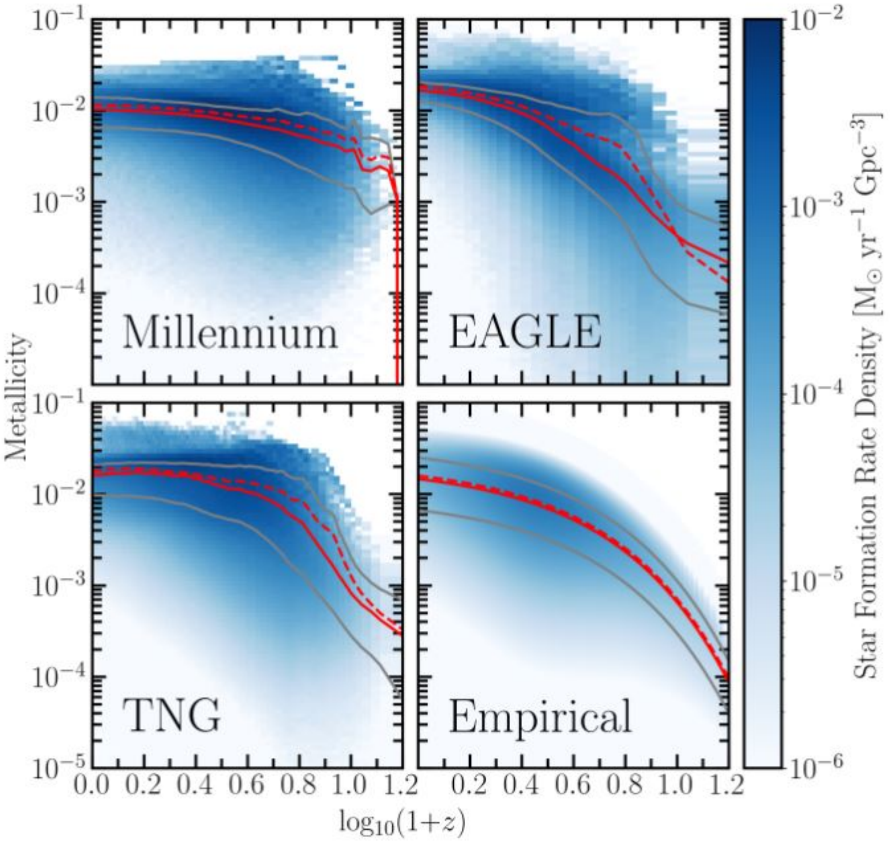

Figure 3: The evolution of metallicity and SFR density as a function of redshift, shown for cosmological simulations (Millennium, EAGLE, and TNG) and empirical results. Figure from Briel et al. 2022 [12]. The median metallicity is indicated with the red solid line and one sigma uncertainties with grey lines. The blue color shows the SFR density. The solar metallicity is at Z = 0.020 and the metallicity appears to increase over cosmic age.

According to Briel et al. (2022), transient rates with high delay times (time between the formation of a progenitor star and the end product, for example SN explosion) should be approached with caution when modelling the metallicity, as these cases can be expected to have the largest discrepancies between simulated and empirical results. On the other hand, transients with low delay times, such as CCSN, did not show a significant difference between the two. [12]

1.3 Classification of Core-Collapse Supernovae Based on Spectral Features

This thesis focuses on the various types of CCSN, which occur when massive stars with more than eight solar masses run out of fuel, as mentioned above. Over the years, CCSN have been classified into different categories and subcategories based on their explosion spectrum, spectral evolution, and brightness evolution. In this study, I specifically examine the various CCSN types based on their spectral features. The explanations of these types is based on the knowledge and insights I gained from the "Spectroscopic Diagnostics" -course held in 2023 at the University of Turku.

The Supernova "zoo" is organized by determining if the spectrum contains hydrogen or not. If hydrogen is present, the type is classified as **Type II**. If not, the type is classified as **Type I**. If the answer is somewhere between yes and no, the type is classified as **Type IIb**. For Type II, further classification is based on the shape of the hydrogen spectral features. Narrow hydrogen lines indicate **Type IIn**, while broader lines indicate either **Type IIP** or **Type IIL**. The "P" in Type IIP stands for "plateau," which refers to a characteristic plateau in the light curve of these supernovae that occurs after the initial brightening. The "L" in Type IIL stands for "linear" light curve. Based on the presence of silicon lines, Type I supernovae can be subdivided into several classes. CCSN lack silicon features, and **Type Ib** and **Ic** supernovae show helium or no helium, respectively. Narrow lines can further divide Type Ib and Ic into **Type Ibn/Icn**. **Type Ic-BL** is the type with with broad line features. Another subclass, Type II/I-Pec, can be distinguished by unusual spectral features or light curve behavior, such as weak hydrogen lines or chemical abundance signatures. One supernova used in this thesis was classified as a "Gap" supernova, due to its faintness.

Previous research has established theoretical explanations for the observed spectral and brightness features of the mentioned types. However, as this topic is beyond the scope of this thesis, it will not be discussed further.

1.3.1 Failed Core-Collapse Supernovae and Islands of Explodability

According to study by O'Connor and Ott (2011) [14] some exploding massive stars result in 'failed' CCSNe. The study investigates how different factors affect the formation of black holes when a massive star collapses in a supernova explosion. The study uses computer simulations to model the collapse of over 100 different types of stars, varying in their initial mass, metallicity, rotation, equation of state and mass-loss. The study finds that a key factor determining whether a star will produce a black hole is the compactness of its core at the moment of collapse. The introduced "compactness" parameter is:

$$\xi_M = \left. \frac{M/M_\odot}{R\left(M_{\text{bary}} = M\right)/1000 \text{ km}} \right|_{t=l_{\text{bounce}}} \tag{2}$$

R is a radial coordinate that has the mass of M within the radius at the time of core bounce.

Study by Sukhbold et al. (2016) [15] uses the "compactness" parameter introduced in the O'Connor and Ott (2011) study with a one-dimensional neutrino transport model to calculate various post-explosion properties. The study models 5 different progenitors and outcomes for the supernova 1987A. Fig 4 shows the resulting outcomes of the supernova explosions for each model at different zero-age main sequence (ZAMS) star masses. Successful explosions that leave behind either a neutron star (NS) or a black hole (BH) are shown in green, the failed explosion, where the explosion fallback directly into a BH without actually exploding, are shown in color black. According to the study, until about 15 solar masses of ZAMS mass, they explode and leave a remnant, but there are "islands of explodability" until 30 solar masses. ZAMS masses above 30 solar masses result in few explosions and high mass-loss rates make the models uncertain. All the progenitors used in the models have solar metallicity. The figure 15 in the Sukhbold et al. (2016) study also shows a good correlation between the "islands of explodability" and the "compactness" parameter. [15]

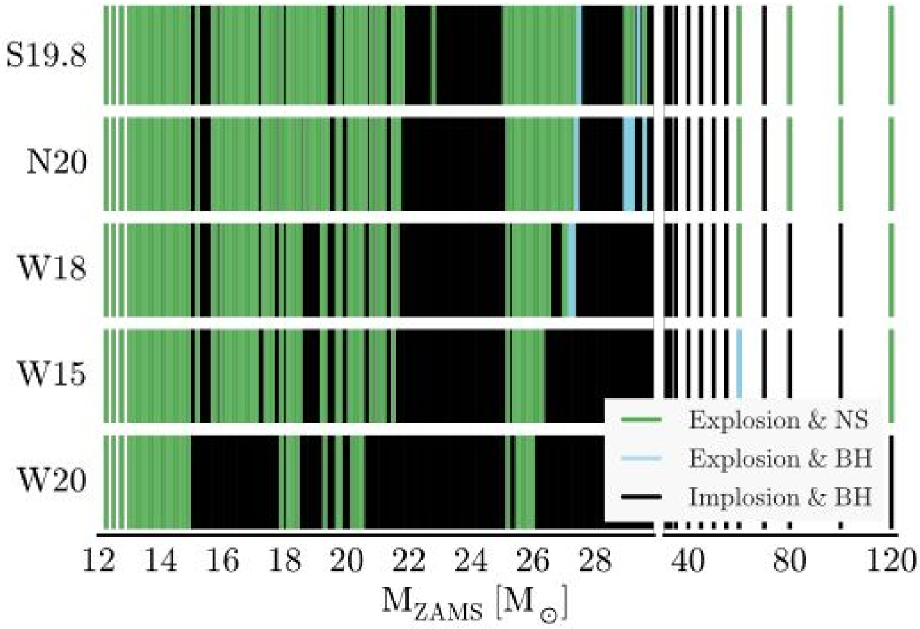

Figure 4: Simulations of explodability as a function of ZAMS mass using 5 progenitor models. ZAMS mass range up to 15 solar masses results in an explosion with all models. "Islands of explodability" begin after 15 solar masses and continue up to 30 solar masses. Results for ZAMS masses higher than 30 solar masses are uncertain. Figure is from Sukhbold et al. (2016) [15]

Sukhbold et al. (2016) [15] do not mention how the outcome of the death of a progenitor depends on the metallicity of the star. The models used in O'Connor and Ott (2011) [14] have different metallicities in the progenitor stars and the results of the explosions as a function of mass are shown in figure 13 of the study. It seems that at lower metallicities progenitors with ZAMS mass above ∼35 solar masses are more likely to result in a BH and the stars with solar metallicity have a larger fraction of supernova explosions. However they also mention that because of the uncertainties in the mass-loss of high mass stars, it is hard to make predictions about the explosion at high ZAMS mass. [14]

2 The Nearby Core-Collapse Supernova Rate: A 0-30 Mpc Survey

Discovering CCSNe poses several challenges. For instance, some SNe are intrinsically too dim to be accurately identified, while others may be hidden behind interstellar dust, resulting in a large extinction and thus going undetected. This is especially true in LIRGs and ULIRGs, where dust is abundant, leading to about 83% of all SNe being undetected. For example, when the redshift value is z $\sim$ 1.2, the missing fraction of SNe rises from 19% to 38% and remains roughly constant until z $\sim$ 2. This implies that the observed number of CCSNe is in correlation with the cosmic formation history of the stars. As ULIRGs and LIRGs are rare in our local space, they can be assumed to have no significant contribution when calculating the local supernova rate. [3]

The local CCSN rate has the potential to shed light on a range of astronomical topics. It can be used to better understand stellar evolution, the distribution of stellar populations in the universe, and the effects of SNe on the interstellar medium, dust and gas distribution, and the chemical composition of galaxies. This work seeks to investigate how the CCSN rate varies as a function of distance.

The first step in calculating the volumetric CCSN rate between 2000-2021 within a distance of 30 Mpc was to search all the observed SNe using the sne.space catalog, which has since been moved to a Github repository [16]. The whole CCSN sample was acquired in July 2022.

Rather than selecting SNe within a Hubble distance for 30 Mpc (which is less accurate at lower redshifts), an initial distance of 45 Mpc was used. The next step was to search the NED [17] and HyperLEDA [18] catalogs for the distance of the galaxy where the observed supernova had occurred.

The distances to most galaxies located below 30 Mpc have been calculated using the Virgo infall method, which is a correction for the Hubble distance at low redshifts. It corrects for the gravitational pull of the Virgo Supercluster, a cluster of galaxies that is located relatively close to our own Milky Way galaxy. The correction accounts for the additional velocity that galaxies in the Virgo Supercluster have due to the gravitational pull of the other galaxies in the cluster. However, for more precise estimations, the Cepheid method (explained below) can be employed. The resulting CCSNe are provided in tables Appendix A and B. After obtaining this sample of CCSNe, additional information was gathered, such as the extinction due to the Milky Way ($A_{\rm V}$ MW), the host galaxy extinction ($A_{\rm V}$ Host), the peak absolute magnitude (M_{peak}), and the age of the SNe at the time of discovery.

Foreground galactic extinction values used in this study were sourced from the (NED) [17]. Host galaxy extinctions were obtained from a variety of sources, as referenced in tables in Appendix A. Peak apparent magnitudes, meanwhile, were sourced from papers found in the NASA Astrophysics Data System (ADS) [19]. The age at discovery of each supernova was determined using its classification spectrum, with papers found in ADS [19] and the Transient Name server (TNS) [20] being searched for classification reports containing this information; these are then referenced in tables in Appendix B. Absolute magnitudes were then calculated using the peak apparent magnitudes, host galaxy extinctions, host galaxy distances, and foreground Galactic extinctions. Equations used for these calculations can be found in Section 2.5.

Methods used to calculate the distance of the host galaxy where the SN is detected are listed below (HyperLeda [18]):

Cepheids: The approach relies on the correlation between the brightness and pulsation period of Cepheid variable stars, which is known as the period-luminosity relationship (PL). Essentially, this relationship links the amount of light emitted by these stars during their fluctuation to the length of their pulsation cycle

Virgo infall: Virgo Infall correction for the redshift is based on the local velocity field model given in Mould et al. (2003) [21] using the term for the influence of the Virgo Cluster.

SBF: TThe SBF technique, also known as Surface Brightness Fluctuations, uses the variations in luminosity resulting from the statistical analysis of stars that contribute to the flux within a pixel of an image. The degree of fluctuation is dependant on the specific types of stellar populations.

TRGB: The Tip of the Red Giant Branch or TRGB is a method, relying on the old stellar population. Method uses the shallow colour-magnitude relation of the TRGB in the I-band.

Sosie: This approach is that galaxies sharing similar characteristics, including type, inclination, and hydrogen I line width, are expected to have identical absolute luminosity.

SN Ia: This method uses the relationship between the light-curve and peak brightness of type a Ia SN. This is a powerful tool to determine cosmological distances since the explosion produces high luminosity and the behaviour is regular.

EPM: The Expanding Photosphere Method or EPM is a geometric distance determination technique based on the velocities of and expanding SN explosion.

The distance method used for each CCSN is listed in tables in Appendix A.

2.1 Cumulative Volume Rates

The CCSN rate can be calculated cumulatively in order to obtain information about the number of CCSN in an entire spherical volume of space as a function of distance. This approach also has its drawbacks, as the changes in CCSN numbers at different distances affects the rate value differently. This makes it more difficult to accurately analyse the changes in the CCSN rate. The results are expressed in units of per year per volume. The equation used to calculate the cumulative CCSN rate is as follows:

$$CCSN\ rate = N_{CCSN} \times \frac{1}{N_y} \times \frac{1}{V} \tag{3}$$

Where N_{SN} is the number of events (cumulative) and N_y is the number of years. They can be obtained from the gathered data. Volume V is calculated as a sphere $V = 4\ \pi\ r^3/3$, where r is the radius of the sphere (in Mpc).

The approach proposed by Gehrels [22] is used to calculate the small number statistical uncertainties throughout this thesis. For values above 50, the square root of the value is used to calculate both upper and lower limits.

The cumulative CCSN rates obtained using the events from Appendix B are listed in Table II. The cumulative CCSN rates and their uncertainties are shown in Figure 5. The x axis of the graphs show the distance bins in Mpc, for example distance bin 6 Mpc means distances 5 - 6 Mpc and distance bin 10 Mpc means 9 - 10 Mpc. Figure 5 (left) shows that the CCSN rates at distances below 6 Mpc are high. This might be the effect of a local overdensity of star formation observed within $\sim$ 10 Mpc (Karachentsev [6]). Another analysis of Figure 5 (right), where the CCSN sample is cut into sub samples by year of observation, suggests that the high CCSN rate is produced by supernovae observed in 2000-2006. The 2007-2013 CCSN rates are lower and the 2014-2021 CCSN rate seems to be constant over the distance. This might be the result of SN observations relying more on amateur observers in the earlier years, and shifting into more professional observations in the more recent years. Amateur observers often observe the most popular galaxies, such as the Andromeda Galaxy (M31) and the Whirlpool Galaxy (M51), because they are easily visible and well-studied. These galaxies are also relatively nearby in astronomical terms, which makes them easier to observe and study in detail. This can cause a bias in the observed rates of CCSN. Using the CCSN sample I examined the fractions of amateur discovery reports compared to all discovery reports for each yearly sample. The results indicate that amateur astronomers make up a significant percentage of all discovery reports, with the percentage around 50% in the 2000-2006 and 2007-2013 yearly bins. However, in the 2014-2021 bin, the percentage drops down to around 30%.

Table II: Cumulative CCSN rates from 0 to 30 Mpc and from 5 to 30 Mpc, excluding CCSN from 0 to 5 Mpc (listed in cols. 2 and 4) with the cumulative number of CCSN events at each distance (listed in cols. 3 and 5).

Distance [Mpc]	CCSN rate 5-30 Mpc $[10^{-4}\ \mathrm{yr}^{-1}\ \mathrm{Mpc}^{-3}]$	Number of CCSN 5-30 Mpc	CCSN rate $[10^{-4}\ \mathrm{yr}^{-1}\ \mathrm{Mpc}^{-3}]$	Number of CCSN
< 1	0.0	0	0.0	0
< 2	0.0	0	0.0	0
< 3	0.0	0	0.0	0
< 4	0.0	0	$10.17^{+6.08}_{-4.04}$	6
< 5	0.0	0	$5.21^{+3.11}_{-2.07}$	6
< 6	$3.58^{+3.48}_{-1.95}$	3	$4.52^{+2.06}_{-1.48}$	9
< 7	$1.99^{+1.57}_{-0.95}$	4	$3.16^{+1.35}_{-0.98}$	10
< 8	$2.24^{+1.11}_{-0.78}$	8	$2.97^{+1.02}_{-0.78}$	14
< 9	$1.98^{+0.79}_{-0.59}$	11	$2.53^{+0.77}_{-0.61}$	17
< 10	$2.11^{+0.64}_{-0.51}$	17	$2.50^{+0.64}_{-0.52}$	23
< 11	$2.34^{+0.55}_{-0.46}$	26	$2.61^{+0.55}_{-0.46}$	32
< 12	$1.96^{+0.44}_{-0.36}$	29	$2.20^{+0.44}_{-0.37}$	35
< 13	$1.94^{+0.37}_{-0.32}$	37	$2.12^{+0.38}_{-0.32}$	43
< 14	$1.70^{+0.31}_{-0.26}$	41	$1.86^{+0.31}_{-0.27}$	47
< 15	$1.97^{+0.26}_{-0.26}$	59	$2.09^{+0.26}_{-0.26}$	65
< 16	$1.97^{+0.23}_{-0.23}$	72	$2.07^{+0.23}_{-0.23}$	78
< 17	$1.79^{+0.20}_{-0.20}$	79	$1.88^{+0.20}_{-0.20}$	85
< 18	$1.60^{+0.17}_{-0.17}$	84	$1.67^{+0.18}_{-0.18}$	90
< 19	$1.48^{+0.15}_{-0.15}$	92	$1.55^{+0.16}_{-0.16}$	98
< 20	$1.36^{+0.14}_{-0.14}$	99	$1.42^{+0.14}_{-0.14}$	105
< 21	$1.31^{+0.12}_{-0.12}$	110	$1.36^{+0.13}_{-0.13}$	116
< 22	$1.26^{+0.11}_{-0.11}$	122	$1.30^{+0.12}_{-0.12}$	128
< 23	$1.20^{+0.10}_{-0.10}$	133	$1.24^{+0.11}_{-0.11}$	139
< 24	$1.15^{+0.10}_{-0.10}$	145	$1.19^{+0.10}_{-0.10}$	151
< 25	$1.09^{+0.09}_{-0.09}$	155	$1.12^{+0.09}_{-0.09}$	161
< 26	$1.05^{+0.08}_{-0.08}$	169	$1.08^{+0.08}_{-0.08}$	175
< 27	$1.03^{+0.08}_{-0.08}$	186	$1.06^{+0.08}_{-0.08}$	192
< 28	$0.96^{+0.07}_{-0.07}$	193	$0.98^{+0.07}_{-0.07}$	199
< 29	$0.92^{+0.06}_{-0.06}$	205	$0.94^{+0.06}_{-0.06}$	211
< 30	$0.85^{+0.06}_{-0.06}$	211	$0.87^{+0.06}_{-0.06}$	217

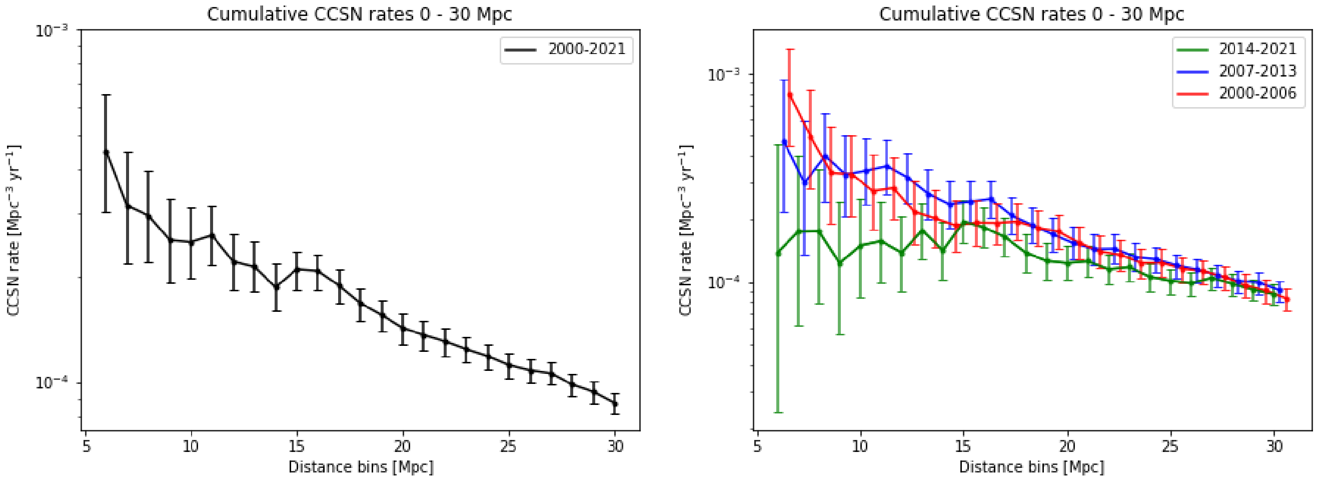

Figure 5: The cumulative CCSN rates for the range of 0 - 30 Mpc (zoomed to 5 - 30 Mpc) are shown. The left graph displays the combined CCSN sample of all CCSNe observed between 2000 - 2021, while the right graph displays separate CCSN samples for each of the three time ranges broken down: 2000 - 2006, 2007 - 2013, and 2014 - 2021. For clarity, the data points on the right graph have been shifted along the x-axis by +0.3 Mpc (2007 - 2013) and +0.6 Mpc (2000 - 2006).

The cumulative CCSN rates were calculated after excluding supernovae within a distance of 5 Mpc, and the results with their associated uncertainties are presented in Table II and Figure 6. This sample was used to determine the CCSN rate by subtracting the 5 Mpc sphere from the calculation volume. The graph shows that the CCSN rate remains constant from 5 Mpc to approximately 18 Mpc, although uncertainties are large at lower distances. A statistical test to determine the distance at which the CCSN begins to decrease significantly is conducted below.

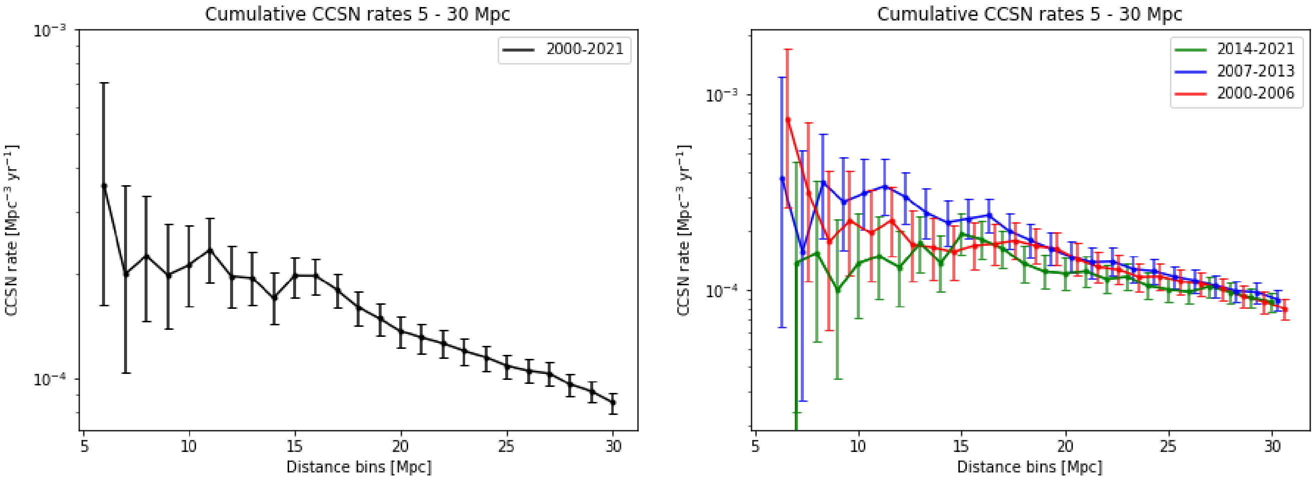

Figure 6: The cumulative CCSN rates for the range of 5 - 30 Mpc are shown. The left graph displays the combined CCSN sample of all CCSNe observed between 2000 - 2021, while the right graph displays separate CCSN samples for each of the three time ranges broken down: 2000 - 2006, 2007 - 2013, and 2014 - 2021. For clarity, the data points on the right graph have been shifted along the x-axis by +0.3 Mpc (2007 - 2013) and +0.6 Mpc (2000 - 2006).

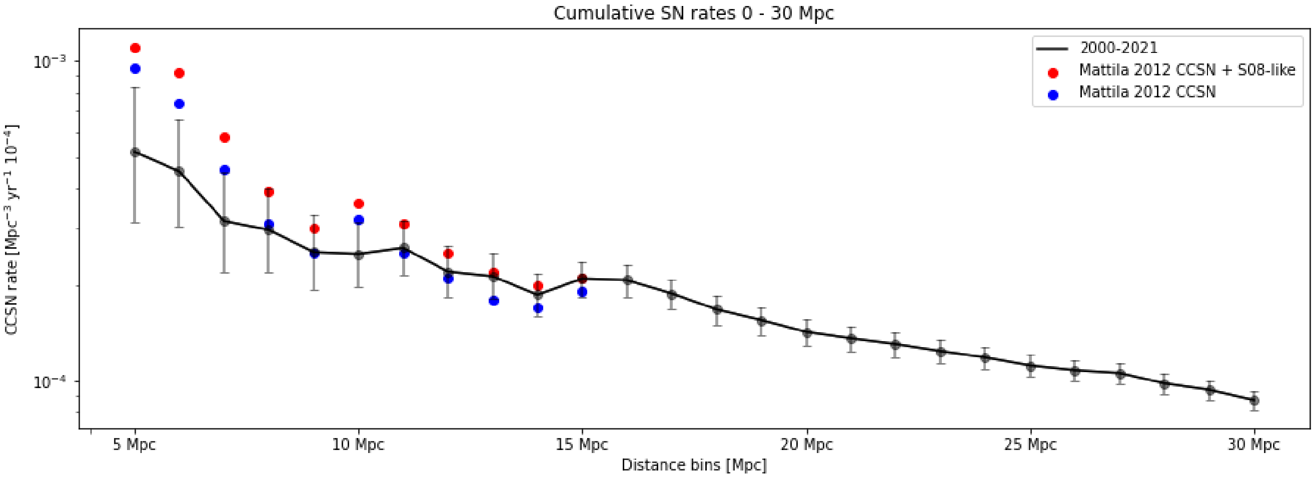

Figure 7: Cumulative CCSN rate (black) graph for the 0 - 30 Mpc sample + CCSN rates (blue) and S08-like rates (red) from Mattila et al. (2012) [3]. The graph is zoomed to 5 - 30 Mpc.

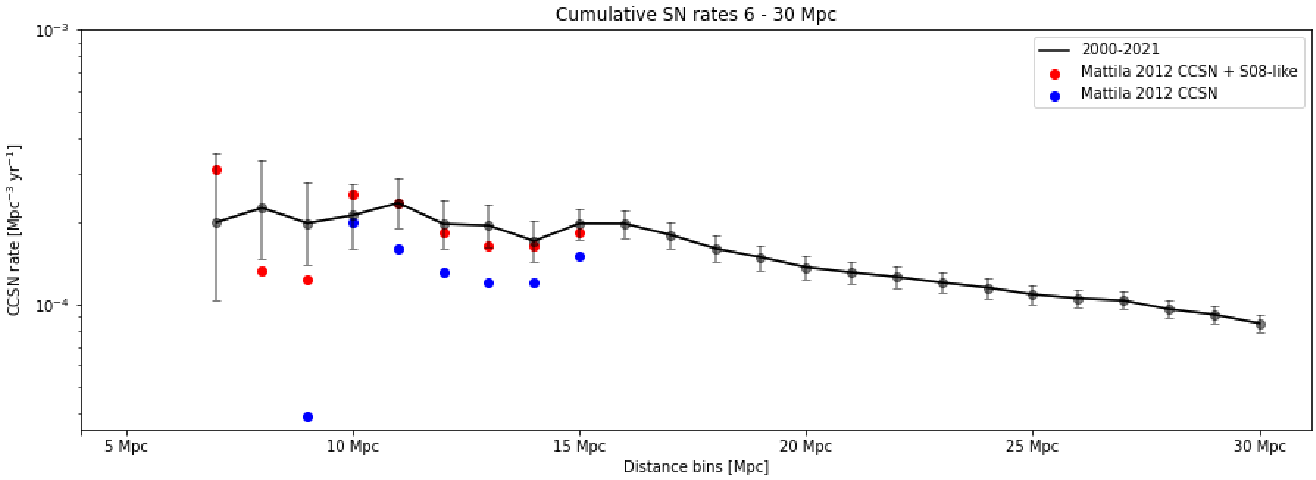

Figure 8: Cumulative CCSN rate (black) graph for the 6 - 30 Mpc sample + CCSN rates (blue) and S08-like rates (red) from Mattila et al. (2012) [3]. The graph is zoomed to 6 - 30 Mpc.

2.2 Co-Moving CCSN Rates

The calculation of co-moving CCSN rates is a useful tool for describing the number of CCSNe occurring in a given region of space. This approach is more accurate to analyse the changes in the rate than the cumulative method, as it adjusts the CCSN rate equation (7) to exclude shorter distance CCSNe from the calculation. The volume is divided into 5 Mpc bins, and all CCSNe inside each volume bin are included in the equation. The CCSN rate equation remains the same, however the volume term is adjusted accordingly ($V_{co-moving} = 4\ \pi\ r_n^3/3 - 4\ \pi\ r_{n-1}^3/3$).

$$CCSN\ rate = N_{CCSN} \times \frac{1}{N_y} \times \frac{1}{V_{co-moving}} \tag{4}$$

Where r_n is the radius of the sphere and r_{n-1} is the radius of the excluded sphere, resulting in the spherical volume $V_{co-moving}$. Here N_{CCSN} only includes the CCSNe inside the spherical volume.

Table III displays the co-moving CCSN rates obtained from Appendix B. The rates and uncertainties are also presented in Figure 9 (left). It can be seen that the CCSN rate is high in the 0 - 5 Mpc bin, as previously indicated by the cumulative CCSN rates.

Table III: Co-moving CCSN rates from 0 to 30 Mpc with the co-moving number of CCSN events at each distance.

Distance [Mpc]	CCSN rate [10^{-4} yr^{-1} Mpc^{-3}]	Number of CCSN
$0-5$	$5.21^{+3.11}_{-2.07}$	6
$5-10$	$2.11^{+0.64}_{-0.51}$	17
$10-15$	$1.92^{+0.34}_{-0.29}$	42
$15-20$	$0.94^{+0.17}_{-0.15}$	40
$20-25$	$0.80^{+0.11}_{-0.11}$	56
$25-30$	$0.53^{+0.07}_{-0.07}$	56

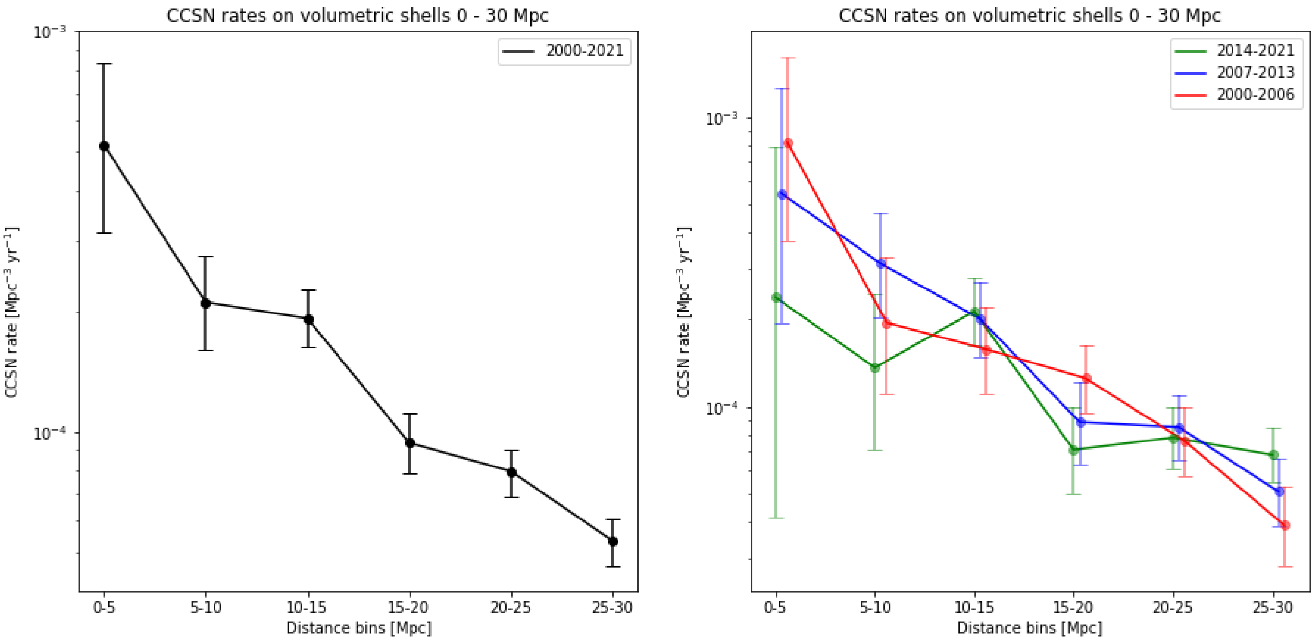

Figure 9: Co-moving CCSN rates. Combined supernova sample with all the CCSN from years 2000 to 2021 on the left and separate supernova samples with CCSN from years 2000-2006, 2007-2013 and 2014-2021 on the right. For clarity, data points have been shifted along the x-axis by +0.3 Mpc (2007-2013) and +0.6 Mpc (2000-2006).

2.2.1 Analysis of the Significance of Decrease Using Statistics

In this section, the CCSN rate was examined over a distance range of 30 Mpc. Specifically, the CCSN rate was transformed into bins of 2 Mpc, starting from 4 Mpc, and analysed using the co-moving way of counting CCSNe. A bin size of 2 Mpc was employed in order to optimize the balance between distance resolution and statistical errors. The results of this analysis are presented in Figure 10. This study was conducted to determine if the CCSN rate decreases statistically significantly at some distance.

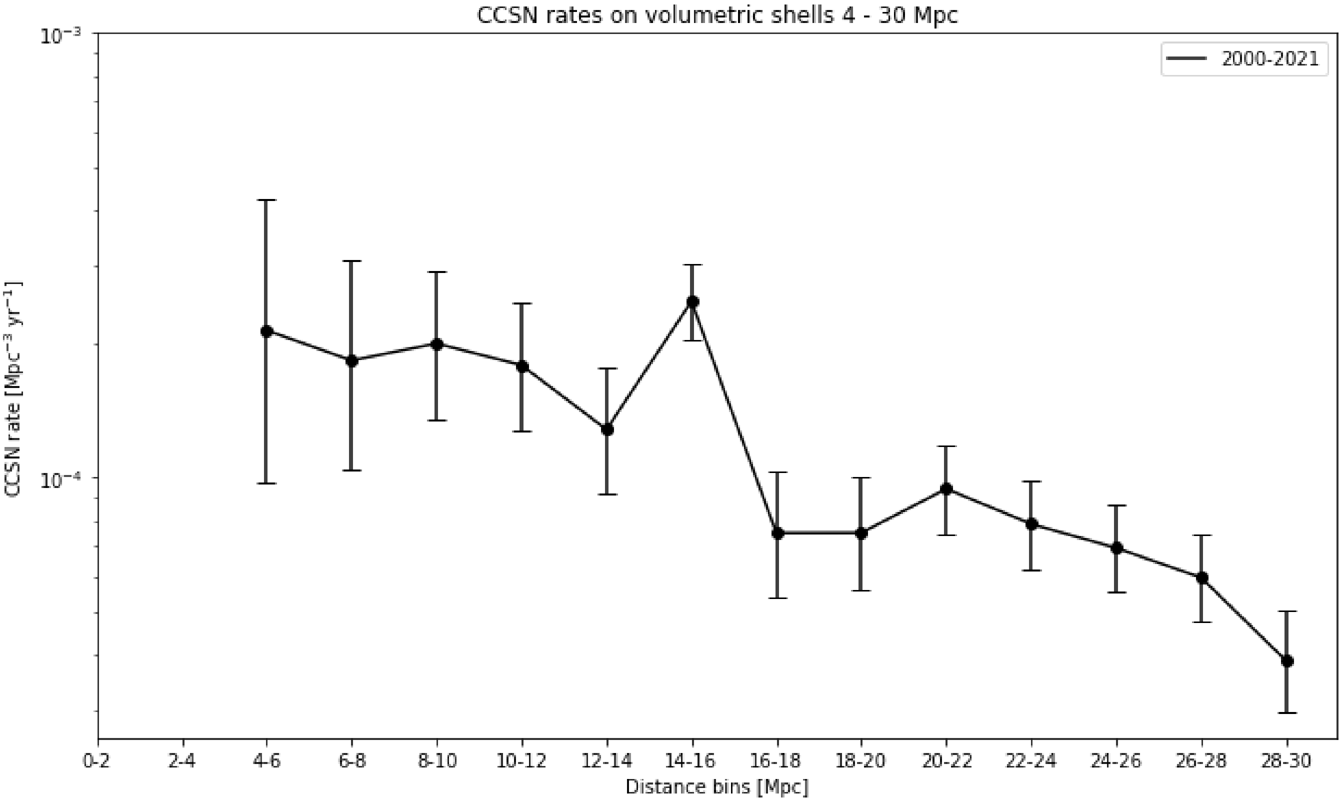

Figure 10: CCSN rates using shell volumes calculated every 2 Mpc from 4 Mpc to 30 Mpc.

The significant decrease in the CCSN rate was analyzed in this study using the statistical method of bootstrapping. Bootstrapping is a non-parametric approach to estimating the sampling distribution of an estimator by resampling a dataset with replacement. Multiple samples were created from the original dataset, and the values for each sample were estimated. The difference between the two samples was assessed using a statistical test, as explained below.

I planned to compare the distributions of the CCSN rates when the CCSN rate is constant and when it is bootstrapped. I analyzed Figure 10 and observed that the CCSN rate did not seem to change significantly in the distance range of 4-16 Mpc, even considering the statistical errors. To confirm this a mean subtraction method was applied. A total of 10,000 bootstrapped values were generated and the mean differences in CCSN rates between two distance ranges (4 to 16 Mpc and 16 to 30 Mpc) were calculated in my approach. Multiple distributions of the subtracted means were obtained by performing this calculation at every distance. It was found that the greatest difference in mean CCSN rate occurred between the distance range of 4 to 16 Mpc and 16 to 30 Mpc based on the results. The 4-16 Mpc distance range was chosen as the constant distribution value for the analysis based on this finding.

Bootstrapping was used to simulate a new CCSN rate within the provided statistical errors. A Poisson distribution centered at the original value was employed to generate the values on each distance bin. The statistical error limits were kept constant. The bootstrapping process was repeated 10,000 times, and the mean value of the CCSN rate between distances of 4-16 Mpc was calculated. Figure 11 displays the bootstrapped CCSN rates in red and the mean values between 4-16 Mpc in blue.

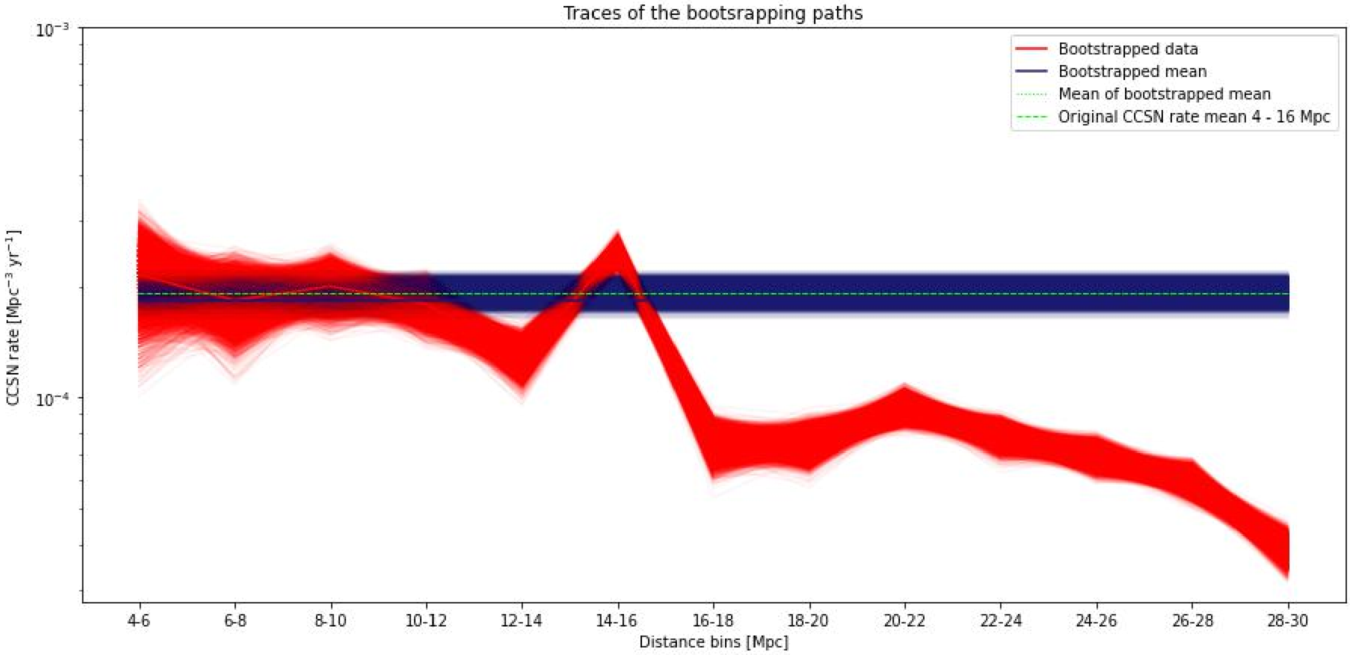

Figure 11: Bootstrapping results for the mean subtraction method

After each simulation of the bootstrapped values and the mean, the relationship of the two distributions was analyzed. I used the Kolmogorov-Smirnov test (KS-test) to determine if the cumulative distributions differ from each other significantly. The KS test compares two samples and determines if the samples are from the same population. The test is based on the maximum absolute difference between the cumulative distribution functions of the two samples. The *scipy.stats.ks2samp* function from the *SciPy* Python package was used to test the null hypothesis that two samples were drawn from the same distribution. Calculating the p-values for each simulation, the null hypothesis was rejected at a 95% confidence level if the p-value was less than 0.05. Figure 12 shows a distribution of the KS-test p-values from all of the 10000 simulations and the result suggests that the two samples were not drawn from the same distribution.

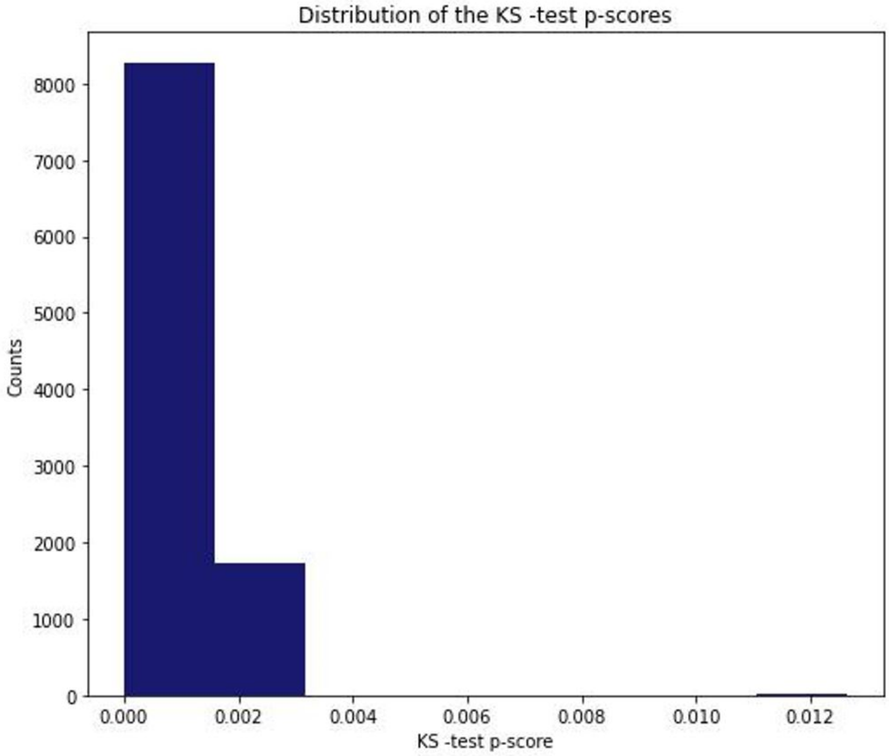

Figure 12: Bootstrapping results for KS-test, when comparing the bootstrapped CCSN rate values with a mean CCSN rate values from 4-16 Mpc.

2.3 The Impact of Galaxy Orientation on Observations

Galaxy inclination is an important factor to consider when detecting a CCSN. The inclination of a galaxy refers to the angle at which it is viewed from the Earth. This angle can affect the visibility of a CCSN signal and can affect how it is interpreted. For example, if a galaxy is viewed from an edge-on orientation, the transient signal may be obscured by dust in the galaxy. This can make it difficult to detect the signal, as it may be faint or only visible in certain wavelengths. On the other hand, if a galaxy is viewed from a face-on orientation, the transient signal may be more easily detected due to the lack of obscuring dust. This can allow for more accurate measurements of the CCSN properties, as well as better understanding of the source of the CCSN. Inclination can also affect the interpretation of the CCSN. For example, a supernova explosion viewed from a face-on orientation may appear brighter and may have different features than a supernova explosion viewed from an edge-on orientation.

2.3.1 Inclination Analysis of Nearby Host Galaxies and Non-Elliptical Galaxies

The galaxy inclination values were found at HyperLeda. The inclination is defined in HyperLeda with the equation:

$$\sin^2(i) = \frac{1 - 10^{-2 \cdot \log r25}}{1 - 10^{-2 \cdot \log r_0}} \tag{5}$$

where i is the galaxy inclination. The parameter logr25 refers to the logarithmic ratio between the major and minor axes lengths of galaxies in the B-band, derived from the isophote at a surface brightness of 25 mag/arcsec^2. r_0 is a constant that is determined based on the morphology of the galaxy.[18] Galaxies with the inclination of 90 degrees is called an edge on galaxy, and 0 degrees is called a face-on galaxy.

The next step was to gather the inclination data from all galaxies within 30 Mpc, in addition to the host galaxies of CCSNe. This was done by using the SQL search feature in HyperLeda. From this search, I excluded any galaxy with the typing of elliptical or probably elliptical galaxies (types 'E' and 'E?'). These types of galaxies have very little star formation and therefore very few CCSNe. Elliptical galaxies have evolved to the point where the remaining stars are too old to produce CCSNe. The distance was determined with the distance modulus, that corresponds to 30 Mpc distance. In addition, only the galaxies with inclination values were chosen in the data. In the end I have the inclination datasets for the CCSN host galaxies and non elliptical galaxies in general within 30 Mpc.

The next thing I did was to plot histograms of the inclinations for the two datasets. The histrograms have 3 bins ($0° - 30°$, $30° - 60°$ and $60° - 90°$). Figure 13 displays histograms describing the inclinations of host galaxies for the CCSN sample with three distance ranges: 0 Mpc to 15 Mpc, 15 Mpc to 30 Mpc, and 0 Mpc to 30 Mpc. The histogram of all galaxy inclinations from HyperLeda is shown in Figure 14. The values of each bin and their statistical errors are presented as percentages from the whole sample.

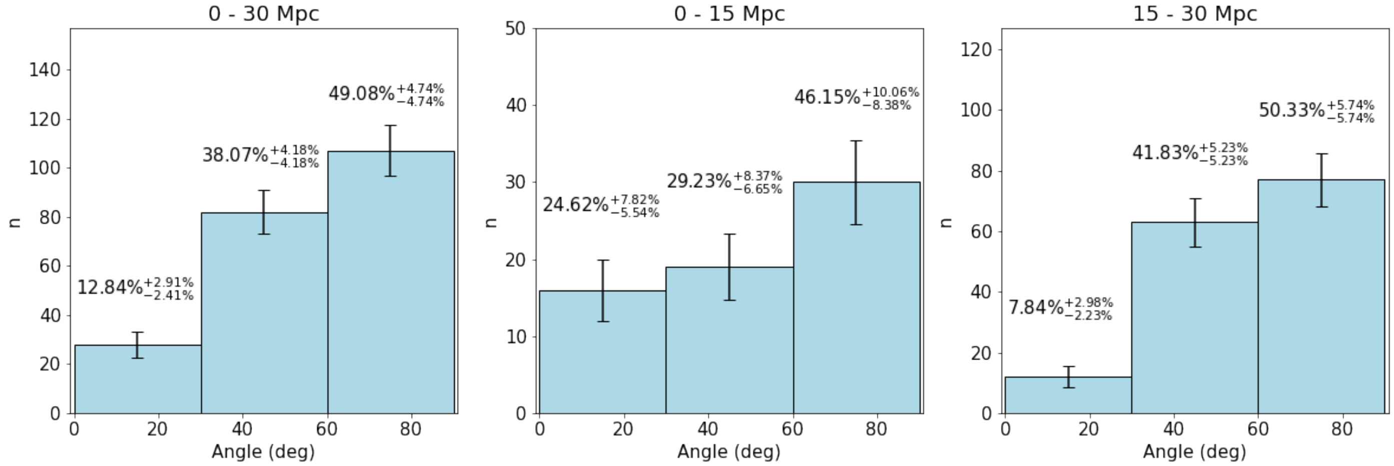

Figure 13: Inclinations of all galaxies from the CCSN sample at distances 0 - 30 Mpc (left), 0 - 15 Mpc (middle) and 15 -30 Mpc (right) with statistical errors.

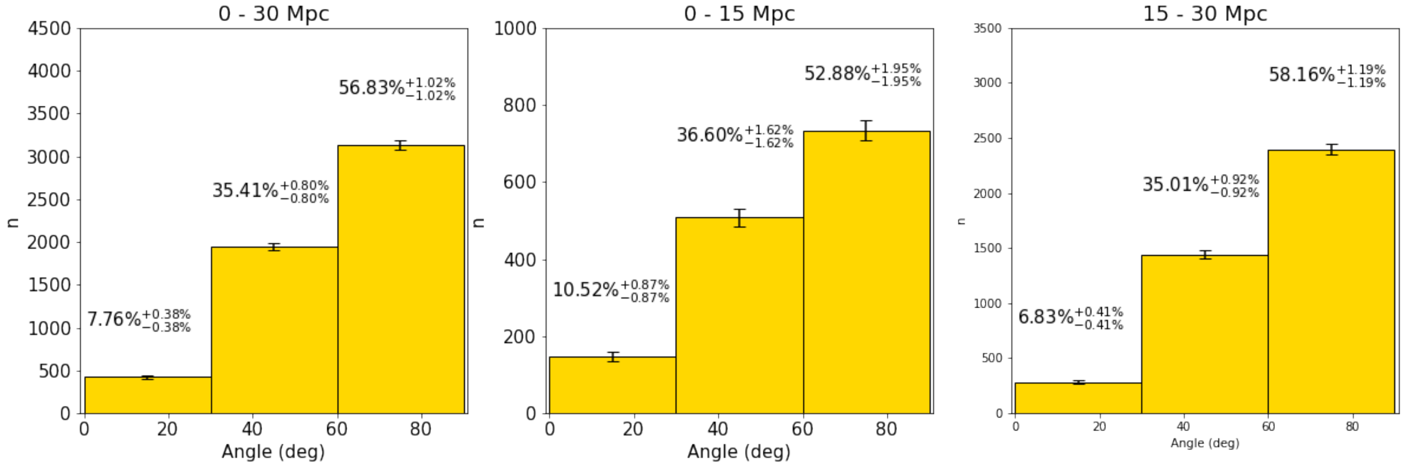

Figure 14: Inclinations of all non elliptical galaxies from HyperLeda at distances 0 - 30 Mpc (left), 0 - 15 Mpc (middle) and 15 -30 Mpc (right) with statistical errors.

When comparing the Figures 13 to Figure 14, in the CCSN host galaxy sample, the distribution is shifted a little bit to the smaller inclinations. This change is outside the statistical uncertainties and might have an actual physical reason. It is hard to compare the distributions at 0 - 15 Mpc since the CCSN host galaxy sample at this distance is quite small and thus has large uncertainties.

2.3.2 Comparing Two Samples with the CDF and KS-test

I present the cumulative distribution functions (CDFs) for the observed CCSN host galaxy sample, the non-elliptical galaxy sample from HyperLeda [18], and a theoretical distribution in Figure 15. The KS-test was used to compare the CCSN host galaxy sample to the non-elliptical galaxy sample.

The theoretical distribution can be explained by considering a model in which an observer is located at the origin of a symmetrical spherical coordinate system, and a galaxy is situated at a distance r from the origin. If the observer is located at a random position, the same is true for the galaxy being located at the origin. Consequently, there is a greater number of possible locations for the observer when the inclination i is high, since the area for a given angular range is larger near the xy-plane. As a result, $1 - \cos(i)$ is the fraction of galaxies with inclination smaller than i.

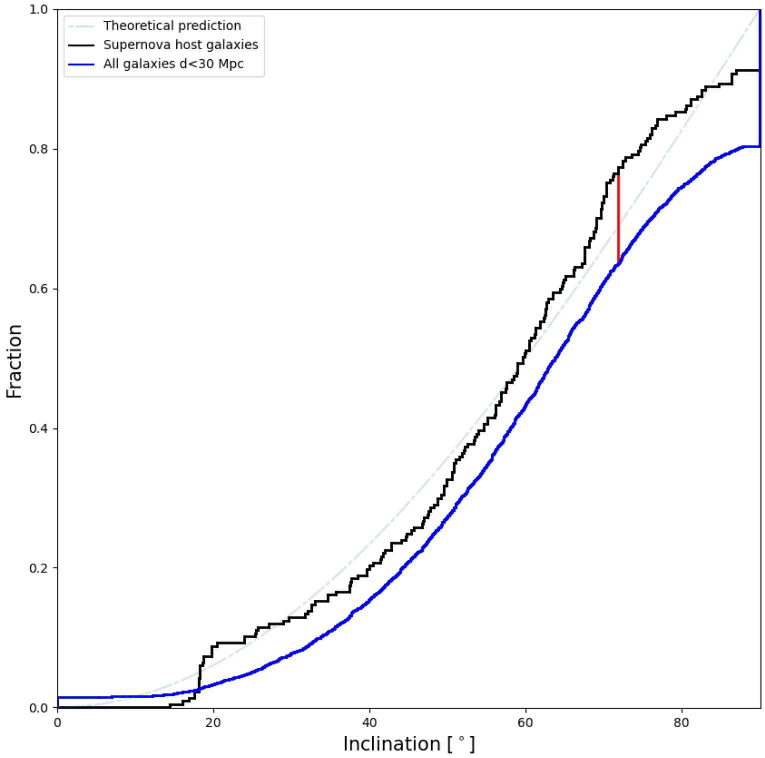

Figure 15: The figure shows the cumulative distribution function of the inclination of supernova host galaxies, all non elliptical galaxies and the predicted distribution from spherical symmetry. The red line indicates the largest distance between supernova host galaxy and all non elliptical galaxy CDFs.

KS-test was conducted at a significance level of $\alpha = 0.05$ to assess the statistical significance of the deviation between two samples. The greatest difference between the samples was 0.134 at $i = 72°$ (shown in figure 15 with red line). According to the KS-test, if the statistic $D_{n,m}$ is greater than the critical value of $c(\alpha)\sqrt{\frac{n+m}{n \cdot m}}$, then the hypothesis of the samples originating from the same population can be rejected at a confidence level of 95%. In the present study, n and m are the sizes of the sample, respectively 217 and 5504. With the value $c(\alpha) = 1.358$, the critical value with the sample size becomes 0.0978. Since $D_{n,m} = 0.134 > 0.0978$, the hypothesis of the samples originating from the same population can be rejected with a confidence level of 95%.

2.4 Extinction in Host Galaxies

The extinction in the line of sight is a key consideration when attempting to detect a CCSN or other transients. Scattering and absorption of light by dust particles situated in the line of sight cause extinction, which can significantly lessen the observed brightness of CCSNe. This can make it more difficult to detect and measure the transient. By accounting for extinction, astronomers can more accurately estimate the true brightness and color of a CCSN, allowing them to gain a better understanding of its properties.

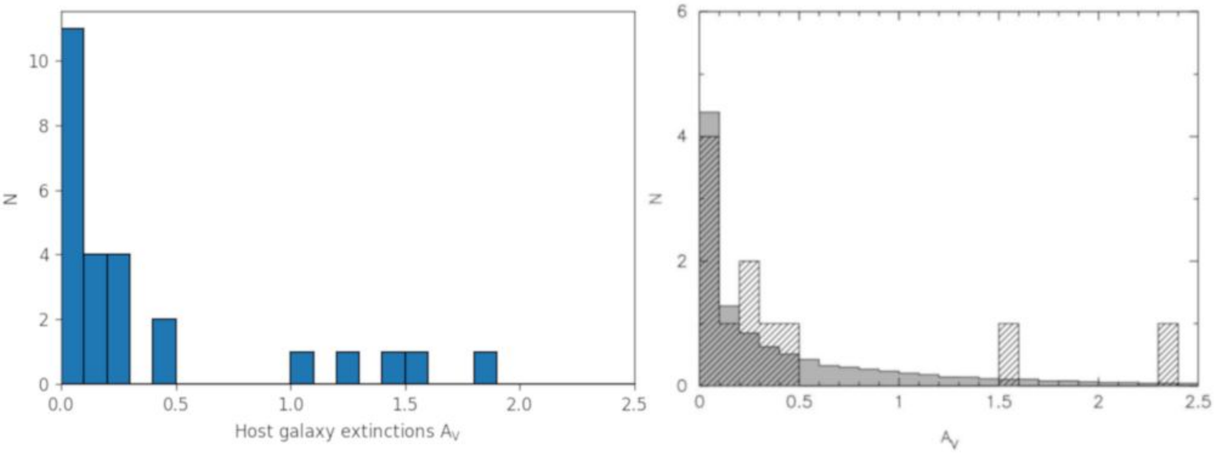

Figure 16: The extinctions of host galaxies of CCSN in this study (left) and Mattila et al. (2012) [3] (right) are shown in the histograms. The x-axis is zoomed to the range 0-2.5 mag of A_V. The hatched area (right) corresponds to the extinctions of observed CCSN, and the grey area (right) is a predicted distribution for CCSN, as presented in Riello & Patat (2005) [23].

This host galaxy extinction analysis focuses on a sample of 28 CCSNe with host galaxy inclinations ranging from 0° to 60° and located within a distance of 16 Mpc.

For comparison I used the predicted values used Mattila et al. 2012 [3] table 3. The extinction analysis reveals that the observed average extinction for the 0°–60° inclination range, $< A_V > = 0.67$, is higher than the predicted value of $< A_V > =$

0.48. The median extinction value is 0.15, which is similar to the predicted value of 0.18. However, when the two events with the highest host galaxy extinctions (SNe 2003jg and 2002hh with $< A_V > = 4$ and 5, respectively) are excluded, the observed average extinction becomes $< A_V > = 0.37$, which is closer to the predicted value. The median extinction value remains unchanged. The standard deviations of the observed and predicted distributions are now very similar, with values of 0.53 and 0.68, respectively.

The events with the highest extinction have a host galaxy extinction of $A_V = 4 - 5$ ($A_B = 5.3 - 6.7$). At a redshift of 0.5, a typical Type II-P event with an absolute peak magnitude of $M(B) = -16.80$ [24] would have an apparent peak magnitude of $m(B) \approx 37$ if the host galaxy extinction is $A_B = 6.7$. This makes detecting CCSN more difficult with current telescopes, especially at higher redshifts where the effects of extinction are even more significant for an optical CCSN search [3]. As a result, it is crucial to consider the potential impact of host galaxy extinction on observed magnitudes of SNe to accurately observe, identify and classify these events at higher redshifts.

Using the sample of 28 CCSNe within 16 Mpc and host galaxy inclination of 0° - 60°, as well as the two outlier events with the highest host galaxy extinctions, I estimate that surveys in normal galaxies may miss a fraction of CCSNe in the range of $7^{+10}_{-5}\%$.

2.5 Calculating Brightness: Absolute Magnitudes

The peak absolute magnitude of CCSNe is an important parameter for astronomers to measure as it provides insight into the type of the progenitor star and the amount of energy released during the explosion. This helps astronomers to classify the type of supernova and to study the physical processes underlying the supernova event. Thus, the measurement of peak absolute magnitude is a key component in understanding the physics of CCSN and their role in the life cycle of stars.

By utilizing the host galaxy distance, peak apparent magnitude, and the extinction of light in the line of sight, I calculated peak absolute magnitudes M for the sample of CCSNe. The peak absolute magnitudes are computed from the peak apparent magnitudes m, the host galaxy distance d, and the extinction values A_V for the Milky Way and the host galaxy:

$$M = m - 5 \cdot \log 10(\frac{d}{10\ \mathrm{pc}}) - A_V^{MW} - A_V^{Host} \tag{6}$$

In some cases, the peak apparent magnitudes are not reported in the V band. In these instances, the extinction values can be transformed from the V band to the reported band using Cardelli's law [25]:

$$\langle A_\lambda / A_V \rangle = a(x) + b(x)/R_V \tag{7}$$

Where A_λ is the extinction in the wanted band, A_V is the extinction in the V band, $a(x)$ and $b(x)$ are the wavelength-dependent coefficients and R_V is a constant with the value $R_V = 3.1$. The $a(x)$ and $b(x)$ values are given in Cardelli et al. 1989, table 3 [25].

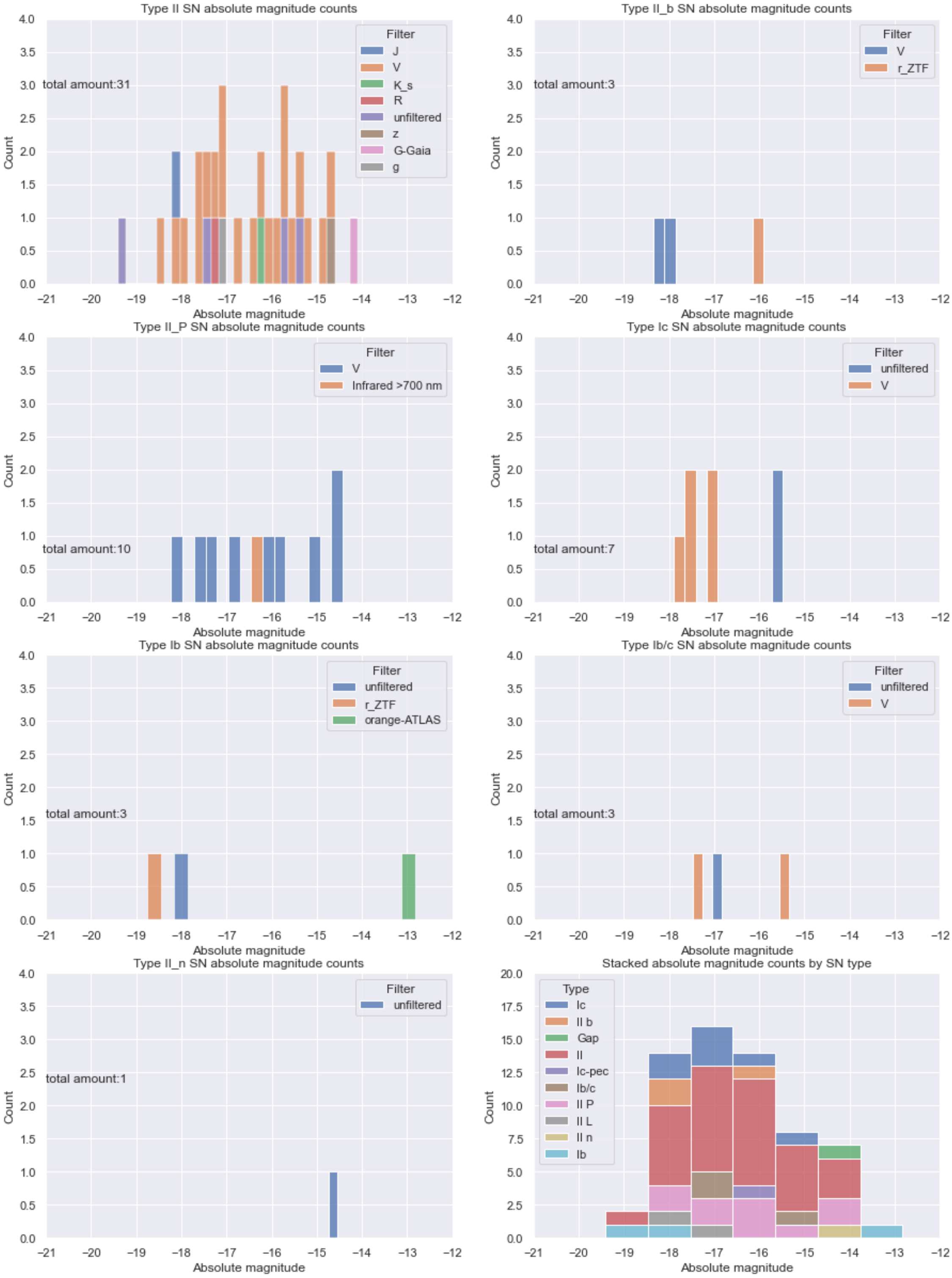

Figure 17: The absolute magnitudes of CCSN are presented in histograms, with the bin heights representing the total number of supernovae in each magnitude range. The first seven histograms show the data for different filters, while the bottom right histogram shows the data for each CCSN type, with counts stacked in each bin and color-coded for easy reference. The final histogram is constructed from data from all filters.

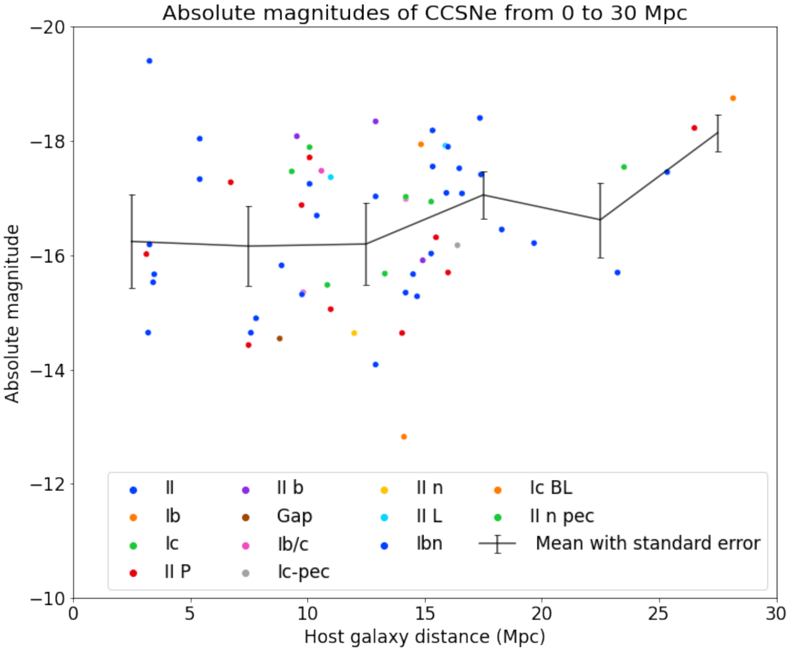

Figure 18: Absolute magnitudes presented as a function of host galaxy distance. The mean absolute magnitudes are calculated with distance bins of 5 Mpc between 0 Mpc and 30 Mpc. The statistical errors are calculated as one sigma standard deviation from the mean.

2.5.1 The Dimmest Supernovae

Table IV presents the faintest CCSNe in the sample. The faintest CCSNe in the sample have the lowest peak absolute magnitudes, ranging from -12.82 to -15.91. This suggests they may have had intrinsically low luminosities or could have been underluminous due to various physical conditions. Additionally, it is possible that the properties of the CCSNe were measured incorrectly, leading to an underestimation of their peak brightness.

Table IV: Table of the faint supernovae in the sample and their absolute peak magnitudes

Supernova	Absolute magnitude	Filter	Type
SN2000ew	$-15.48^{-0.61}_{+0.84}$	unfiltered	Ic
SN2002bu	$-14.54^{-0.15}_{+0.16}$	V	Gap
SN2005af	$-15.67^{-0.02}_{+0.03}$	V	II
SN2005cs	$-15.82^{-0.15}_{+0.16}$	V	II
SN2006ov	$-15.67^{-0.20}_{+0.22}$	unfiltered	II
SN2008bk	$-14.65^{-0.15}_{+0.16}$	V	II
SN2009N	$-14.64^{-0.15}_{+0.16}$	V	II P
SN2009ib	$-15.70^{-0.26}_{+0.29}$	V	II P
SN2009js	$-15.70^{-0.15}_{+0.16}$	V	II
SN2009kr	$-15.35^{-0.41}_{+0.50}$	unfiltered	II
SN2011dh	$-14.43^{-0.04}_{+0.04}$	V	II P
SN2012fh	$-15.35^{-0.26}_{+0.30}$	V	Ib/c
SN2013am	$-14.90^{-0.15}_{+0.16}$	V	II
SN2013dk	$-15.68^{-0.17}_{+0.18}$	unfiltered	Ic
SN2013gc	$-14.64^{-0.14}_{+0.15}$	unfiltered	II n
SN2014bc	$-14.64^{-0.06}_{+0.06}$	z	II
SN2016adj	$-15.53^{-0.20}_{+0.22}$	V	II
SN2016aqf	$-15.28^{-0.16}_{+0.16}$	V	II
SN2016bkv	$-15.32^{-0.16}_{+0.16}$	V	II
SN2016cok	$-15.05^{-0.09}_{+0.08}$	V	II P
SN2019ehk	$-15.91^{-0.07}_{+0.07}$	r_ZTF	II b
SN2019ejj	$-14.09^{-0.15}_{+0.16}$	G-Gaia	II
SN2021gno	$-12.82^{-0.19}_{+0.21}$	orange-ATLAS	Ib

3 The Core-Collapse Supernova-Star Formation Connection

The rate of CCSNe is closely linked to the SFR. This is because the timescale of the stars leading up to a CCSN is much shorter than the cosmic timescale. The lifetime of a massive star is therefore about 0.1 percent of the lifetime of the universe. The CCSN rate (r_{CCSN}) can be estimated by utilizing the SFR, the IMF, marked by ϕ, and the lower and upper mass limits (m_l and m_u) of the stars that cause the collapse supernova. Values m_{min} and m_{max} are the mass limits of all objects that can be classified as stars. Thus, the annual occurrence of CCSNe per volume ($\text{yr}^{-1}\text{Mpc}^{-3}$) can be calculated as: [26]

$$r_{\text{CCSN}} = \frac{\int_{m_l}^{m_u} \phi(m)\text{d}m}{\int_{m_{\text{min}}}^{m_{\text{max}}} m\phi(m)\text{d}m} \times \text{SFR} \tag{8}$$

The IMF used in this study is the Salpeter IMF:

$$\phi(m) = \phi_0 m^{-2{,}35} \tag{9}$$

where ϕ_0 is a constant that describes the density of stars of a given location. The ratio of the CCSN rate to the SFR is affected by two uncertain factors. One of these is the adopted IMF, which has only a minor effect on the result. The other variation is caused by the limits on the mass of the stars that explode as supernovae. The lower limit typically ranges between $7 < \text{M}_\odot < 9.5$. The upper limit is usually set at $40\text{M}_\odot$ or $50\text{M}_\odot$, as stars with masses greater than these are thought to undergo direct collapse into black holes instead of producing a supernova explosion. [27]

By using formulas (1), (8) and (9), it is possible to compare the CCSN rate with the SFR as a function of redshift. These formulas can be used to explore different mass limits and investigate the effects of varying IMF values.

3.1 The Universe in Our Backyard

Using equations (8) and (9), the SFR was determined from the CCSN rate value between 6 and 15 Mpc. A lower limit of 8 solar masses and a higher limit of 50 solar masses were imposed as the progenitors of CCSNe. My results, presented in Table V, indicate that the calculated local CCSN rate and corresponding SFR are slightly higher than the four other results. Nevertheless, my result is consistent within the uncertainties of Botticella et al. (2012) [28].

Table V: Results for the local CCSN rate and corresponding SFR. The distance within which the rates are calculated are in column 4.

Origin	SNR [10^{-4} yr^{-1} Mpc^{-3}]	SFR [M$_\odot$ yr^{-1} Mpc^{-3}]	Distance [Mpc]
This work	$2.09\ ^{+0.26}_{-0.26}$	$0.030\ ^{+0.004}_{-0.004}$	15
Mattila et al. (2012) [3]	$1.50\ ^{+0.40}_{-0.30}$	$0.021\ ^{+0.006}_{-0.005}$	15
Botticella et al. (2012) [28]	$2.00\ ^{+0.50}_{-0.50}$	$0.029\ ^{+0.007}_{-0.007}*$	11
Bothwell et al. (2011) [29]	$1.60\ ^{+0.14}_{-0.14}*$	$0.023\ ^{+0.002}_{-0.002}$	11
Horiuchi et al. (2011) [30]	$1.33\ ^{+0.10}_{-0.10}*$	$0.019\ ^{+0.001}_{-0.001}$	11

* These values were calculated in this work using the same mass limits in equation (11).

3.2 The Distant Universe

We used equation (11) and the SFR as a function of redshift (equation (1)) from Madau & Dickinson (2014) [1] to calculate the CCSN rates for various mass limits of the progenitor stars and models from Heger et al. (2003) [31], O'Connor & Ott (2011) [14], and Sukhbold et al. (2016) [15]. The observed CCSN rates were taken from the study by Strolger et al. (2015) [32] and compared to the predicted rates.

3.2.1 Adjusting Observed Rates

The detection of CCSNe is hindered by a variety of issues. Faint CCSNe may go undetected, while some may be obscured by interstellar dust. This is especially significant in LIRGs and ULIRGs where high dust content renders the majority of CCSNe undetectable. Horiuchi et al. (2011) proposed the 'supernova rate problem' to explain the observation of a CCSN rate that was approximately two times lower than that predicted from the SFR. This mismatch could be caused by a large fraction of CCSNe being obscured, an overestimation of the amount of stars born, or a fundamental misunderstanding of star formation. If the latter is the case, then theoretical models of star formation must be reassessed. [30].

However, a likely solution to this problem is that in LIRGs and ULIRGs, CCSNe are difficult to detect optically due to the dust extinction. While these galaxies are rare in the local Universe, they are common at redshifts of z $\sim 1-2$. A study has revealed that approximately $83^{+9}_{-15}\%$ of SNe remain undetected. This leads to an increase in the average number of supernovae explosions behind the dust extinction, which is approximately $38^{+19}_{-8}\%$ at redshift z $\sim$ 1.2 and remains constant up to z $\sim$ 2. As a result, the observed CCSN rate in the 2011 study [30] is two times lower than predicted CCSN rate. When these supernovae obscured by dust are included in the calculation, the observed number of CCSN is in agreement with the cosmic star formation history. [3]

Near-infrared (NIR) observations are advantageous due to their lower extinction coefficient, allowing for a more detailed investigation of nearby LIRG with core extinction values of $A_V \sim$ 4 - 5 mag. In a few LIRGs, values of $A_V > 10$ mag have been reported [3]. An example of this is the nearby LIRG, Arp 299, where optical observations fail to detect SNe in its nuclei, while only one is detected in the NIR.

The estimated lower limit of CCSN rate for the space surrounding the nuclei of Arp 299 is $0.29^{+0.23}_{-0.14}$ yr^{-1}. Compared to the predicted CCSN rate of 0.30-0.61 yr^{-1}, the suggested missed fraction is 37^{+38}_{-37}%. In comparison, the estimated total CCSN rate for unobserved CCSNe in Arp 299 is 1.59-1.91 yr^{-1}, with an estimated missed fraction of 83^{+9}_{-15}%. [3]

In normal galaxies, where the dust content is lower than in LIRGs and ULIRGs, a small proportion of CCSNe also remain undetected. Dahlen et al. (2012) [27] present the "Normal Galaxy Extinction Correction model", which postulates different distributions of dust and CCSNe in galaxies, with the effects of the spiral structure of spiral galaxies thought to be insignificant.

In this study, I use the observed values between redshifts of 0.3 and 2.3 presented in Strolger et al. (2015). This work employed the supernova surveys CANDELS and CLASH to determine the CCSN rate at higher redshifts in six redshift bins, as shown in Table VI. The table displays the CCSN rates in each redshift bin along with their corresponding statistical errors.

Table VI: Observed CCSN rate from Strolger et al (2015) table 2 [32]

Redshift	CCSN rate [10^{-4} yr^{-1} Mpc^{-3}]
$0.3\ ^{+0.2}_{-0.2}$	$1.97\ ^{+1.4}_{-0.85}$
$0.7\ ^{+0.2}_{-0.2}$	$2.68\ ^{+1.54}_{-1.04}$
$1.1\ ^{+0.2}_{-0.2}$	$1.70\ ^{+1.19}_{-0.71}$
$1.5\ ^{+0.2}_{-0.2}$	$3.25\ ^{+2.03}_{-1.32}$
$1.9\ ^{+0.2}_{-0.2}$	$3.16\ ^{+3.37}_{-1.77}$
$2.3\ ^{+0.2}_{-0.2}$	$6.17\ ^{+6.76}_{-3.52}$

The observed rates of CCSNe have not been corrected for those missed in the surveys. To assess the effects of this, I used correction values derived by Mattila et al. (2012) [3]. These corrections consider the contribution of missed supernovae in LIRGs and ULIRGs, as well as normal galaxies, as a function of redshift. The fraction of CCSN that are potentially missed in observations, as presented by Mattila et al. (2012) [3] table 10, is used to scale the observed rates. The corrections to the observed values are shown in Figure 19 as blue regions with various shades of blue. These corrections shift the observed values to higher values with their corresponding statistical errors. The figure also illustrates the shift of the upper limits of the observed rates to higher values, depending on the fractional correction used: high, nominal, or low.

3.2.2 Comparing Observed and Predicted Rates

In this section I describe the CCSN rates as a function of redshift obtained from three studies; Heger et al. (2003) [31], O'Connor & Ott (2011) [14] and Sukhbold et al. (2016) [15].

In Heger (2003) [31], the SN budgets for different metallicities, IMFs and mass limits were studied. The maximum mass limit was set to 20 solar masses (low $M_{\mathrm{FBH}}^{\mathrm{lim}}$) and 25 solar masses (high $M_{\mathrm{FBH}}^{\mathrm{lim}}$). Using the results given with the Salpeter IMF for zero metallicity, the high SN fraction was found to be 0.76 and the low SN fraction was 0.67. The rest were BHs and fallback blackholes (FBH). The main difference in formation between regular BH and FBH is the amount of mass available to form the BH. Regular BHs are formed from the complete collapse of a massive star, whereas FBHs are formed from the incomplete collapse of a massive star, resulting in a lower mass BH. Correspondingly, the high and low CCSN rate values were determined to be $r_{CCSNHigh} = 0.0051784\ \frac{\mathrm{SFR}}{\mathrm{M_{Sun}}}$ and $r_{CCSNLow} = 0.004557\ \frac{\mathrm{SFR}}{\mathrm{M_{Sun}}}$. A similar analysis was performed for the solar metallicity progenitors, yielding a high supernova fraction of 0.87 and a low supernova fraction of 0.75, as presented in Table VII. The corresponding supernova rate values were determined to be $r_{High} = 0.005941\ \frac{\mathrm{SFR}}{\mathrm{M_{Sun}}}$ and $r_{Low} = 0.005121\ \frac{\mathrm{SFR}}{\mathrm{M_{Sun}}}$. The results indicate that higher metallicity models result in higher supernova rates, as seen in Table VIII.

Table VII: Heger et al. (2003) fractions of massive stars that explode as CCSN. [31].

	Solar metallicity	Zero metallicity
High $\mathrm{M}_{\mathrm{FBH}}^{\mathrm{lim}}$	0.87	0.76
low $\mathrm{M}_{\mathrm{FBH}}^{\mathrm{lim}}$	0.75	0.67

Table VIII: Calculated CCSN rate (r_{CCSN}) values using equation (8), with two different mass limits and metallicities.

	Solar metallicity	Zero metallicity
High $\mathrm{M}_{\mathrm{FBH}}^{\mathrm{lim}}$	0.005941 $\frac{\mathrm{SFR}}{\mathrm{M}_\odot}$	0.005178 $\frac{\mathrm{SFR}}{\mathrm{M}_\odot}$
low $\mathrm{M}_{\mathrm{FBH}}^{\mathrm{lim}}$	0.005121 $\frac{\mathrm{SFR}}{\mathrm{M}_\odot}$	0.004557 $\frac{\mathrm{SFR}}{\mathrm{M}_\odot}$

In Sukhbold et al. (2016) [15], the observable supernova fractions were calculated for a mass range of 9 to 120 solar masses using Table 4. The fractions were determined to be 66%, 67%, 55%, and 74%. The remaining fraction do not produce observable supernovae. Utilizing these fractions to calculate the supernova rates (r_{CCSN}) between 9 to 120 solar masses and 100% for masses between 8 to 9, the corresponding supernova rates were determined to be 0.004860 $\frac{\mathrm{SFR}}{\mathrm{M}_\odot}$, 0.004918 $\frac{\mathrm{SFR}}{\mathrm{M}_\odot}$, 0.004223 $\frac{\mathrm{SFR}}{\mathrm{M}_\odot}$, and 0.005323 $\frac{\mathrm{SFR}}{\mathrm{M}_\odot}$ respectively (Table IX).

Table IX: Sukhbold et al. (2016) CCSN rate (r_{CCSN}) values [15].

Model	r_{CCSN} [$\frac{\mathrm{SFR}}{\mathrm{M}_\odot}$]
W15.0	0.004860
W18.0	0.004918
W20.0	0.004223
N20.0	0.005323

In O'Connor & Ott (2011) [14], the black hole fractions for six different models of metallicity and other properties were studied. The fractions were found to be 13%, 15%, 0%, 7%, 1%, and 4%. Using mass limits of 8 and 125 solar masses for the progenitors, the resulting supernova rates were found to be $r_{WHW02} = 0.005941\ \frac{\mathrm{SFR}}{\mathrm{M_{Sun}}}$, $r_{WHW02} = 0.005804\ \frac{\mathrm{SFR}}{\mathrm{M_{Sun}}}$, $r_{WHW02} = 0.006760\ \frac{\mathrm{SFR}}{\mathrm{M_{Sun}}}$, $r_{LC06B} = 0.006829\ \frac{\mathrm{SFR}}{\mathrm{M_{Sun}}}$, $r_{LC06A} = 0.006351\ \frac{\mathrm{SFR}}{\mathrm{M_{Sun}}}$, and $r_{WH07} = 0.006555\ \frac{\mathrm{SFR}}{\mathrm{M_{Sun}}}$, as shown in Table X. The differences between models with varying metallicity are illustrated in Figure 5. It is also worth noting that the CCSN rates include possible fallback blackholes, which are not taken into account when calculating the observed supernova fractions.

Table X: O'Connor & Ott (2011) r_{CCSN} values. [14]

Model	r_{CCSN} [$\frac{\mathrm{SFR}}{\mathrm{M_\odot}}$]
WHW02 (zero metallicity)	0.005941
WHW02 (10^{-4} metallicity)	0.005804
WHW02 (solar metallicity)	0.006760
LC06B (solar metallicity)	0.006829
LC06A (solar metallicity)	0.006351
WH07 (solar metallicity)	0.006555

By combining the CCSN rate values from the three studies with the Madau & Dickinson SFR (equation (1)), I plotted them in Figure 19 alongside the observed rates discussed earlier.

The Figure 19 allows us to make some deductions about the predicted and observed CCSN rates. The top panel (Heger et al. (2003)) shows that the solar metallicity model is better suited for redshifts z = 0-1, while the zero-metallicity model appears to fit the data more accurately at higher redshifts (z = 2). The middle panel (O'Connor & Ott 2011) shows a similar trend, while the bottom panel (Sukhbold et al. 2016) seems to have the opposite effect. We should bear in mind that these models also have varying parameters other than metallicity, and thus should not be compared in isolation.

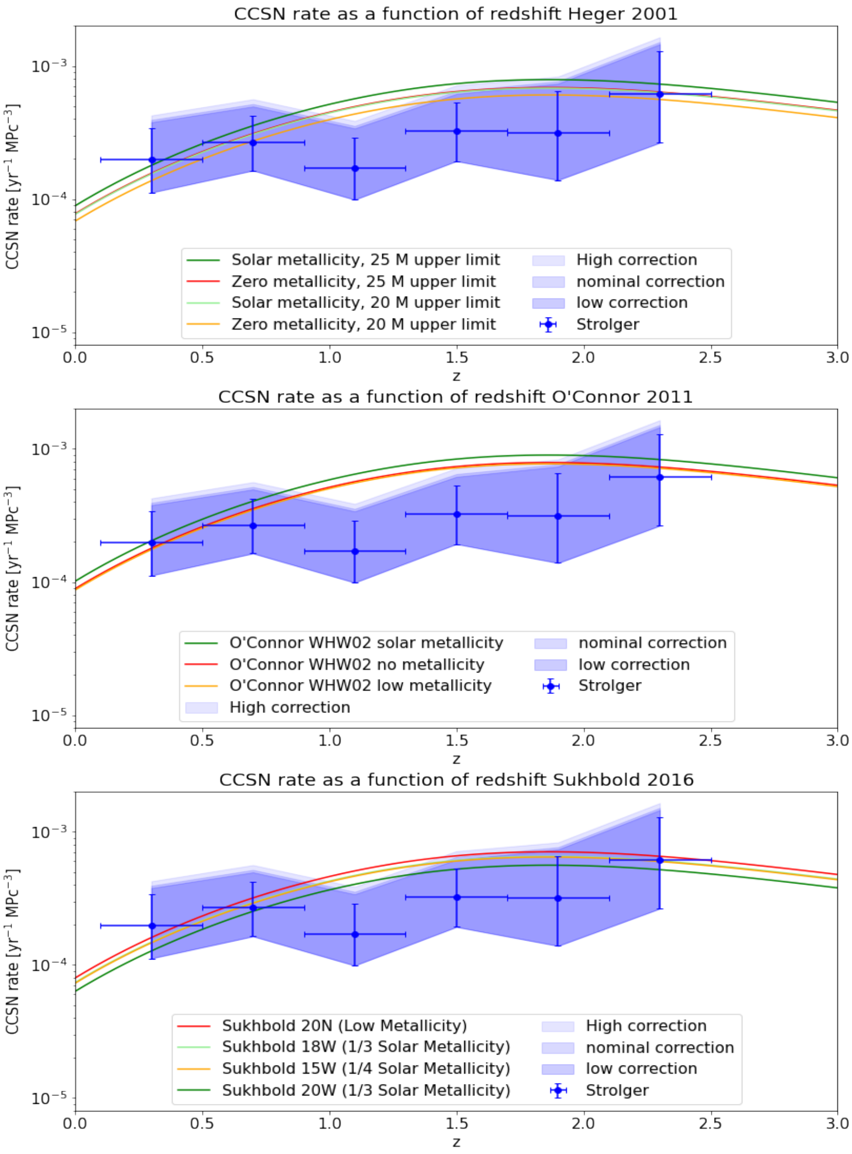

Figure 19: The figure displays the CCSN rate as a function of redshift for different theoretical models. The top panel shows four models from Heger et al. (2003) [31], the middle panel three models from O'Connor & Ott (2011) [14], and the bottom panel four models from Sukhbold et al. (2016) [15]. The blue dots represent observed CCSN rate values from Strolger et al. (2015) with errorbars indicating statistical errors, while the blue-filled regions show the effect of different corrections [3] on the upper limits of the observed CCSN rates.

4 Discussion

Having analyzed and presented the main findings from the preceding sections, this discussion section aims to provide more interpretation and evaluation of the results. In this section, I will delve into the implications, explore possible explanations, and highlight areas for further investigation.

As discussed earlier in the Cumulative Rates section, the accuracy and completeness of supernova observations can be influenced by various factors, such as the availability of resources and the expertise of the observers. In this context, it is important to consider that professional astronomers may have had fewer resources available for SN observations in the early years, which could have limited their ability to make significant contributions. An example of this could be the lack of advanced telescopes and imaging technologies that are available today. In the early years, astronomers had to rely on less sophisticated equipment, which made it more difficult to observe and study supernovae accurately. Additionally, the field of astronomy may not have been as well-funded as it is today, which could have limited the resources available to astronomers for their research. Moreover, relying on amateur reports of SN might have biased the observations towards shorter distances, potentially affecting the estimated CCSN rate.

In Mattila et al. (2012) [3], the volumetric CCSN rate was examined from 0 to 15 Mpc as well as from 6 to 15 Mpc. This sample covered supernovae from 2000 to 2011, with the CCSN rate being calculated with and without 08S-like supernovae. The study has suggested that SN 2008S may be representative of a new class of transients, distinct from traditional supernovae, due to its low peak luminosity. This new class has been categorised as 08S-like supernovae. This thesis does not differentiate between the two. Figure 7 compares the CCSN rate from 0 to 15 Mpc and the CCSN + 08S-like rate from 0 to 30 Mpc in Mattila et al. [3] with the cumulative CCSN rates of this study. There is some discrepancy between the two rates at distances 4 - 7 Mpc, which is likely due to the Mattila (2012) sample being somewhat biased by amateur observations. That said, the rates at distances 8 - 15 Mpc appear to be in good agreement.

In order to further compare the results of this study, a supernova sample was created that excluded supernovae closer than 6 Mpc. The CCSN and CCSN + 08S-like rates from 6 to 15 Mpc, as well as the cumulative CCSN rates from 6 to 30 Mpc are displayed in Figure 8. It appears that the Mattila 2012 CCSN + 08S-like rates are more similar to my results than the Mattila 2012 CCSN rates, likely because the S08-like supernovae were not taken into account in this study and were instead included in the CCSN sample used to calculate the rates.

The CCSN rate in Figure 9 appears to be relatively constant in the 5 - 10 Mpc and 10 - 15 Mpc bins, before dropping sharply between 15 - 20 Mpc. This suggests that supernovae become increasingly difficult to observe beyond 15 Mpc. A more in-depth statistical analysis of this significant decrease is presented in the subsequent subsection. Additionally, the sphere shell CCSN rates remain fairly similar across different years of observation, within the uncertainties.

The results of the KS-test showed that bootstrapped values and constant values are not drawn from the same population, thus the decrease of the CCSN rate beyond 16 Mpc can be considered statistically significant. This suggests that CCSN rates are likely to be lower at larger distances, and that the decrease is not a result of random fluctuations or sampling bias. This could suggest various explanations, such as a decrease in CCSN rates with increasing distance due to some underlying physical phenomenon or an increased difficulty in detecting CCSNe at greater distances.

The angle of galaxy orientation to the observer can affect the visibility of a CCSN signal and can affect how it is interpreted. For example, if a galaxy is viewed from an edge-on orientation, the transient signal may be obscured by dust in the galaxy. This can make it difficult to detect the signal, as it may be faint or only visible in certain wavelengths. On the other hand, if a galaxy is viewed from a face-on orientation, the transient signal may be more easily detected due to the lack of obscuring dust. This can allow for more accurate measurements of the CCSN properties, as well as better understanding of the source of the CCSN. Inclination can also affect the interpretation of the CCSN. For example, a supernova explosion viewed from a face-on orientation may appear brighter and may have different features than a supernova explosion viewed from an edge-on orientation.

In this work, I compare the CCSN host galaxies data sample to the sample of all non-elliptical galaxies and the theoretical distribution of galaxy inclinations. I find that the total galaxy sample does not follow the theoretical prediction of a monotonically increasing slope. Instead, the slope begins to decrease at around 70° and jumps to 100 % at 90°. I propose that this is because galaxies at high inclination $\gtrsim 75$ are difficult to distinguish from those that have an inclination of 90°, and are therefore often assigned an inclination of 90°. This effect can also be seen to a lesser degree at 0° and in the supernova host sample. In contrast, the central region of the picture shows the CDF from the sample of all galaxies matching the shape of the theoretical prediction. These findings are illustrated in Figure 15.

The sample of supernova host galaxies is significantly distinct from the sample of all galaxies. This is remarkable considering the large sample size and the fact that the majority of the inclination data comes from the same source. If inclination had no influence, then it can be assumed that the CDF of CCSN host galaxies would be nearly identical to that of all galaxies.

Figure 16 shows the distributions of extinction for this study and Mattila et al. (2012). The peak of the extinction distribution at 0-0.1 is significantly higher in this study than that of Mattila et al. (2012). However, the sample size of Mattila et al. (2012) is smaller than that of this study, making a direct comparison difficult. However, this difference could also be due to other factors, such as the different regions of the sky that are being studied or the different methods used to measure extinction. A more detailed comparison of the two studies, including a comparison of the methods used, could help to determine the exact cause of the difference in the extinction distributions.

Figure 16 shows the host galaxy extinctions of CCSN up to 2.5 magnitudes, which is quite a significant amount of obscuration. However, some CCSN in the sample had more than 2.5 magnitudes extinction, which makes them especially difficult to detect. This could be because their brightness is so heavily reduced by the dust and gas along the line of sight, making them much fainter than they would be otherwise. As a result, these CCSN can be difficult to detect and study, and may be missed entirely in surveys that only consider brighter sources. For this reason, it is important to take into account the host galaxy extinction when searching for CCSN.

Richardson et al. (2014) [24] investigated the average peak absolute magnitudes of various types of CCSNe in the B-band. Building upon this work, the present study expands the scope to include absolute magnitudes in multiple observational filters. With a limited sample size, the uncertainties in the results for each CCSN type are considerable. To reduce complexity and provide an appropriate overview of the data, the results are presented in a histogram format (Figure 17) instead of a table. The lack of data limits the ability to draw conclusions from the study, and further research is needed to refine the results and better understand the average peak absolute magnitudes for each CCSN type. Additionally, the current results may be used to improve classification system for CCSNe, providing more detail to categorize the different types of CCSNe based on their peak absolute magnitude values. This could aid future studies by improving the accuracy of their results.

The peak absolute magnitude of CCSN was an intriguing parameter to consider when examining the sample. Figure 18 illustrates the peak absolute magnitude of all CCSNe in the sample as a function of distance, using data from all filters. It was discovered that the observed number of sources with peak absolute magnitudes above 18 Mpc decreases. This is likely due to the reduced amount of available apparent magnitude data or host galaxy extinction data in this distance range. As displayed in Tables II and III, there are numerous sources categorized as CCSN above 18 Mpc. However, a substantial proportion of them lacked the necessary information to determine their absolute magnitudes.

An increase in the average peak absolute magnitude was also observed with increasing distance, which could be attributed to a combination of factors. Firstly, the luminosity of the source decreases with distance, making it more difficult to detect dimmer CCSNe at larger distances. Secondly, the effects of dust extinction become more significant farther away from us, resulting in a reduction of the source's apparent magnitude and thus its peak absolute magnitude. Lastly, the number of sources with accurate magnitudes decreases with distance due to the limited amount of available data.

These faint CCSNe could have been missed at peak brightness due to inadequate detection techniques or observational bias. The physical causes of the faintness of these CCSNe are still unknown, and further research is needed to better understand the underlying mechanisms. Moreover, further observations of these faint CCSNe could lead to new insights into their properties and the physics at work.

Several faint supernovae have been discovered and studied in detail. For example, SN2002bu, SN2005cs, SN2013am, SN2019ejj, and SN2021gno have all been identified as being fainter than the typical CCSN.

Szczygiel et al. (2002) researched SN2002bu and noted disparities in its physical properties when compared to usual CCSN. This could be proof of a previously unknown subset of CCSNe which are dimmer than the traditional type. Kozyreva et al. (2022) explained the low brightness of SN2005cs as a result of a low-energy explosion from a low-mass iron-core progenitor. Tomasella et al. (2017) [33] reported that SN2013am was fainter than the standard luminosity type IIP supernova. They suggested that the supernova was produced by a moderate-mass red supergiant. Gill et al. (2022) [34] studied the time of gravitational wave emission from CCSN and reported the peak brightness of SN2019ejj to be around -14 mag in the V-band. Furthermore, Bo Jacobson-Galan et al. (2022) [35] reported on SN2021gno, which has a peak absolute magnitude of -14.9 ± 0.1 in the g-band. This is much fainter than the typical luminosity of type Ib CCSN, and it was classified as a "Ca-strong transient" in the study.

My results for the local CCSN rate and the SFR were slightly higher than the four other studies. This could be because the studies conducted by the four other authors are more than 10 years old and the techniques for observing supernovae have advanced significantly in that time. Amateur observations were often used in the past to discover supernovae, but now more professional surveys are used for this purpose. This could account for the slight difference in the results. It is important to note, however, that the difference between my results and those of the other papers is quite small and could be due to other factors such as observational bias or errors in the data.

In the more distant universe, results of Figure 19 suggest that, at redshifts of 0.5 to 1, corrections with smaller missing supernova fractions better fit the observed CCSN rate. At higher redshifts, however, corrections with higher missing fractions seem to provide a better match to the predicted CCSN rate. It is important to note, however, that errors become large when observing at redshifts greater than 2, due to the logarithmic scale of the y-axis. Further research is needed in order to accurately understand the relationship between the observed and predicted CCSN rates at higher redshifts. A more detailed examination of Figure 19 led me to evaluate which models were most consistent with the observed data. In the top panel, only the model with zero metallicity and an upper mass limit of 20 solar masses matched the observed values at redshifts between 1 and 1.5. For the middle panel, all models of the CCSN rate were too high when compared to observations between redshifts of 1 and 2. In the bottom panel, the Sukhbold 20W 1/3 solar metallicity model performed the best, with the other models being too high at redshifts between 1 and 1.5. The Heger zero metallicity, 20 solar mass and the Sukhbold 20W 1/3 solar metallicity models provided the best performance for this comparison.

5 Conclusions

The evolution of SFR with redshift peaks at z = 2, and dust obscures most SN explosions in galaxies with high star formation rates, such as LIRGs and ULIRGs.

There is a correlation between galaxy mass and metallicity, known as the MZR, and an anti-correlation between gas metallicity and SFR, known as the FMR. The MZR evolves with increasing redshift, with a decrease in metallicity at different rates depending on the mass of the galaxy. The SFR weighted metallicity appears to increase over time, reaching the highest value at present day.

The local CCSN rate within 30 Mpc is estimated as cumulative rates and co-moving rates. The rate is higher at close distances for earlier years, likely due to reliance on amateur observations in those years. The rate decreases significantly after a distance of 16 Mpc.

The inclination distributions of CCSN host galaxies suggest that the sample of supernova host galaxies is significantly distinct from the sample of all galaxies. The overall trend is that CCSN are observed more easily in lower inclination galaxies. A substantial number of CCSN may be missed from galaxies with high inclinations.

The observed average peak absolute magnitude distribution of CCSNe increases with distance, likely due to a combination of undetected faint CCSNe, dust extinction, and data availability.

The correlation between CCSN rate and SFR in both the local and higher redshift universe suggests that at redshifts of 0.5 to 1, corrections with smaller missing supernova fractions better fit the observed CCSN rate. However, at higher redshifts, corrections with higher missing fractions seem to provide a better agreement with the predicted CCSN rate.

Acknowledgements

Completing a master's thesis was a challenging but rewarding journey. It taught me the importance of dedication, organization, and staying focused. I was able to develop my research, writing and critical thinking skills, as well as gain a better understanding of my chosen field. The process of writing and revising my thesis was difficult, but I was able to overcome the obstacles and ultimately succeed. I am proud of the work I put into my thesis and the knowledge I gained through the process. I would like to express my sincere gratitude to Doctor Steven Williams for helping me to gather the supernova data from Github, Niko Pyykkinen for his invaluable assistance with the host galaxy inclination analysis, Johannes Rajala for conversations about possible statistical methods and Professor Seppo Mattila for his guidance and support throughout my master's thesis research.

References

[1] P. Madau and M. Dickinson, “Cosmic star-formation history”, Annual Review of Astronomy and Astrophysics **52**, 415–486 (2014).

[2] S. M. Wilkins, C. C. Lovell, and E. R. Stanway, “Recalibrating the cosmic star formation history”, Monthly Notices of the Royal Astronomical Society **490**, 5359–5365 (2019).

[3] S. Mattila, T. Dahlen, A. Efstathiou, E. Kankare, J. Melinder, A. Alonso-Herrero, M. Á. Pérez-Torres, S. Ryder, P. Väisänen, and G. Östlin, “Core-collapse supernovae missed by optical surveys”, Astrophysical Journal **756**, `10.1088/0004-637X/756/2/111` (2012).

[4] D. B. Sanders and I. F. Mirabel, “Luminous Infrared Galaxies”, Annual review of Astronomy and Astrophysics **34**, 749 (1996).

[5] M. Pérez-Torres, S. Mattila, A. Alonso-Herrero, S. Aalto, and A. Efstathiou, “Star formation and nuclear activity in luminous infrared galaxies: an infrared through radio review”, Astronomy and Astrophysics Reviews **29**, 2, 2 (2021).

[6] I. D. Karachentsev, V. E. Karachentseva, W. K. Huchtmeier, and D. I. Makarov, “A Catalog of Neighboring Galaxies”, The Astronomical Journal **127**, 2031–2068 (2004).

[7] R. J. Cooke, M. Pettini, and R. A. Jorgenson, “The most metal-poor damped Lyα systems: An insight into dwarf galaxies at high-redshift”, Astrophysical Journal **800**, `10.1088/0004-637X/800/1/12` (2015).

[8] S. Garrison-Kimmel, A. Wetzel, P. F. Hopkins, R. Sanderson, K. El-Badry, A. Graus, T. K. Chan, R. Feldmann, M. Boylan-Kolchin, C. C. Hayward, J. S. Bullock, A. Fitts, J. Samuel, C. Wheeler, D. Kereš, and C. A. Faucher-Giguère, “Star formation histories of dwarf galaxies in the FIRE simulations: Dependence on mass and Local Group environment”, Monthly Notices of the Royal Astronomical Society **489**, 4574–4588 (2019).

[9] E. N. Kirby, J. G. Cohen, P. Guhathakurta, L. Cheng, J. S. Bullock, and A. Gallazzi, “The universal stellar mass-stellar metallicity relation for dwarf galaxies”, Astrophysical Journal **779**, `10.1088/0004-637X/779/2/102` (2013).

[10] R. Maiolino and F. Mannucci, “De re metallica: the cosmic chemical evolution of galaxies”, Astronomy and Astrophysics Review **27**, 1–187 (2019).

[11] R. Genzel, L. J. Tacconi, D. Lutz, A. Saintonge, S. Berta, B. Magnelli, F. Combes, S. García-Burillo, R. Neri, A. Bolatto, T. Contini, S. Lilly, J. Boissier, F. Boone, N. Bouché, F. Bournaud, A. Burkert, M. Carollo, L. Colina, M. C. Cooper, P. Cox, C. Feruglio, N. M. Förster Schreiber, J. Freundlich, J. Gracia-Carpio, S. Juneau, K. Kovac, M. Lippa, T. Naab, P. Salome, A. Renzini, A. Sternberg, F. Walter, B. Weiner, A. Weiss, and S. Wuyts, “Combined CO and dust scaling relations of depletion time and molecular gas fractions with cosmic time, specific star-formation rate, and stellar mass”, Astrophysical Journal **800**, `10.1088/0004-637X/800/1/20` (2015).

[12] M. M. Briel, J. J. Eldridge, E. R. Stanway, H. F. Stevance, and A. A. Chrimes, “Estimating transient rates from cosmological simulations and BPASS”, Monthly Notices of the Royal Astronomical Society **514**, 1315–1334 (2022).

[13] N. Langer and C. A. Norman, “On the collapsar model of long gamma-ray bursts:constraints from cosmic metallicity evolution”, The Astrophysical Journal **638**, L63–L66 (2006).

[14] E. O’Connor and C. D. Ott, “Black hole formation in failing core-collapse supernovae”, Astrophysical Journal **730**, `10.1088/0004-637X/730/2/70` (2011).

[15] T. Sukhbold, T. Ertl, S. E. Woosley, J. M. Brown, and H.-T. Janka, “Core-Collapse Supernovae From 9 To 120 Solar Masses Based on Neutrino-Powered Explosions”, The Astrophysical Journal **821**, 38 (2016).

[16] Https://sne.space/, *Sne.space catalog.*

[17] Https://ned.ipac.caltech.edu/, *NED.*

[18] Http://leda.univ-lyon1.fr/, *HyperLEDA.*

[19] *Https://ui.adsabs.harvard.edu/.*

[20] *Https://www.wis-tns.org/.*

[21] E. A. Corbett, L. Kewley, P. N. Appleton, V. Charmandaris, M. A. Dopita, C. A. Heisler, R. P. Norris, A. Zezas, and A. Marston, “The American Astronomical Society. All rights reserved. Printed in U.S.A.”, **10**, 670–688 (2003).

[22] N. Gehrels, "Errors Calculation", The Astrophysical Journal **303**, 336–346 (1986).

[23] M. Riello and F. Patat, "Extinction correction for Type Ia supernova rates - I. The model", mnras **362**, 671–680 (2005).

[24] D. Richardson, R. L. J. III, J. Wright, and L. Maddox, "ABSOLUTE-MAGNITUDE DISTRIBUTIONS OF SUPERNOVAE", The Astronomical Journal **147**, 118 (2014).

[25] Jason A. Cardelli, Geoffrey C. Clayton and J. S. Mathis, "THE RELATIONSHIP BETWEEN INFRARED, OPTICAL, AND ULTRAVIOLET EXTINCTION", The Astrophysical Journal **345**, 245–256 (1989).

[26] P. Madau, M. Della Valle, and N. Panagia, "On the evolution of the cosmic supernova rates", Monthly Notices of the Royal Astronomical Society **297**, 1–6 (1998).

[27] T. Dahlen, L. G. Strolger, A. G. Riess, S. Mattila, E. Kankare, and B. Mobasher, "The extended hubble space telescope supernova survey: The rate of core collapse supernovae to z $\sim$ 1", Astrophysical Journal **757**, `10.1088/0004-637X/757/1/70` (2012).

[28] M. T. Botticella, S. J. Smartt, R. C. Kennicutt, E. Cappellaro, M. Sereno, and J. C. Lee, "A comparison between SFR diagnostics and CC SN rate within 11 Mpc.", Memorie della Societa Astronomica Italiana - Journal of the Italian Astronomical Society **19**, 158–165 (2012).

[29] M. S. Bothwell, R. C. Kenicutt, B. D. Johnson, Y. Wu, J. C. Lee, D. Dale, C. Engelbracht, D. Calzetti, and E. Skillman, "The star formation rate distribution function of the local Universe", Monthly Notices of the Royal Astronomical Society **415**, 1815–1826 (2011).

[30] S. Horiuchi, J. F. Beacom, C. S. Kochanek, J. L. Prieto, K. Z. Stanek, and T. A. Thompson, "The cosmic core-collapse supernova rate does not match the massive-star formation rate", Astrophysical Journal **738**, `10.1088/0004-637X/738/2/154` (2011).

[31] A. Heger, C. L. Fryer, S. E. Woosley, N. Langer, and D. H. Hartmann, "How Massive Single Stars End Their Life", The Astrophysical Journal **591**, 288–300 (2003).

[32] L. G. Strolger, T. Dahlen, S. A. Rodney, O. Graur, A. G. Riess, C. McCully, S. Ravindranath, B. Mobasher, and A. K. Shahady, "THE RATE of CORE COLLAPSE SUPERNOVAE to REDSHIFT 2.5 from the CANDELS and CLASH SUPERNOVA SURVEYS", Astrophysical Journal **813**, 93 (2015).

[33] L. Tomasella, E. Cappellaro, M. L. Pumo, A. Jerkstrand, S. Benetti, N. Elias-Rosa, M. Fraser, C. Inserra, A. Pastorello, M. Turatto, J. P. Anderson, L. Galbany, C. P. Gutiérrez, E. Kankare, G. Pignata, G. Terreran, S. Valenti, C. Barbarino, F. E. Bauer, M. T. Botticella, T. .-. Chen, A. Gal-Yam, A. Harutyunyan, D. A. Howell, K. Maguire, A. Morales Garoffolo, P. Ochner, S. J. Smartt, S. Schulze, D. R. Young, and L. Zampieri, "SNe 2013K and 2013am: observed and physical properties of two slow, normal Type IIP events", Monthly Notices of the RAS **475**, 1937–1959 (2018).

[34] K. Gill, G. Hosseinzadeh, E. Berger, M. Zanolin, and M. Szczepańczyk, "Constraining the Time of Gravitational-wave Emission from Core-collapse Supernovae", Astrophysical Journal **931**, 159, 159 (2022).

[35] W. V. Jacobson-Galán, P. Venkatraman, R. Margutti, D. Khatami, G. Terreran, R. J. Foley, R. Angulo, C. R. Angus, K. Auchettl, P. K. Blanchard, A. Bobrick, J. S. Bright, D. Brout, K. C. Chambers, C. D. Couch, D. A. Coulter, K. Clever, K. W. Davis, T. J. L. de Boer, L. DeMarchi, S. A. Dodd, D. O. Jones, J. Johnson, C. D. Kilpatrick, N. Khetan, Z. Lai, D. Langeroodi, C. .-. Lin, E. A. Magnier, D. Milisavljevic, H. B. Perets, J. D. R. Pierel, J. Raymond, S. Rest, A. Rest, R. Ridden-Harper, K. J. Shen, M. R. Siebert, C. Smith, K. Taggart, S. Tinyanont, F. Valdes, V. A. Villar, Q. Wang, S. K. Yadavalli, Y. Zenati, and A. Zenteno, "The Circumstellar Environments of Double-peaked, Calcium-strong Transients 2021gno and 2021inl", Astrophysical Journal **932**, 58, 58 (2022).

[36] J. L. Tonry, A. Dressler, J. P. Blakeslee, E. A. Ajhar, A. B. Fletcher, G. A. Luppino, M. R. Metzger, and C. B. Moore, "The SBF Survey of Galaxy Distances. IV. SBF Magnitudes, Colors, and Distances", Astrophysical Journal **546**, 681–693 (2001).

[37] S. D. Van Dyk, W. Li, and A. V. Filippenko, "A Search for Core-Collapse Supernova Progenitors in Hubble Space Telescope Images", Publications of the Astronomical Society of the Pacific **115**, 1–20 (2003).

[38] W. L. Freedman, B. F. Madore, B. K. Gibson, L. Ferrarese, D. D. Kelson, S. Sakai, J. R. Mould, J. Kennicutt Robert C., H. C. Ford, J. A. Graham, J. P. Huchra, S. M. G. Hughes, G. D. Illingworth, L. M. Macri, and P. B. Stetson, "Final Results from the Hubble Space Telescope Key Project to Measure the Hubble Constant", Astrophysical Journal **553**, 47–72 (2001).

[39] J. N. Terry, G. Paturel, and T. Ekholm, "Local velocity field from sosie galaxies. I. The Peebles' model", Astronomy and Astrophysics **393**, 57–68 (2002).

[40] J. M. Silverman, P. Mazzali, R. Chornock, A. V. Filippenko, A. Clocchiatti, M. M. Phillips, M. Ganeshalingam, and R. J. Foley, "Optical Spectroscopy of the Somewhat Peculiar Type IIb Supernova 2001ig", Publications of the Astronomical Society of the Pacific **121**, 689 (2009).

[41] I. S. Jang and M. G. Lee, "The Tip of the Red Giant Branch Distance to the Perfect Spiral Galaxy M74 Hosting Three Core-collapse Supernovae", Astrophysical Journal **792**, 52, 52 (2014).

[42] M. Takada-Hidai, W. Aoki, and G. Zhao, "Na I D Lines in the SN 2002ap Spectrum *", Publications of the Astronomical Society of Japan **54**, 899–903 (2002).

[43] D. M. Szczygieł, C. S. Kochanek, and X. Dai, "SN 2002bu—Another SN 2008S-like Transient", Astrophysical Journal **760**, 20, 20 (2012).

[44] S. Bose and B. Kumar, "Distance Determination to Eight Galaxies Using Expanding Photosphere Method", Astrophysical Journal **782**, 98, 98 (2014).

[45] P. Meikle, S. Mattila, S. Smartt, E. MacDonald, L. Clewley, and G. Dalton, "Supernova 2002hh in NGC 6946", IAU Cirulars **8024**, 1 (2002).

[46] J. M. Silverman, R. J. Foley, A. V. Filippenko, M. Ganeshalingam, A. J. Barth, R. Chornock, C. V. Griffith, J. J. Kong, N. Lee, D. C. Leonard, T. Matheson, E. G. Miller, T. N. Steele, B. J. Barris, J. S. Bloom, B. E. Cobb, A. L. Coil, L.-B. Desroches, E. L. Gates, L. C. Ho, S. W. Jha, M. T. Kandrashoff, W. Li, K. S. Mandel, M. Modjaz, M. R. Moore, R. E. Mostardi, M. S. Papenkova, S. Park, D. A. Perley, D. Poznanski, C. A. Reuter, J. Scala, F. J. D. Serduke, J. C. Shields, B. J. Swift, J. L. Tonry, S. D. Van Dyk, X. Wang, and D. S. Wong, "Berkeley Supernova Ia Program - I. Observations, data reduction and spectroscopic sample of 582 low-redshift Type Ia supernovae", Monthly Notices of the RAS **425**, 1789–1818 (2012).

[47] M. Hamuy, J. Deng, P. A. Mazzali, N. I. Morrell, M. M. Phillips, M. Roth, S. Gonzalez, J. Thomas-Osip, W. Krzeminski, C. Contreras, J. Maza, L. González, L. Huerta, G. Folatelli, R. Chornock, A. V. Filippenko, S. E. Persson, W. L. Freedman, K. Koviak, N. B. Suntzeff, and K. Krisciunas, "Supernova 2003bg: The First Type IIb Hypernova", Astrophysical Journal **703**, 1612–1623 (2009).

[48] S. J. Smartt, J. J. Eldridge, R. M. Crockett, and J. R. Maund, "The death of massive stars - I. Observational constraints on the progenitors of Type II-P supernovae", Monthly Notices of the RAS **395**, 1409–1437 (2009).

[49] M. I. Jones, M. Hamuy, P. Lira, J. Maza, A. Clocchiatti, M. Phillips, N. Morrell, M. Roth, N. B. Suntzeff, T. Matheson, A. V. Filippenko, R. J. Foley, and D. C. Leonard, "Distance Determination to 12 Type II Supernovae Using the Expanding Photosphere Method", Astrophysical Journal **696**, 1176–1194 (2009).

[50] K. S. Mandel, W. M. Wood-Vasey, A. S. Friedman, and R. P. Kirshner, "Type Ia Supernova Light-Curve Inference: Hierarchical Bayesian Analysis in the Near-Infrared", Astrophysical Journal **704**, 629–651 (2009).

[51] M. C. Bersten and M. Hamuy, "Bolometric Light Curves for 33 Type II Plateau Supernovae", Astrophysical Journal **701**, 200–208 (2009).

[52] N. Elias-Rosa, "The progenitors of stripped-envelope supernovae", edited by J. C. Guirado, L. M. Lara, V. Quilis, and J. Gorgas, 649–649 (2013).

[53] L. Martinez and M. C. Bersten, “Mass discrepancy analysis for a select sample of Type II-Plateau supernovae”, Astronomy and Astrophysics **629**, A124, A124 (2019).

[54] R. J. Foley, O. D. Fox, C. McCully, M. M. Phillips, D. J. Sand, W. Zheng, P. Challis, A. V. Filippenko, G. Folatelli, W. Hillebrandt, E. Y. Hsiao, S. W. Jha, R. P. Kirshner, M. Kromer, G. H. Marion, M. Nelson, R. Pakmor, G. Pignata, F. K. Röpke, I. R. Seitenzahl, J. M. Silverman, M. Skrutskie, and M. D. Stritzinger, “Extensive HST ultraviolet spectra and multiwavelength observations of SN 2014J in M82 indicate reddening and circumstellar scattering by typical dust”, Monthly Notices of the RAS **443**, 2887–2906 (2014).

[55] S. Mattila, M. Fraser, S. J. Smartt, W. P. S. Meikle, C. Romero-Cañizales, R. M. Crockett, and A. Stephens, “Supernovae and radio transients in M82”, Monthly Notices of the RAS **431**, 2050–2062 (2013).

[56] W. L. Freedman, B. F. Madore, B. K. Gibson, L. Ferrarese, D. D. Kelson, S. Sakai, J. R. Mould, J. Kennicutt Robert C., H. C. Ford, J. A. Graham, J. P. Huchra, S. M. G. Hughes, G. D. Illingworth, L. M. Macri, and P. B. Stetson, “Final Results from the Hubble Space Telescope Key Project to Measure the Hubble Constant”, Astrophysical Journal **553**, 47–72 (2001).

[57] S. M. Kanbur, C. Ngeow, S. Nikolaev, N. R. Tanvir, and M. A. Hendry, “The extra-galactic Cepheid distance scale from LMC and Galactic period-luminosity relations”, Astronomy and Astrophysics **411**, 361–379 (2003).

[58] B. A. Jacobs, L. Rizzi, R. B. Tully, E. J. Shaya, D. I. Makarov, and L. Makarova, “The Extragalactic Distance Database: Color-Magnitude Diagrams”, Astronomical Journal **138**, 332–337 (2009).

[59] A. Pereyra, A. M. Magalhães, C. V. Rodrigues, C. R. Silva, R. Campos, G. Hickel, and D. Cieslinski, “Optical polarimetric monitoring of the type II-plateau SN 2005af”, Astronomy and Astrophysics **454**, 827–831 (2006).

[60] E. Kankare, M. Fraser, S. Ryder, C. Romero-Cañizales, S. Mattila, R. Kotak, P. Laursen, L. A. G. Monard, M. Salvo, and P. Väisänen, “SN 2005at - A neglected type Ic supernova at 10 Mpc”, Astronomy and Astrophysics **572**, A75, A75 (2014).

[61] D. Y. Tsvetkov, A. A. Volnova, A. P. Shulga, S. A. Korotkiy, A. Elmhamdi, I. J. Danziger, and M. V. Ereshko, “Observations and analysis of two type IIP supernovae: the intrinsically faint object SN 2005cs and the ambiguous object SN 2005ay”, Astronomy and Astrophysics **460**, 769–776 (2006).

[62] J. B. Jensen, J. L. Tonry, B. J. Barris, R. I. Thompson, M. C. Liu, M. J. Rieke, E. A. Ajhar, and J. P. Blakeslee, “Measuring Distances and Probing the Unresolved Stellar Populations of Galaxies Using Infrared Surface Brightness Fluctuations”, Astrophysical Journal **583**, 712–726 (2003).

[63] S. Spiro, A. Pastorello, M. L. Pumo, L. Zampieri, M. Turatto, S. J. Smartt, S. Benetti, E. Cappellaro, S. Valenti, I. Agnoletto, G. Altavilla, T. Aoki, E. Brocato, E. M. Corsini, A. Di Cianno, N. Elias-Rosa, M. Hamuy, K. Enya, M. Fiaschi, G. Folatelli, S. Desidera, A. Harutyunyan, D. A. Howell, A. Kawka, Y. Kobayashi, B. Leibundgut, T. Minezaki, H. Navasardyan, K. Nomoto, S. Mattila, A. Pietrinferni, G. Pignata, G. Raimondo, M. Salvo, B. P. Schmidt, J. Sollerman, J. Spyromilio, S. Taubenberger, G. Valentini, S. Vennes, and Y. Yoshii, “Low luminosity Type II supernovae - II. Pointing towards moderate mass precursors”, Monthly Notices of the RAS **439**, 2873–2892 (2014).

[64] D. J. Hunter, S. Valenti, R. Kotak, W. P. S. Meikle, S. Taubenberger, A. Pastorello, S. Benetti, V. Stanishev, S. J. Smartt, C. Trundle, A. A. Arkharov, F. Bufano, E. Cappellaro, E. Di Carlo, M. Dolci, N. Elias-Rosa, S. Frandsen, J. U. Fynbo, U. Hopp, V. M. Larionov, P. Laursen, P. Mazzali, H. Navasardyan, C. Ries, A. Riffeser, L. Rizzi, D. Y. Tsvetkov, M. Turatto, and S. Wilke, “Extensive optical and near-infrared observations of the nearby, narrow-lined type Ic SN 2007gr: days 5 to 415”, Astronomy and Astrophysics **508**, 371–389 (2009).

[65] J. E. Andrews, B. E. K. Sugerman, G. C. Clayton, J. S. Gallagher, M. J. Barlow, J. Clem, B. Ercolano, J. Fabbri, M. Meixner, M. Otsuka, D. L. Welch, and R. Wesson, “Photometric and Spectroscopic Evolution of the IIP SN 2007it to Day 944”, Astrophysical Journal **731**, 47, 47 (2011).

[66] R. Chornock, A. V. Filippenko, W. Li, G. H. Marion, R. J. Foley, M. Modjaz, M. Rafelski, G. D. Becker, W. H. de Vries, P. Garnavich, R. A. Jorgenson, D. K. Lynch, A. L. Malec, E. C. Moran, M. T. Murphy, R. J. Rudy, R. W. Russell, J. M. Silverman, T. N. Steele, A. Stockton, A. M. Wolfe, and C. E. Woodward, "The Transitional Stripped-envelope SN 2008ax: Spectral Evolution and Evidence for Large Asphericity", Astrophysical Journal **739**, 41, 41 (2011).

[67] S. D. Van Dyk, T. J. Davidge, N. Elias-Rosa, S. Taubenberger, W. Li, E. M. Levesque, S. Howerton, G. Pignata, N. Morrell, M. Hamuy, and A. V. Filippenko, "Supernova 2008bk and Its Red Supergiant Progenitor", Astronomical Journal **143**, 19, 19 (2012).

[68] R. Amanullah, C. Lidman, D. Rubin, G. Aldering, P. Astier, K. Barbary, M. S. Burns, A. Conley, K. S. Dawson, S. E. Deustua, M. Doi, S. Fabbro, L. Faccioli, H. K. Fakhouri, G. Folatelli, A. S. Fruchter, H. Furusawa, G. Garavini, G. Goldhaber, A. Goobar, D. E. Groom, I. Hook, D. A. Howell, N. Kashikawa, A. G. Kim, R. A. Knop, M. Kowalski, E. Linder, J. Meyers, T. Morokuma, S. Nobili, J. Nordin, P. E. Nugent, L. Östman, R. Pain, N. Panagia, S. Perlmutter, J. Raux, P. Ruiz-Lapuente, A. L. Spadafora, M. Strovink, N. Suzuki, L. Wang, W. M. Wood-Vasey, N. Yasuda, and T. Supernova Cosmology Project, "Spectra and Hubble Space Telescope Light Curves of Six Type Ia Supernovae at $0.511 < z < 1.12$ and the Union2 Compilation", Astrophysical Journal **716**, 712–738 (2010).

[69] J. L. Prieto, J. C. Lee, A. J. Drake, R. McNaught, G. Garradd, J. F. Beacom, E. Beshore, M. Catelan, S. G. Djorgovski, G. Pojmanski, K. Z. Stanek, and D. M. Szczygieł, "SN 2008jb: A "Lost" Core-collapse Supernova in a Star-forming Dwarf Galaxy at ~10 Mpc", Astrophysical Journal **745**, 70, 70 (2012).

[70] K. Takáts, M. L. Pumo, N. Elias-Rosa, A. Pastorello, G. Pignata, E. Paillas, L. Zampieri, J. P. Anderson, J. Vinkó, S. Benetti, M. .-. Botticella, F. Bufano, A. Campillay, R. Cartier, M. Ergon, G. Folatelli, R. J. Foley, F. Förster, M. Hamuy, V. .-. Hentunen, E. Kankare, G. Leloudas, N. Morrell, M. Nissinen, M. M. Phillips, S. J. Smartt, M. Stritzinger, S. Taubenberger, S. Valenti, S. D. Van Dyk, J. B. Haislip, A. P. LaCluyze, J. P. Moore, and D. Reichart, "SN 2009N: linking normal and subluminous Type II-P SNe", Monthly Notices of the RAS **438**, 368–387 (2014).

[71] C. Inserra, M. Turatto, A. Pastorello, M. L. Pumo, E. Baron, S. Benetti, E. Cappellaro, S. Taubenberger, F. Bufano, N. Elias-Rosa, L. Zampieri, A. Harutyunyan, A. S. Moskvitin, M. Nissinen, V. Stanishev, D. Y. Tsvetkov, V. P. Hentunen, V. N. Komarova, N. N. Pavlyuk, V. V. Sokolov, and T. N. Sokolova, "The bright Type IIP SN 2009bw, showing signs of interaction", Monthly Notices of the RAS **422**, 1122–1139 (2012).

[72] C. Inserra, A. Pastorello, M. Turatto, M. L. Pumo, S. Benetti, E. Cappellaro, M. T. Botticella, F. Bufano, N. Elias-Rosa, A. Harutyunyan, S. Taubenberger, S. Valenti, and L. Zampieri, "Moderately luminous Type II supernovae", Astronomy and Astrophysics **555**, A142, A142 (2013).

[73] N. Elias-Rosa, S. D. Van Dyk, W. Li, J. M. Silverman, R. J. Foley, M. Ganeshalingam, J. C. Mauerhan, E. Kankare, S. Jha, A. V. Filippenko, J. E. Beckman, E. Berger, J.-C. Cuillandre, and N. Smith, "The Massive Progenitor of the Possible Type II-Linear Supernova 2009hd in Messier 66", Astrophysical Journal **742**, 6, 6 (2011).

[74] R. G. Eastman, B. P. Schmidt, and R. Kirshner, "The Atmospheres of Type II Supernovae and the Expanding Photosphere Method", Astrophysical Journal **466**, 911 (1996).

[75] K. Takáts, G. Pignata, M. L. Pumo, E. Paillas, L. Zampieri, N. Elias-Rosa, S. Benetti, F. Bufano, E. Cappellaro, M. Ergon, M. Fraser, M. Hamuy, C. Inserra, E. Kankare, S. J. Smartt, M. D. Stritzinger, S. D. Van Dyk, J. B. Haislip, A. P. LaCluyze, J. P. Moore, and D. Reichart, "SN 2009ib: a Type II-P supernova with an unusually long plateau", Monthly Notices of the RAS **450**, 3137–3154 (2015).

[76] P. Gandhi, M. Yamanaka, M. Tanaka, T. Nozawa, K. S. Kawabata, I. Saviane, K. Maeda, T. J. Moriya, T. Hattori, M. Sasada, and R. Itoh, "SN 2009js at the Crossroads between Normal and Subluminous Type IIP Supernovae: Optical and Mid-infrared Evolution", Astrophysical Journal **767**, 166, 166 (2013).

[77] I. Arcavi, A. Gal-Yam, O. Yaron, A. Sternberg, I. Rabinak, E. Waxman, M. M. Kasliwal, R. M. Quimby, E. O. Ofek, A. Horesh, S. R. Kulkarni, A. V. Filippenko, J. M. Silverman, S. B. Cenko, W. Li, J. S. Bloom, M. Sullivan, P. E. Nugent, D. Poznanski, E. Gorbikov, B. J. Fulton, D. A. Howell, D. Bersier, A. Riou, S. Lamotte-Bailey, T. Griga, J. G. Cohen, S. Hachinger, D. Polishook, D. Xu, S. Ben-Ami, I. Manulis, E. S. Walker, K. Maguire, Y.-C. Pan, T. Matheson, P. A. Mazzali, E. Pian, D. B. Fox, N. Gehrels, N. Law, P. James, J. M. Marchant, R. J. Smith, C. J. Mottram, R. M. Barnsley, M. T. Kandrashoff, and K. I. Clubb, "SN 2011dh: Discovery of a Type IIb Supernova from a Compact Progenitor in the Nearby Galaxy M51", Astrophysical Journal, Letters **742**, L18, L18 (2011).

[78] V. P. Utrobin and N. N. Chugai, "Parameters of type IIP SN 2012A and clumpiness effects", Astronomy and Astrophysics **575**, A100, A100 (2015).

[79] G. Theureau, M. O. Hanski, N. Coudreau, N. Hallet, and J. .-. Martin, "Kinematics of the Local Universe. XIII. 21-cm line measurements of 452 galaxies with the Nançay radiotelescope, JHK Tully-Fisher relation, and preliminary maps of the peculiar velocity field", Astronomy and Astrophysics **465**, 71–85 (2007).

[80] S. Bose, B. Kumar, F. Sutaria, B. Kumar, R. Roy, V. K. Bhatt, S. B. Pandey, H. C. Chandola, R. Sagar, K. Misra, and S. Chakraborti, "Supernova 2012aw - a high-energy clone of archetypal Type IIP SN 1999em", Monthly Notices of the RAS **433**, 1871–1891 (2013).

[81] J. L. Tonry, A. Dressler, J. P. Blakeslee, E. A. Ajhar, A. B. Fletcher, G. A. Luppino, M. R. Metzger, and C. B. Moore, "The SBF Survey of Galaxy Distances. IV. SBF Magnitudes, Colors, and Distances", Astrophysical Journal **546**, 681–693 (2001).

[82] A. Jerkstrand, S. J. Smartt, J. Sollerman, C. Inserra, M. Fraser, J. Spyromilio, C. Fransson, T. .-. Chen, C. Barbarino, M. Dall'Ora, M. T. Botticella, M. Della Valle, A. Gal-Yam, S. Valenti, K. Maguire, P. Mazzali, and L. Tomasella, "Supersolar Ni/Fe production in the Type IIP SN 2012ec", Monthly Notices of the RAS **448**, 2482–2494 (2015).

[83] S. A. Johnson, C. S. Kochanek, and S. M. Adams, "On the progenitor of the Type Ibc supernova 2012fh", Monthly Notices of the RAS **472**, 3115–3119 (2017).

[84] S. Bose, S. Valenti, K. Misra, M. L. Pumo, L. Zampieri, D. Sand, B. Kumar, A. Pastorello, F. Sutaria, T. J. Maccarone, B. Kumar, M. L. Graham, D. A. Howell, P. Ochner, H. C. Chandola, and S. B. Pandey, "SN 2013ab: a normal Type IIP supernova in NGC 5669", Monthly Notices of the RAS **450**, 2373–2392 (2015).

[85] S. A. Johnson, C. S. Kochanek, and S. M. Adams, "The quiescent progenitors of four Type II-P/L supernovae", Monthly Notices of the RAS **480**, 1696–1704 (2018).

[86] S. Valenti, D. A. Howell, M. D. Stritzinger, M. L. Graham, G. Hosseinzadeh, I. Arcavi, L. Bildsten, A. Jerkstrand, C. McCully, A. Pastorello, A. L. Piro, D. Sand, S. J. Smartt, G. Terreran, C. Baltay, S. Benetti, P. Brown, A. V. Filippenko, M. Fraser, D. Rabinowitz, M. Sullivan, and F. Yuan, "The diversity of Type II supernova versus the similarity in their progenitors", Monthly Notices of the RAS **459**, 3939–3962 (2016).

[87] T. Szalai, J. Vinkó, A. P. Nagy, J. M. Silverman, J. C. Wheeler, G. Dhungana, G. H. Marion, R. Kehoe, O. D. Fox, K. Sárneczky, G. Marschalkó, B. I. Bı'ró, T. Borkovits, T. Hegedüs, R. Szakáts, F. V. Ferrante, E. Bányai, G. Hodosán, J. Kelemen, and A. Pál, "The continuing story of SN IIb 2013df: new optical and IR observations and analysis", Monthly Notices of the RAS **460**, 1500–1518 (2016).

[88] I. Saviane, Y. Momany, G. S. Da Costa, R. M. Rich, and J. E. Hibbard, "A New Red Giant-based Distance Modulus of 13.3 Mpc to the Antennae Galaxies and Its Consequences", Astrophysical Journal **678**, 179–186 (2008).

[89] N. Elias-Rosa, A. Pastorello, J. R. Maund, K. Takats, M. Fraser, S. J. Smartt, S. Benetti, G. Pignata, D. Sand, and S. Valenti, "On the progenitor of the type IC SN 2013dk in the antennae galaxies.", Monthly Notices of the RAS **436**, L109–L113 (2013).

[90] A. Reguitti, A. Pastorello, G. Pignata, S. Benetti, E. Cappellaro, M. Turatto, C. Agliozzo, F. Bufano, N. I. Morrell, F. Olivares E., D. E. Reichart, J. B. Haislip, V. Kouprianov, S. J. Smartt, and S. Ciroi,

"Signatures of an eruptive phase before the explosion of the peculiar core-collapse SN 2013gc", Monthly Notices of the RAS **482**, 2750–2769 (2019).

[91]O. D. Fox, S. D. Van Dyk, B. F. Williams, M. Drout, E. Zapartas, N. Smith, D. Milisavljevic, J. E. Andrews, K. A. Bostroem, A. V. Filippenko, S. Gomez, P. L. Kelly, S. E. de Mink, J. Pierel, A. Rest, S. Ryder, N. Sravan, L. Strolger, Q. Wang, and K. E. Weil, "The Candidate Progenitor Companion Star of the Type Ib/c SN 2013ge", Astrophysical Journal, Letters **929**, L15, L15 (2022).

[92]S. M. Kanbur, C. Ngeow, S. Nikolaev, N. R. Tanvir, and M. A. Hendry, "The extra-galactic Cepheid distance scale from LMC and Galactic period-luminosity relations", Astronomy and Astrophysics **411**, 361–379 (2003).

[93]N.-C. Sun, J. R. Maund, and P. A. Crowther, "The changing-type SN 2014C may come from an 11-$M_\odot$ star stripped by binary interaction and violent eruption", Monthly Notices of the RAS **497**, 5118–5135 (2020).

[94]J. Polshaw, R. Kotak, K. C. Chambers, S. J. Smartt, S. Taubenberger, M. Kromer, E. E. E. Gall, W. Hillebrandt, M. Huber, K. W. Smith, and R. J. Wainscoat, "A supernova distance to the anchor galaxy NGC 4258", Astronomy and Astrophysics **580**, L15, L15 (2015).

[95]S. Jha, A. G. Riess, and R. P. Kirshner, "Improved Distances to Type Ia Supernovae with Multicolor Light-Curve Shapes: MLCS2k2", Astrophysical Journal **659**, 122–148 (2007).

[96]B. A. Jacobs, L. Rizzi, R. B. Tully, E. J. Shaya, D. I. Makarov, and L. Makarova, "The Extragalactic Distance Database: Color-Magnitude Diagrams", Astronomical Journal **138**, 332–337 (2009).

[97]F. Huang, X. .-. Wang, G. Hosseinzadeh, P. J. Brown, J. Mo, J. .-. Zhang, K. .-. Zhang, T. .-. Zhang, D. .-. Howell, I. Arcavi, C. McCully, S. Valenti, L. .-. Rui, H. Song, D. .-. Xiang, W. .-. Li, H. Lin, and L. .-. Wang, "SN 2016X: a type II-P supernova with a signature of shock breakout from explosion of a massive red supergiant", Monthly Notices of the RAS **475**, 3959–3973 (2018).

[98]L. Ferrarese, J. R. Mould, P. B. Stetson, J. L. Tonry, J. P. Blakeslee, and E. A. Ajhar, "The Discovery of Cepheids and a Distance to NGC 5128", Astrophysical Journal **654**, 186–218 (2007).

[99]D. P. K. Banerjee, V. Joshi, A. Evans, M. Srivastava, N. M. Ashok, R. D. Gehrz, M. S. Connelley, T. R. Geballe, J. Spyromilio, J. Rho, and R. Roy, "Early formation of carbon monoxide in the Centaurus A supernova SN 2016adj", Monthly Notices of the RAS **481**, 806–818 (2018).

[100]T. E. Müller-Bravo, C. P. Gutiérrez, M. Sullivan, A. Jerkstrand, J. P. Anderson, S. González-Gaitán, J. Sollerman, I. Arcavi, J. Burke, L. Galbany, A. Gal-Yam, M. Gromadzki, D. Hiramatsu, G. Hosseinzadeh, D. A. Howell, C. Inserra, E. Kankare, A. Kozyreva, C. McCully, M. Nicholl, S. Smartt, S. Valenti, and D. R. Young, "The low-luminosity Type II SN 2016aqf: a well-monitored spectral evolution of the Ni/Fe abundance ratio", Monthly Notices of the RAS **497**, 361–377 (2020).

[101]G. Hosseinzadeh, S. Valenti, C. McCully, D. A. Howell, I. Arcavi, A. Jerkstrand, D. Guevel, L. Tartaglia, L. Rui, J. Mo, X. Wang, F. Huang, H. Song, T. Zhang, and K. Itagaki, "Short-lived Circumstellar Interaction in the Low-luminosity Type IIP SN 2016bkv", Astrophysical Journal **861**, 63, 63 (2018).

[102]C. S. Kochanek, M. Fraser, S. M. Adams, T. Sukhbold, J. L. Prieto, T. Müller, G. Bock, J. S. Brown, S. Dong, T. W. .-. Holoien, R. Khan, B. J. Shappee, and K. Z. Stanek, "Supernova progenitors, their variability and the Type IIP Supernova ASASSN-16fq in M66", Monthly Notices of the RAS **467**, 3347–3360 (2017).

[103]N. A. Tikhonov, "Stellar content and distances to the isolated spiral galaxies NGC 6503 and NGC 6946", Astronomy Letters **40**, 537–550 (2014).

[104]S. D. Van Dyk, W. Zheng, T. G. Brink, A. V. Filippenko, D. Milisavljevic, J. E. Andrews, N. Smith, M. Cignoni, O. D. Fox, P. L. Kelly, A. Adamo, S. Yunus, K. Zhang, and S. Kumar, "SN 2017ein and the Possible First Identification of a Type Ic Supernova Progenitor", Astrophysical Journal **860**, 90, 90 (2018).

[105] J. E. Andrews, D. J. Sand, S. Valenti, N. Smith, R. Dastidar, D. K. Sahu, K. Misra, A. Singh, D. Hiramatsu, P. J. Brown, G. Hosseinzadeh, S. Wyatt, J. Vinko, G. C. Anupama, I. Arcavi, C. Ashall, S. Benetti, M. Berton, K. A. Bostroem, M. Bulla, J. Burke, S. Chen, L. Chomiuk, A. Cikota, E. Congiu, B. Cseh, S. Davis, N. Elias-Rosa, T. Faran, M. Fraser, L. Galbany, C. Gall, A. Gal-Yam, A. Gangopadhyay, M. Gromadzki, J. Haislip, D. A. Howell, E. Y. Hsiao, C. Inserra, E. Kankare, H. Kuncarayakti, V. Kouprianov, B. Kumar, X. Li, H. Lin, K. Maguire, P. Mazzali, C. McCully, P. Milne, J. Mo, N. Morrell, M. Nicholl, P. Ochner, F. Olivares, A. Pastorello, F. Patat, M. Phillips, G. Pignata, S. Prentice, A. Reguitti, D. E. Reichart, Ó. Rodrı’guez, L. Rui, P. Sanwal, K. Sárneczky, M. Shahbandeh, M. Singh, S. Smartt, J. Strader, M. D. Stritzinger, R. Szakáts, L. Tartaglia, H. Wang, L. Wang, X. Wang, J. C. Wheeler, D. Xiang, O. Yaron, D. R. Young, and J. Zhang, “SN 2017gmr: An Energetic Type II-P Supernova with Asymmetries”, Astrophysical Journal **885**, 43, 43 (2019).

[106] L. Bottinelli, L. Gouguenheim, G. Paturel, and P. Teerikorpi, “The Malmquist bias and the value of H zero from the Tully-Fisher relation.”, Astronomy and Astrophysics **156**, 157–171 (1986).

[107] D. O’Neill, R. Kotak, M. Fraser, S. A. Sim, S. Benetti, S. J. Smartt, S. Mattila, C. Ashall, E. Callis, N. Elias-Rosa, M. Gromadzki, and S. J. Prentice, “A progenitor candidate for the type II-P supernova SN 2018aoq in NGC 4151”, Astronomy and Astrophysics **622**, L1, L1 (2019).

[108] S. Tinyanont, M. Millar-Blanchaer, M. M. Kasliwal, D. Mawet, D. C. Leonard, M. Bulla, K. De, N. Jovanovic, M. Hankins, G. Vasisht, and E. Serabyn, “Infrared spectropolarimetric detection of intrinsic polarization from a core-collapse supernova”, Nature Astronomy **5**, 544–551 (2021).

[109] K. A. Bostroem, S. Valenti, D. J. Sand, J. E. Andrews, S. D. Van Dyk, L. Galbany, D. Pooley, R. C. Amaro, N. Smith, S. Yang, G. C. Anupama, I. Arcavi, E. Baron, P. J. Brown, J. Burke, R. Cartier, D. Hiramatsu, R. Dastidar, J. M. DerKacy, Y. Dong, E. Egami, S. Ertel, A. V. Filippenko, O. D. Fox, J. Haislip, G. Hosseinzadeh, D. A. Howell, A. Gangopadhyay, S. W. Jha, V. Kouprianov, B. Kumar, M. Lundquist, D. Milisavljevic, C. McCully, P. Milne, K. Misra, D. E. Reichart, D. K. Sahu, H. Sai, A. Singh, P. S. Smith, J. Vinko, X. Wang, Y. Wang, J. C. Wheeler, G. G. Williams, S. Wyatt, J. Zhang, and X. Zhang, “Discovery and Rapid Follow-up Observations of the Unusual Type II SN 2018ivc in NGC 1068”, Astrophysical Journal **895**, 31, 31 (2020).

[110] W. V. Jacobson-Galán, R. Margutti, C. D. Kilpatrick, D. Hiramatsu, H. Perets, D. Khatami, R. J. Foley, J. Raymond, S.-C. Yoon, A. Bobrick, Y. Zenati, L. Galbany, J. Andrews, P. J. Brown, R. Cartier, D. L. Coppejans, G. Dimitriadis, M. Dobson, A. Hajela, D. A. Howell, H. Kuncarayakti, D. Milisavljevic, M. Rahman, C. Rojas-Bravo, D. J. Sand, J. Shepherd, S. J. Smartt, H. Stacey, M. Stroh, J. J. Swift, G. Terreran, J. Vinko, X. Wang, J. P. Anderson, E. A. Baron, E. Berger, P. K. Blanchard, J. Burke, D. A. Coulter, L. DeMarchi, J. M. DerKacy, C. Fremling, S. Gomez, M. Gromadzki, G. Hosseinzadeh, D. Kasen, L. Kriskovics, C. McCully, T. E. Müller-Bravo, M. Nicholl, A. Ordasi, C. Pellegrino, A. L. Piro, A. Pál, J. Ren, A. Rest, R. M. Rich, H. Sai, K. Sárneczky, K. J. Shen, P. Short, M. R. Siebert, C. Stauffer, R. Szakáts, X. Zhang, J. Zhang, and K. Zhang, “SN 2019ehk: A Double-peaked Ca-rich Transient with Luminous X-Ray Emission and Shock-ionized Spectral Features”, Astrophysical Journal **898**, 166, 166 (2020).

[111] K. Gill, G. Hosseinzadeh, E. Berger, M. Zanolin, and M. Szczepańczyk, “Constraining the Time of Gravitational-wave Emission from Core-collapse Supernovae”, Astrophysical Journal **931**, 159, 159 (2022).

[112] C. D. Kilpatrick, M. R. Drout, K. Auchettl, G. Dimitriadis, R. J. Foley, D. O. Jones, L. DeMarchi, K. D. French, C. Gall, J. Hjorth, W. V. Jacobson-Galán, R. Margutti, A. L. Piro, E. Ramirez-Ruiz, A. Rest, and C. Rojas-Bravo, “A cool and inflated progenitor candidate for the Type Ib supernova 2019yvr at 2.6 yr before explosion”, Monthly Notices of the RAS **504**, 2073–2093 (2021).

[113] J. Rho, A. Evans, T. R. Geballe, D. P. K. Banerjee, P. Hoeflich, M. Shahbandeh, S. Valenti, S. .-. Yoon, H. Jin, M. Williamson, M. Modjaz, D. Hiramatsu, D. A. Howell, C. Pellegrino, J. Vinkó, R. Cartier, J. Burke, C. McCully, H. An, H. Cha, T. Pritchard, X. Wang, J. Andrews, L. Galbany, S. Van Dyk, M. L.

Graham, S. Blinnikov, V. Joshi, A. Pál, L. Kriskovics, A. Ordasi, R. Szakats, K. Vida, Z. Chen, X. Li, J. Zhang, and S. Yan, "Near-infrared and Optical Observations of Type Ic SN 2020oi and Broad-lined Type Ic SN 2020bvc: Carbon Monoxide, Dust, and High-velocity Supernova Ejecta", Astrophysical Journal **908**, 232, 232 (2021).

[114] A. G. Riess, L. M. Macri, S. L. Hoffmann, D. Scolnic, S. Casertano, A. V. Filippenko, B. E. Tucker, M. J. Reid, D. O. Jones, J. M. Silverman, R. Chornock, P. Challis, W. Yuan, P. J. Brown, and R. J. Foley, "A 2.4% Determination of the Local Value of the Hubble Constant", Astrophysical Journal **826**, 56, 56 (2016).

[115] W. Jacobson-Galán, P. Venkatraman, R. Margutti, D. Khatami, G. Terreran, R. J. Foley, R. Angulo, C. R. Angus, K. Auchettl, P. K. Blanchard, A. Bobrick, J. S. Bright, C. D. Couch, D. A. Coulter, K. Clever, K. W. Davis, T. de Boer, L. DeMarchi, S. A. Dodd, D. O. Jones, J. Johnson, C. D. Kilpatrick, N. Khetan, Z. Lai, D. Langeroodi, C.-C. Lin, E. A. Magnier, D. Milisavljevic, H. B. Perets, J. D. R. Pierel, J. Raymond, S. Rest, A. Rest, R. Ridden-Harper, K. J. Shen, M. R. Siebert, C. Smith, K. Taggart, S. Tinyanont, F. Valdes, V. A. Villar, Q. Wang, S. Karthik Yadavalli, Y. Zenati, and A. Zenteno, "The Circumstellar Environments of Double-Peaked, Calcium-strong Supernovae 2021gno and 2021inl", arXiv e-prints, arXiv:2203.03785, arXiv:2203.03785 (2022).

[116] J. Ripero, D. Rodriquez, and F. Pujol, "Supernovae Studied by the M-1 Group in 2000", Journal of the American Association of Variable Star Observers **30**, 130–138 (2002).

[117] S. Nakano and M. Aoki, "Supernova 2000db in NGC 3949", IAU Cirulars **7475**, 1 (2000).

[118] J. R. Maund and S. J. Smartt, "Hubble Space Telescope imaging of the progenitor sites of six nearby core-collapse supernovae", Monthly Notices of the RAS **360**, 288–304 (2005).

[119] T. Puckett and G. Dowdle, "Supernova 2000ds in NGC 2768", IAU Cirulars **7507**, 2 (2000).

[120] T. Puckett, A. Langoussis, and G. J. Garradd, "Supernova 2000ew in NGC 3810", IAU Cirulars **7530**, 1 (2000).

[121] R. Chornock and A. V. Filippenko, "Supernova 2001B in IC 391", IAU Cirulars **7577**, 2 (2001).

[122] D. W. Xu and Y. L. Qiu, "Supernova 2001B in IC 391", IAU Cirulars **7555**, 2 (2001).

[123] A. Gal-Yam, O. Shemmer, and J. Dann, "Supernova 2001X in NGC 5921", IAU Cirulars **7602**, 2 (2001).

[124] W. Li, Y. Fan, Y. L. Qiu, J. Y. Hu, and M. Schwartz, "Supernova 2001X in NGC 5921", IAU Cirulars **7591**, 1 (2001).

[125] L. Wang, D. Baade, C. Fransson, P. Hoeflich, P. Lundqvist, and J. C. Wheeler, "Supernova 2001du in NGC 1365", IAU Cirulars **7704**, 2 (2001).

[126] R. Evans, G. Bock, P. Marples, G. J. Garradd, M. Salvo, B. Schmidt, M. Ashley, A. Phillips, C. Stubbs, P. Francis, and A. Hale, "Supernova 2001du in NGC 1365", IAU Cirulars **7690**, 1 (2001).

[127] T. Matheson, S. Jha, P. Challis, R. Kirshner, and P. Berlind, "Supernova 2001fv in NGC 3512", IAU Cirulars **7756**, 4 (2001).

[128] G. M. Hurst and M. Armstrong, "Supernova 2001fv in NGC 3512", IAU Cirulars **7750**, 1 (2001).

[129] T. Matheson, S. Jha, P. Challis, R. Kirshner, and K. Rines, "Supernova 2001fz in NGC 2280", IAU Cirulars **7759**, 2 (2001).

[130] Y. L. Qiu and J. Y. Hu, "Supernova 2001fz in NGC 2280", IAU Cirulars **7753**, 2 (2001).

[131] S. Nakano, K. Itagaki, Y. Kushida, R. Kushida, and A. Dimai, "Supernova 2001gd in NGC 5033", IAU Cirulars **7761**, 1 (2001).

[132] T. Matheson, S. Jha, P. Challis, R. Kirshner, and P. Berlind, "Supernova 2001gd in NGC 5033", IAU Cirulars **7765**, 2 (2001).

[133] T. Matheson, S. Jha, P. Challis, R. Kirshner, and E. Falco, "Supernova 2001hg in NGC 4162", IAU Cirulars **7770**, 3 (2001).

[134] T. Puckett and A. Sehgal, "Supernova 2001hg in NGC 4162", IAU Cirulars **7766**, 1 (2001).

[135] C. Bembrick, A. Pearce, and R. Evans, "Supernova 2001ig in NGC 7424", IAU Cirulars **7804**, 2 (2002).

[136] J. R. Maund, J. C. Wheeler, F. Patat, L. Wang, D. Baade, and P. A. Höflich, “Spectropolarimetry of the Type IIb Supernova 2001ig”, Astrophysical Journal **671**, 1944–1958 (2007).

[137] R. O. Evans, B. White, and C. Bembrick, “Supernova 2001ig in NGC 7424”, IAU Cirulars **7772**, 1 (2001).

[138] B. Swift and W. D. Li, “Supernovae 2002D, 2002E, 2002F, and 2002G”, IAU Cirulars **7797**, 1 (2002).

[139] T. Matheson, S. Jha, P. Challis, R. Kirshner, and P. Berlind, “Supernova 2002E in NGC 4129”, IAU Cirulars **7800**, 4 (2002).

[140] A. Gal-Yam, O. Shemmer, and J. Dann, “Supernova 2002ao in UGC 9299”, IAU Cirulars **7810**, 3 (2002).

[141] P. Martin, W. D. Li, Y. L. Qiu, and D. West, “Supernova 2002ao in UGC 9299”, IAU Cirulars **7809**, 3 (2002).

[142] L. M. Cook, E. V. Katkova, N. A. Sokolov, and I. S. Guseva, “BVRI photometry of the type Ic Hypernova SN 2002ap”, Information Bulletin on Variable Stars **5283**, 1 (2002).

[143] A. V. Filippenko and R. Chornock, “Supernovae 2002ao, 2002ap, 2002ar, 2002au, 2002av”, IAU Cirulars **7825**, 1 (2002).

[144] S. Nakano, Y. Hirose, R. Kushida, Y. Kushida, and W. Li, “Supernova 2002ap in M74”, IAU Cirulars **7810**, 1 (2002).

[145] N. Smith, W. Li, J. M. Silverman, M. Ganeshalingam, and A. V. Filippenko, “Luminous blue variable eruptions and related transients: diversity of progenitors and outburst properties”, Monthly Notices of the RAS **415**, 773–810 (2011).

[146] C. Ransome, “Transient Classification Report for 2021-08-24”, Transient Name Server Classification Report **2021-2919**, 1–2919 (2021).

[147] T. Puckett and S. Gauthier, “Supernova 2002bu in NGC 4242”, IAU Cirulars **7863**, 1 (2002).

[148] W. M. Wood-Vasey, G. Aldering, P. Nugent, B. Beutler, P. Martin, M. Papenkova, A. V. Filippenko, and M. Hamuy, “Supernovae 2002hb, 2002hc, 2002hd”, IAU Cirulars **7999**, 1 (2002).

[149] A. V. Filippenko, R. J. Foley, and B. Swift, “Supernovae 2002hf and 2002hh”, IAU Cirulars **8007**, 2 (2002).

[150] W. Li, “Supernova 2002hh in NGC 6946”, IAU Cirulars **8005**, 1 (2002).

[151] P. Ruiz-Lapuente, S. Benetti, A. Balastegui, S. Basa, D. Guide, J. Mendez, J. Raux, and M. Turatto, “Supernova 2002ji in NGC 3655”, IAU Cirulars **8028**, 3 (2002).

[152] Y. L. Qiu and J. Y. Hu, “Supernova 2002ji in NGC 3655”, IAU Cirulars **8025**, 1 (2002).

[153] T. Puckett, D. Tigner, and A. Sehgal, “Supernova 2002jz in UGC 2984”, IAU Cirulars **8037**, 1 (2002).

[154] M. Hamuy, M. Roth, and N. Morrell, “Supernova 2002jz in UGC 2984”, IAU Cirulars **8037**, 2 (2002).

[155] R. Evans and S. Quirk, “Supernova 2003B near NGC 1097”, IAU Cirulars **8042**, 1 (2003).

[156] A. V. Filippenko and R. Chornock, “Supernova 2003B near NGC 1097”, IAU Cirulars **8042**, 3 (2003).

[157] R. Kushida, S. Nakano, T. Puckett, J. Newton, A. Langoussis, T. Boles, M. Schwartz, B. Swift, W. Li, T. Kobayashi, and Y. Koshida, “Supernovae 2003J, 2003K, 2003L, 2003M”, IAU Cirulars **8048**, 1 (2003).

[158] K. Ayani, T. Hashimoto, and H. Yamaoka, “Supernovae 2003J, 2003K, 2003L, 2003M”, IAU Cirulars **8048**, 2 (2003).

[159] T. Matheson, P. Challis, R. Kirshner, and M. Calkins, “Supernovae 2003Y and 2003Z”, IAU Cirulars **8063**, 2 (2003).

[160] T. Boles, B. Beutler, W. Li, Y. L. Qiu, J. Y. Hu, and M. Schwartz, “Supernovae 2003X, 2003Y, and 2003Z”, IAU Cirulars **8062**, 1 (2003).

[161] A. V. Filippenko and R. Chornock, “Supernovae”, IAU Cirulars **8085**, 2 (2003).

[162] H. C. Ferguson, GOODS Treasury Team, Hubble Higher-Z Supernova Team, K. S. Lee, Lotoss, D. Weisz, and W. Li, “Supernovae 2003aj, 2003ak, 2003al, 2003am, and 2003an”, IAU Cirulars **8069**, 1 (2003).

[163] W. M. Wood-Vasey, G. Aldering, P. Nugent, and R. Chassagne, “Supernovae 2003bf and 2003bg”, IAU Cirulars **8082**, 1 (2003).

[164] A. M. Soderberg, S. R. Kulkarni, E. Berger, and D. A. Frail, “Supernova 2003bg in MCG -05-10-15”, IAU Cirulars **8087**, 2 (2003).

[165] M. Hamuy, M. Phillips, and J. Thomas-Osip, “Supernova 2003bg in MCG -05-10-15”, IAU Cirulars **8088**, 3 (2003).

[166] M. Phillips, M. Hamuy, M. Roth, and N. Morrell, “Supernovae 2003bj, 2003bk, 2003bl, and 2003bm”, IAU Cirulars **8086**, 2 (2003).

[167] B. Swift, D. Weisz, W. Li, and T. Boles, “Supernovae 2003bj, 2003bk, 2003bl, and 2003bm”, IAU Cirulars **8086**, 1 (2003).

[168] S. Nakano, R. Arbour, B. Swift, W. Li, Y. Kushida, and R. Kushida, “Supernovae 2003cg, 2003ch, and 2003ci”, IAU Cirulars **8097**, 1 (2003).

[169] M. Salvo, B. Schmidt, and J. Tonry, “Supernovae 2003bn, 2003bu, 2003cb, 2003ch, and 2003ci”, IAU Cirulars **8098**, 2 (2003).

[170] D. C. Leonard, R. Chornock, and A. V. Filippenko, “Supernova 2003ed in NGC 5303A”, IAU Cirulars **8144**, 2 (2003).

[171] S. Nakano, R. Kushida, Y. Kushida, and K. Kadota, “Supernova 2003ed in NGC 5303A”, Central Bureau Electronic Telegrams **14**, 1 (2003).

[172] R. Evans and R. H. McNaught, “Supernova 2003gd in M74”, IAU Cirulars **8150**, 2 (2003).

[173] S. J. Smartt, J. R. Maund, M. A. Hendry, and C. R. Benn, “Supernova 2003gd in M74”, IAU Cirulars **8152**, 4 (2003).

[174] R. Kotak, W. P. S. Meikle, S. J. Smartt, European Supernova Collaboration, and C. Benn, “Supernova 2003gd in M74”, IAU Cirulars **8152**, 1 (2003).

[175] A. V. Filippenko, R. J. Foley, and F. J. D. Serduke, “Supernovae 2003gv, gw, hc, he, hf, hi, hj, hk, hl, hm, 2003hp”, IAU Cirulars **8189**, 2 (2003).

[176] M. Moore, W. Li, and T. Boles, “Supernovae 2003hg, 2003hh, 2003hi, 2003hj, 2003hk, 2003hl”, IAU Cirulars **8184**, 2 (2003).

[177] R. Evans, G. Bock, K. Krisciunas, and J. Espinoza, “Supernova 2003hn in NGC 1448”, IAU Cirulars **8186**, 1 (2003).

[178] M. Salvo, M. Bessell, and B. Schmidt, “Supernova 2003hn in NGC 1448”, IAU Cirulars **8187**, 1 (2003).

[179] R. Arbour and T. Boles, “Supernova 2003ie in NGC 4051”, IAU Cirulars **8205**, 1 (2003).

[180] I. Arcavi, A. Gal-Yam, and S. G. Sergeev, “Supernova 2003ie Was Likely a Faint Type IIP Event”, Astronomical Journal **145**, 99, 99 (2013).

[181] T. Matheson, P. Challis, R. Kirshner, and P. Berlind, “Supernovae 2003io, 2003iq, and 2003is”, IAU Cirulars **8225**, 2 (2003).

[182] J. .-. Llapasset, H. Yamaoka, and K. Ayani, “Supernovae 2003hl and 2003iq in NGC 772.”, Central Bureau Electronic Telegrams **48**, 1 (2003).

[183] R. Martin and J. Biggs, “Supernova 2003jg in NGC 2997”, IAU Cirulars **8235**, 1 (2003).

[184] D. A. Howell, “Supernovae 2003jh and 2003jg”, IAU Cirulars **8241**, 2 (2003).

[185] D. Y. Tsvetkov, “Photometric Observations of Two Type II-P Supernovae: Normal SN II-P2004A and Unusual SN 2004ek”, Peremennye Zvezdy **28**, 3 (2008).

[186] H. Kawakita, K. Kinugasa, K. Ayani, and H. Yamaoka, “Supernova 2004A in NGC 6207”, IAU Cirulars **8266**, 2 (2004).

[187] S. Nakano, K. Itagaki, R. Kushida, and Y. Kushida, “Supernova 2004A in NGC 6207”, IAU Cirulars **8265**, 1 (2004).

[188] W. P. S. Meikle, S. Mattila, D. Carter, and R. J. Smith, “Supernova 2004C in NGC 3683”, IAU Cirulars **8270**, 2 (2004).

[189] C. C. Dudley and J. Fischer, “Supernova 2004C in NGC 3683”, Central Bureau Electronic Telegrams **57**, 1 (2004).

[190] N. Elias-Rosa, G. Pignata, S. Benetti, G. Blanc, A. Della Valle, A. Pastorello, G. Altavilla, H. Navasardyan, M. Turatto, L. Zampieri, E. Cappellaro, and F. Patat, “Supernova 2004G in NGC 5668”, IAU Cirulars **8273**, 2 (2004).

[191] S. Nakano, R. Kushida, Y. Kushida, and K. Itagaki, “Supernova 2004G in NGC 5668”, IAU Cirulars **8272**, 1 (2004).

[192] S. Mattila, W. P. S. Meikle, P. Groeningsson, R. Greimel, M. Schirmer, J. A. Acosta-Pulido, and W. Li, “Supernova 2004am in M82”, IAU Cirulars **8299**, 2 (2004).

[193] R. J. Beswick, T. W. B. Muxlow, M. K. Argo, and A. Pedlar, “Supernova 2004am in M82”, IAU Cirulars **8332**, 2 (2004).

[194] D. Singer, H. Pugh, and W. Li, “Supernovae 2004ak, 2004al, and 2004am”, IAU Cirulars **8297**, 2 (2004).

[195] T. Matheson, P. Challis, R. Kirshner, and P. Berlind, “Supernovae 2004an, 2004ao, and 2004at”, IAU Cirulars **8304**, 4 (2004).

[196] D. Singer and W. Li, “Supernovae 2004an and 2004ao”, IAU Cirulars **8299**, 1 (2004).

[197] R. J. Foley, D. S. Wong, M. Ganeshalingam, A. V. Filippenko, and R. Chornock, “Supernovae 2004bm, 2004bp, and 2004bq”, IAU Cirulars **8339**, 2 (2004).

[198] D. Singer and W. Li, “Supernova 2004bm in NGC 3437”, Central Bureau Electronic Telegrams **65**, 1 (2004).

[199] R. J. Foley, D. S. Wong, M. Moore, and A. V. Filippenko, “Supernovae 2004bu, 2004bw, 2004bz, 2004cb, and 2004cc”, IAU Cirulars **8353**, 3 (2004).

[200] L. A. G. Monard and W. Li, “Supernovae 2004bz, 2004ca, 2004cb, 2004cc”, IAU Cirulars **8350**, 2 (2004).

[201] A. Connolly, “Supernovae 2004cj-2004cq”, IAU Cirulars **8359**, 1 (2004).

[202] R. J. Foley, H. Pugh, and A. V. Filippenko, “Supernovae 2004by, 2004cz, and 2004dd”, IAU Cirulars **8374**, 2 (2004).

[203] C. Jacques and T. Napoleao, “Supernova 2004cz in ESO 407-G9”, IAU Cirulars **8368**, 1 (2004).

[204] N.-C. Sun, J. R. Maund, P. A. Crowther, X. Fang, and E. Zapartas, “Towards a better understanding of supernova environments: a study of SNe 2004dg and 2012P in NGC 5806 with HST and MUSE”, Monthly Notices of the RAS **504**, 2253–2272 (2021).

[205] A. Vagnozzi, D. de Pasquale, F. Guerri, G. Guerri, M. Cristofanelli, S. Romanelli, S. Valentini, H. Yamaoka, and K. Itagaki, “Supernova 2004dg”, IAU Cirulars **8375**, 1 (2004).

[206] J. Vinkó, K. Takáts, K. Sárneczky, G. M. Szabó, S. Mészáros, R. Csorvási, T. Szalai, A. Gáspár, A. Pál, S. Csizmadia, A. Kóspál, M. Rácz, M. Kun, B. Csák, G. Fürész, H. DeBond, J. Grunhut, J. Thomson, S. Mochnacki, and T. Koktay, “The first year of SN 2004dj in NGC 2403”, Monthly Notices of the RAS **369**, 1780–1796 (2006).

[207] F. Patat, S. Benetti, A. Pastorello, A. V. Filippenko, and J. Aceituno, “Supernova 2004dj in NGC 2403”, IAU Cirulars **8378**, 1 (2004).

[208] S. Nakano and K. Itagaki, “Supernova 2004dj in NGC 2403”, Central Bureau Electronic Telegrams **74**, 1 (2004).

[209] F. Patat, G. Pignata, S. Benetti, and J. Aceituno, “Supernova 2004dk in NGC 6118”, IAU Cirulars **8379**, 3 (2004).

[210] J. Graham and W. Li, “Supernova 2004dk in NGC 6118”, Central Bureau Electronic Telegrams **75**, 1 (2004).

[211] A. V. Filippenko, R. J. Foley, R. Chornock, and T. Matheson, “Supernovae 2004dx, 2004eh, 2004ep, 2004eq, 2004ev, 2004ex-2004ez”, IAU Cirulars **8420**, 2 (2004).

[212] M. Moore and W. Li, “Superbova 2004ep in IC 2152”, Central Bureau Electronic Telegrams **91**, 1 (2004).

[213] H. Yamaoka, K. Itagaki, A. Klotz, C. Pollas, and M. Boer, “Supernova 2004et in NGC 6946”, IAU Cirulars **8413**, 2 (2004).

[214] A. V. Filippenko, R. J. Foley, T. Treu, and M. A. Malkan, “Supernovae 2004es and 2004et”, IAU Cirulars **8414**, 1 (2004).

[215] T. Zwitter, U. Munari, and S. Moretti, “Supernova 2004et in NGC 6946”, Central Bureau Electronic Telegrams **95**, 1 (2004).

[216] M. Salvo, B. Schmidt, and S. Keller, “Supernova 2004fc in NGC 701”, IAU Cirulars **8432**, 2 (2004).

[217] K. Shimasaki, W. Li, H. Yamaoka, and K. Itagaki, “Supernovae 2004ex and 2004fc”, IAU Cirulars **8422**, 2 (2004).

[218] W. Li, H. Yamaoka, and K. Itagaki, “Supernova 2004gn in NGC 4527”, Central Bureau Electronic Telegrams **100**, 1 (2004).

[219] R. Barbon, V. Buondi, E. Cappellaro, and M. Turatto, "VizieR Online Data Catalog: Asiago Supernova Catalogue.", VizieR Online Data Catalog (2008).

[220] H. Pugh, W. Li, F. Manzini, and R. Behrend, "Supernovae 2004gq and 2004gr", IAU Cirulars **8452**, 2 (2004).

[221] M. Modjaz, R. Kirshner, P. Challis, and E. Falco, "Supernovae 2004gq and 2005A", IAU Cirulars **8461**, 3 (2005).

[222] F. J. D. Serduke, M. Ganeshalingam, B. J. Swift, and A. V. Filippenko, "Supernovae 2004gt and 2004gv", IAU Cirulars **8456**, 4 (2004).

[223] L. A. G. Monard, R. Quimby, C. Gerardy, P. Hoeflich, J. C. Wheeler, Y. .-. Chen, H. J. Smith, and A. Bauer, "Supernovae 2004gt, 2004gu, 2004gv", IAU Cirulars **8454**, 1 (2004).

[224] S. Taubenberger, A. Pastorello, S. Benetti, and J. Aceituno, "Supernova 2005V in NGC 2146", IAU Cirulars **8474**, 3 (2005).

[225] S. Mattila, R. Greimel, C. Gerardy, W. P. S. Meikle, L. A. G. Monard, T. Boles, H. Pugh, J. Graham, and W. Li, "Supernova 2005V in NGC 2146", IAU Cirulars **8474**, 1 (2005).

[226] N. Morrell, M. Hamuy, G. Folatelli, and F. Olivares, "Supernovae 2005Q, 2005S, 2005Y, 2005Z, 2005ad", IAU Cirulars **8482**, 2 (2005).

[227] S. Nakano and K. Itagaki, "Supernovae 2005ab and 2005ad", IAU Cirulars **8479**, 1 (2005).

[228] R. Martin, "Supernova 2005ae in ESO 209-9", IAU Cirulars **8480**, 1 (2005).

[229] A. V. Filippenko and R. J. Foley, "Supernovae 2004gw, 2005T, and 2005ae", IAU Cirulars **8486**, 3 (2005).

[230] A. Pearce and W. Souza, "Supernova 2005af in NGC 4945", IAU Cirulars **8487**, 6 (2005).

[231] A. V. Filippenko and R. J. Foley, "Supernova 2005af in NGC 4945", IAU Cirulars **8484**, 2 (2005).

[232] E. Kankare, M. Fraser, S. Ryder, C. Romero-Cañizales, S. Mattila, R. Kotak, P. Laursen, L. A. G. Monard, M. Salvo, and P. Väisänen, "SN 2005at - A neglected type Ic supernova at 10 Mpc", Astronomy and Astrophysics **572**, A75, A75 (2014).

[233] M. Salvo, B. Schmidt, L. Kiss, and A. Derekas, "Supernova 2005av in NGC 6943", IAU Cirulars **8501**, 4 (2005).

[234] L. A. G. Monard, "Supernova 2005av in NGC 6943", Central Bureau Electronic Telegrams **126**, 1 (2005).

[235] S. Taubenberger, S. Benetti, A. Harutyunyan, and A. Zurita, "Supernova 2005ay in NGC 3938", IAU Cirulars **8502**, 3 (2005).

[236] D. Rich, "Supernova 2005ay in NGC 3938", Central Bureau Electronic Telegrams **128**, 1 (2005).

[237] M. Modjaz, R. Kirshner, P. Challis, and R. Hutchins, "Supernova 2005cs in M51", IAU Cirulars **8555**, 1 (2005).

[238] M. Modjaz, R. Kirshner, P. Challis, and R. Hutchins, "Supernovae 2005cp and 2005cs", Central Bureau Electronic Telegrams **174**, 1 (2005).

[239] D. C. Leonard, "Supernova 2005cz in NGC 4589", IAU Cirulars **8579**, 2 (2005).

[240] A. Dimai, A. Sehgal, J. Newton, T. Puckett, K. Itagaki, S. Nakano, and D. George, "Supernovae 2005cx, 2005cy, 2005cz", IAU Cirulars **8569**, 1 (2005).

[241] S. Taubenberger, A. Pastorello, P. A. Mazzali, A. Witham, and A. Guijarro, "Supernova 2005kl in NGC 4369", Central Bureau Electronic Telegrams **305**, 1 (2005).

[242] A. Dimai and M. Migliardi, "Supernova 2005kl in NGC 4369", Central Bureau Electronic Telegrams **300**, 1 (2005).

[243] F. Patat, D. Baade, and L. Wang, "Supernova 2006bc in NGC 2397", Central Bureau Electronic Telegrams **450**, 1 (2006).

[244] R. Martin, "Supernova 2006bc in NGC 2397", Central Bureau Electronic Telegrams **446**, 1 (2006).

[245] R. Quimby, P. Brown, J. Caldwell, and S. Rostopchin, "Supernova 2006bp in NGC 3953", Central Bureau Electronic Telegrams **471**, 1 (2006).

[246] S. Nakano, "Supernova 2006bp in NGC 3953", Central Bureau Electronic Telegrams **470**, 1 (2006).

[247] K. Itagaki, S. Nakano, T. Puckett, R. Gorelli, R. R. Prasad, W. Li, D. Lane, G. Masi, and S. Foglia, "Supernovae 2006jc, 2006jd, 2006je", IAU Cirulars **8762**, 1 (2006).

[248] V. Stanishev and T. B. Nielsen, "Supernovae 2006my in NGC 4651", Central Bureau Electronic Telegrams **737**, 1 (2006).

[249] S. Nakano and K. Itagaki, "Supernova 2006my in NGC 4651", Central Bureau Electronic Telegrams **727**, 1 (2006).

[250] R. Chornock, A. V. Filippenko, W. Li, and J. M. Silverman, "Large Late-Time Asphericities in Three Type IIP Supernovae", Astrophysical Journal **713**, 1363–1375 (2010).

[251] S. Blondin, M. Modjaz, R. Kirshner, P. Challis, and P. Berlind, "Supernova 2006ov in M61", Central Bureau Electronic Telegrams **757**, 1 (2006).

[252] S. Nakano, K. Itagaki, and K. Kadota, "Supernova 2006ov in M61", Central Bureau Electronic Telegrams **756**, 1 (2006).

[253] T. Puckett, T. Orff, D. Madison, W. Li, K. Itagaki, S. Nakano, J. Newton, and K. Kadota, "Supernovae 2007A, 2007B, 2007C", IAU Cirulars **8792**, 2 (2007).

[254] S. Nakano, K. Itagaki, and K. Kadota, "Supernova 2007C in NGC 4981", Central Bureau Electronic Telegrams **798**, 1 (2007).

[255] G. Folatelli, N. Morrell, M. Phillips, and M. Hamuy, "Supernova 2007Y in NGC 1187", Central Bureau Electronic Telegrams **862**, 1 (2007).

[256] L. A. G. Monard, "Supernova 2007Y in NGC 1187", Central Bureau Electronic Telegrams **845**, 1 (2007).

[257] G. Folatelli, S. Gonzalez, and N. Morrell, "Supernova 2007aa in NGC 4030", Central Bureau Electronic Telegrams **850**, 1 (2007).

[258] T. Doi, S. Nakano, K. Itagaki, H. Naito, and R. Iizuka, "Supernova 2007aa in NGC 4030", Central Bureau Electronic Telegrams **848**, 1 (2007).

[259] A. Harutyunyan, I. Agnoletto, S. Benetti, M. Turatto, E. Cappellaro, and V. Lorenzi Telescopio Nazionale Galileo, "Supernova 2007av in NGC 3279", Central Bureau Electronic Telegrams **903**, 1 (2007).

[260] R. Arbour and D. Briggs, "Supernova 2007av in NGC 3279", Central Bureau Electronic Telegrams **901**, 1 (2007).

[261] R. Chornock, A. V. Filippenko, W. Li, R. J. Foley, D. Reitzel, and R. M. Rich, "Supernova 2007gr in NGC 1058", Central Bureau Electronic Telegrams **1036**, 1 (2007).

[262] D. Madison and W. Li, "Supernova 2007gr in NGC 1058", Central Bureau Electronic Telegrams **1034**, 1 (2007).

[263] C. Contreras, N. Morrell, S. Gonzalez, and K. .-. Lee, "Supernova 2007it in NGC 5530", Central Bureau Electronic Telegrams **1068**, 1 (2007).

[264] S. Blondin and M. Calkins, "Supernova 2007od in UGC 12846", Central Bureau Electronic Telegrams **1119**, 1 (2007).

[265] H. Mikuz and S. Maticic, "Supernova 2007od in UGC 12846", Central Bureau Electronic Telegrams **1116**, 1 (2007).

[266] M. T. Botticella, A. Pastorello, S. J. Smartt, W. P. S. Meikle, S. Benetti, R. Kotak, E. Cappellaro, R. M. Crockett, S. Mattila, M. Sereno, F. Patat, D. Tsvetkov, J. T. van Loon, D. Abraham, I. Agnoletto, R. Arbour, C. Benn, G. di Rico, N. Elias-Rosa, D. L. Gorshanov, A. Harutyunyan, D. Hunter, V. Lorenzi, F. P. Keenan, K. Maguire, J. Mendez, M. Mobberley, H. Navasardyan, C. Ries, V. Stanishev, S. Taubenberger, C. Trundle, M. Turatto, and I. M. Volkov, "SN 2008S: an electron-capture SN from a super-AGB progenitor?", Monthly Notices of the RAS **398**, 1041–1068 (2009).

[267] V. Stanishev, A. Pastorello, and T. Pursimo, "Supernova 2008S in NGC 6946", Central Bureau Electronic Telegrams **1235**, 1 (2008).

[268] R. Arbour and T. Boles, "Supernova 2008S in NGC 6946", Central Bureau Electronic Telegrams **1234**, 1 (2008).

[269] S. Taubenberger, H. Navasardyan, J. I. Maurer, L. Zampieri, N. N. Chugai, S. Benetti, I. Agnoletto, F. Bufano, N. Elias-Rosa, M. Turatto, F. Patat, E. Cappellaro, P. A. Mazzali, T. Iijima, S. Valenti, A. Harutyunyan, R. Claudi, and M. Dolci, "The He-rich stripped-envelope core-collapse supernova 2008ax", Monthly Notices of the RAS **413**, 2140–2156 (2011).

[270] A. Pastorello, M. M. Kasliwal, R. M. Crockett, S. Valenti, R. Arbour, K. Itagaki, S. Kaspi, A. Gal-Yam, S. J. Smartt, R. Griffith, K. Maguire, E. O. Ofek, N. Seymour, D. Stern, and W. Wiethoff, “The Type IIb SN 2008ax: spectral and light curve evolution”, Monthly Notices of the RAS **389**, 955–966 (2008).

[271] W. Li, “On the progenitor of SN 2008ax in NGC 4490”, The Astronomer’s Telegram **1417**, 1 (2008).

[272] N. Morrell and M. Stritzinger, “Supernovae 2008bk and 2008br”, Central Bureau Electronic Telegrams **1335**, 1 (2008).

[273] L. A. G. Monard, “Supernova 2008bk in NGC 7793”, Central Bureau Electronic Telegrams **1315**, 1 (2008).

[274] H. Navasardyan, S. Benetti, A. Harutyunyan, I. Agnoletto, F. Bufano, E. Cappellaro, and M. Turatto, “Supernova 2008bo in NGC 6643”, Central Bureau Electronic Telegrams **1325**, 1 (2008).

[275] M. Nissinen and A. Oksanen, “Supernova 2008bo in NGC 6643”, Central Bureau Electronic Telegrams **1324**, 1 (2008).

[276] J. Kajava, J. Fynbo, D. Della Monica Ferreira, M. Michalowski, T. Zafar, and J. Sollerman, “Supernova 2008fb in UGC 2813”, Central Bureau Electronic Telegrams **1479**, 2 (2008).

[277] D. W. E. Green, “Supernova 2008fb in UGC 2813”, Central Bureau Electronic Telegrams **1479**, 1 (2008).

[278] R. Roy, B. Kumar, A. S. Moskvitin, S. Benetti, T. A. Fatkhullin, B. Kumar, K. Misra, F. Bufano, R. Martin, V. V. Sokolov, S. B. Pandey, H. C. Chandola, and R. Sagar, “SN 2008gz - most likely a normal Type IIP event”, Monthly Notices of the RAS **414**, 167–183 (2011).

[279] S. Nakano and R. Martin, “Supernova 2008gz in NGC 3672”, Central Bureau Electronic Telegrams **1566**, 1 (2008).

[280] P. Challis, “Supernova 2008ij in NGC 6643”, Central Bureau Electronic Telegrams **1628**, 2 (2008).

[281] S. Nakano, K. Kadota, T. Kryachko, and S. Korotkiy, “Supernova 2008ij in NGC 6643”, Central Bureau Electronic Telegrams **1626**, 1 (2008).

[282] R. Roy, B. Kumar, S. Benetti, A. Pastorello, F. Yuan, P. J. Brown, S. Immler, T. A. Fatkhullin, A. S. Moskvitin, J. Maund, C. W. Akerlof, J. C. Wheeler, V. V. Sokolov, R. M. Quimby, F. Bufano, B. Kumar, K. Misra, S. B. Pandey, N. Elias-Rosa, P. W. A. Roming, and R. Sagar, “SN 2008in—Bridging the Gap between Normal and Faint Supernovae of Type IIP”, Astrophysical Journal **736**, 76, 76 (2011).

[283] M. Stritzinger, “Supernova 2008in in M61”, Central Bureau Electronic Telegrams **1638**, 3 (2008).

[284] S. Nakano, K. Kadota, and W. Wells, “Supernova 2008in in M61”, Central Bureau Electronic Telegrams **1636**, 1 (2008).

[285] A. Brunthaler, K. M. Menten, C. Henkel, M. J. Reid, G. C. Bower, H. Falcke, and D. W. E. Green, “Supernova 2008iz in M82”, Central Bureau Electronic Telegrams **1803**, 1 (2009).

[286] J. L. Prieto, A. J. Drake, R. McNaught, and G. Garradd, “Supernova 2008jb in ESO 302-14”, Central Bureau Electronic Telegrams **2771**, 1 (2011).

[287] M. Stritzinger, F. Forster, G. Folatelli, G. Pignata, and M. Hamuy, “Supernova 2009G in IC 4444.”, Central Bureau Electronic Telegrams **1664**, 1 (2009).

[288] G. Pignata, J. Maza, M. Hamuy, R. Antezana, L. Gonzalez, P. Gonzalez, P. Lopez, S. Silva, G. Folatelli, D. Iturra, R. Cartier, F. Forster, S. Marchi, B. Conuel, D. Reichart, K. Ivarsen, A. Crain, D. Foster, M. Nysewander, and A. Lacluyze, “Supernova 2009G in IC 4441”, Central Bureau Electronic Telegrams **1655**, 1 (2009).

[289] S. Benetti, S. Valenti, A. Magazzu, and A. Harutyunyan, “Supernova 2009H in NGC 1084”, Central Bureau Electronic Telegrams **1667**, 1 (2009).

[290] W. Li, S. B. Cenko, and A. V. Filippenko, “Supernova 2009H in NGC 1084”, Central Bureau Electronic Telegrams **1656**, 1 (2009).

[291] P. Challis and P. Berlind, “Supernova 2009N in NGC 4487”, Central Bureau Electronic Telegrams **1673**, 2 (2009).

[292] S. Nakano, K. Kadota, and L. Buzzi, “Supernova 2009N in NGC 4487”, Central Bureau Electronic Telegrams **1670**, 1 (2009).

[293] A. Harutyunyan, F. Bufano, and S. Benetti, "Supernova 2009at in NGC 5301", Central Bureau Electronic Telegrams **1722**, 1 (2009).

[294] S. Nakano, K. Kadota, Y. Ikari, and K. Itagaki, "Supernova 2009at in NGC 5301", Central Bureau Electronic Telegrams **1718**, 1 (2009).

[295] V. Stanishev, A. Adamo, and G. Micheva, "Supernova 2009bw in UGC 2890", Central Bureau Electronic Telegrams **1746**, 1 (2009).

[296] C. Jacques and E. Pimentel, "Supernova 2009bw in UGC 2890", Central Bureau Electronic Telegrams **1743**, 1 (2009).

[297] N. Elias-Rosa, S. D. van Dyk, I. Agnoletto, and S. Benetti, "Supernova 2009dd in NGC 4088", Central Bureau Electronic Telegrams **1765**, 1 (2009).

[298] G. Cortini and A. Dimai, "Supernova 2009dd in NGC 4088", Central Bureau Electronic Telegrams **1764**, 1 (2009).

[299] D. W. E. Green, "Supernovae 2009dp, 2009dq, 2009ds, and 2009dt", Central Bureau Electronic Telegrams **1789**, 5 (2009).

[300] G. Pignata, J. Maza, M. Hamuy, R. Antezana, L. Gonzalez, P. Gonzalez, P. Lopez, S. Silva, G. Folatelli, D. Iturra, R. Cartier, F. Forster, S. Marchi, A. Rojas, B. Conuel, D. Reichart, K. Ivarsen, A. Crain, D. Foster, M. Nysewander, and A. Lacluyze, "Supernova 2009dq in IC 2554", Central Bureau Electronic Telegrams **1781**, 1 (2009).

[301] D. W. E. Green, "Supernovae 2009el and 2009em", Central Bureau Electronic Telegrams **1807**, 2 (2009).

[302] L. A. G. Monard, "Supernova 2009em in NGC 157", Central Bureau Electronic Telegrams **1798**, 1 (2009).

[303] P. Marples, C. Drescher, S. Quirk, and G. Bock, "Supernova 2009gj in NGC 134", Central Bureau Electronic Telegrams **1856**, 1 (2009).

[304] R. J. Foley, "Supernova 2009gj in NGC 134", Central Bureau Electronic Telegrams **1858**, 1 (2009).

[305] L. A. G. Monard, "Supernova 2009hd in M66", Central Bureau Electronic Telegrams **1867**, 1 (2009).

[306] G. Pignata, J. Maza, M. Hamuy, R. Antezana, L. Gonzalez, P. Gonzalez, P. Lopez, S. Silva, G. Folatelli, D. Iturra, R. Cartier, F. Forster, S. Marchi, A. Rojas, B. Conuel, D. Reichart, K. Ivarsen, A. Crain, D. Foster, M. Nysewander, A. Lacluyze, and M. Stritzinger, "Supernova 2009ib in NGC 1559", Central Bureau Electronic Telegrams **1902**, 1 (2009).

[307] N. Smith and J. Mauerhan, "SN2009ip: New spectrum shows early phases of a luminous Type IIn supernova", The Astronomer's Telegram **4427**, 1 (2012).

[308] J. Maza, M. Hamuy, R. Antezana, L. Gonzalez, P. Lopez, S. Silva, G. Folatelli, D. Iturra, R. Cartier, F. Forster, S. Marchi, A. Rojas, G. Pignata, B. Conuel, D. Reichart, K. Ivarsen, J. Haislip, A. Crain, D. Foster, M. Nysewander, and A. Lacluyze, "Supernova 2009ip in NGC 7259", Central Bureau Electronic Telegrams **1928**, 1 (2009).

[309] J. M. Silverman, M. T. Kandrashoff, and A. V. Filippenko, "Supernova 2009js in NGC 918", Central Bureau Electronic Telegrams **1969**, 2 (2009).

[310] S. Nakano, K. Itagaki, T. Yusa, X. Parisky, S. B. Cenko, W. Li, and A. V. Filippenko, "Supernova 2009js in NGC 918", Central Bureau Electronic Telegrams **1969**, 1 (2009).

[311] S. Nakano, T. Yusa, and K. Kadota, "Supernova 2009kr in NGC 1832", Central Bureau Electronic Telegrams **2006**, 1 (2009).

[312] T. N. Steele, B. Cobb, and A. V. Filippenko, "Supernovae 2009kn, 2009ko, 2009kq, and 2009kr", Central Bureau Electronic Telegrams **2011**, 1 (2009).

[313] W. Li, A. V. Filippenko, A. A. Miller, J. .-. Cuillandre, N. Elias-Rosa, and S. D. van Dyk, "Supernova 2009kr in NGC 1832", Central Bureau Electronic Telegrams **2042**, 1 (2009).

[314] D. W. E. Green, "Supernova 2009ls in NGC 3423", Central Bureau Electronic Telegrams **2041**, 1 (2009).

[315] T. N. Steele, C. V. Griffith, I. K. W. Kleiser, and A. V. Filippenko, "Supernovae 2009lr, 2009ls, 2009lt, 2009lu, and 2009lv", Central Bureau Electronic Telegrams **2049**, 3 (2009).

[316] J. Sollerman, M. Ergon, C. Inserra, S. Valenti, P. A. Wilson, S. Jon Juliusson, H. Holma, M. Ingemyr, O. Saxen, and L. Haukanes, “Supernova 2009md in NGC 3389”, Central Bureau Electronic Telegrams **2068**, 1 (2009).

[317] S. Nakano, T. Yusa, and K. Kadota, “Supernova 2009md in NGC 3389”, Central Bureau Electronic Telegrams **2065**, 1 (2009).

[318] R. Chornock and E. Berger, “Supernova 2009mk in Pgc 474”, Central Bureau Electronic Telegrams **2086**, 1 (2009).

[319] P. Marples and C. Drescher, “Supernova 2009mk in Pgc 474”, Central Bureau Electronic Telegrams **2080**, 1 (2009).

[320] A. Maksym, L. Elenin, and M. Schwartz, “Supernova 2010br in NGC 4051”, Central Bureau Electronic Telegrams **2245**, 1 (2010).

[321] A. J. Maxwell, M. L. Graham, A. Parker, S. Sadavoy, C. J. Pritchet, E. Y. Hsiao, and D. D. Balam, “Supernova 2010br in NGC 4051”, Central Bureau Electronic Telegrams **2245**, 2 (2010).

[322] D. D. Balam, “Supernova 2010gi in IC 4660”, Central Bureau Electronic Telegrams **2376**, 2 (2010).

[323] M. Yamanaka, A. Arai, K. Sakimoto, T. Okushima, and K. S. Kawabata, “Supernova 2010gi in IC 4660”, Central Bureau Electronic Telegrams **2384**, 1 (2010).

[324] G. Pignata, M. Cifuentes, J. Maza, M. Hamuy, R. Antezana, L. Gonzalez, P. Gonzalez, S. Silva, G. Folatelli, R. Cartier, F. Forster, S. Marchi, A. Rojas, B. Conuel, D. Reichart, K. Ivarsen, J. Haislip, A. Crain, D. Foster, M. Nysewander, and A. Lacluyze, “Supernova 2010bi in NGC 3509”, Central Bureau Electronic Telegrams **2229**, 1 (2010).

[325] N. Morrell and M. Stritzinger, “Supernova 2011am in NGC 4219 = Psn J12162600-4319200”, Central Bureau Electronic Telegrams **2667**, 1 (2011).

[326] S. B. Cenko, W. Li, A. V. Filippenko, and J. M. Silverman, “Supernova 2011aq in NGC 1056 = Psn J02424814+2834258”, Central Bureau Electronic Telegrams **2671**, 1 (2011).

[327] S. B. Cenko, W. Li, A. V. Filippenko, and J. M. Silverman, “Supernova 2011aq in NGC 1056 = Psn J02424814+2834258”, Central Bureau Electronic Telegrams **2671**, 1 (2011).

[328] M. Ergon, A. Jerkstrand, J. Sollerman, N. Elias-Rosa, C. Fransson, M. Fraser, A. Pastorello, R. Kotak, S. Taubenberger, L. Tomasella, S. Valenti, S. Benetti, G. Helou, M. M. Kasliwal, J. Maund, S. J. Smartt, and J. Spyromilio, “The Type IIb SN 2011dh: Two years of observations and modelling of the lightcurves”, Astronomy and Astrophysics **580**, A142, A142 (2015).

[329] T. Griga, A. Marulla, A. Grenier, G. Sun, X. Gao, S. Lamotte Bailey, R. A. Koff, H. Mikuz, B. Dintinjana, J. M. Silverman, S. B. Cenko, A. V. Filippenko, W. Li, M. Yamanaka, R. Itoh, A. Arai, M. Nagashima, and K. Kajiawa, “Supernova 2011dh in M51 = Psn J13303600+4706330”, Central Bureau Electronic Telegrams **2736**, 1 (2011).

[330] L. A. G. Monard, S. Valenti, and S. Benetti, “Supernova 2011dq in NGC 337 = Psn J00594775-0734205”, Central Bureau Electronic Telegrams **2749**, 1 (2011).

[331] L. A. G. Monard, M. Stritzinger, and R. J. Foley, “Supernova 2011hp in NGC 4219 = Psn J12162547-4319469”, Central Bureau Electronic Telegrams **2899**, 1 (2011).

[332] D. Milisavljevic, R. Fesen, A. Soderberg, T. Pickering, and P. Kotze, “Supernova 2011hs in IC 5267 = Psn J22571177-4323048”, Central Bureau Electronic Telegrams **2902**, 1 (2011).

[333] J. C. Mauerhan, N. Smith, J. M. Silverman, A. V. Filippenko, A. N. Morgan, S. B. Cenko, M. Ganeshalingam, K. I. Clubb, J. S. Bloom, T. Matheson, and P. Milne, “SN 2011ht: confirming a class of interacting supernovae with plateau light curves (Type IIn-P)”, Monthly Notices of the RAS **431**, 2599–2611 (2013).

[334] J. L. Prieto, R. McMillan, G. Bakos, and D. Grennan, “Supernova 2011ht in UGC 5460 = Psn J10081059+5150570”, Central Bureau Electronic Telegrams **2903**, 1 (2011).

[335]S. Howerton, A. J. Drake, S. G. Djorgovski, A. Mahabal, M. J. Graham, R. Williams, J. L. Prieto, M. Catelan, R. H. McNaught, G. Garradd, E. C. Beshore, S. M. Larson, E. Christensen, J. Brimacombe, F. Luppi, L. Buzzi, S. Baroni, P. Concari, S. Foglia, G. Galli, M. Tombelli, R. J. Foley, and W. Fong, "Supernova 2011jm in NGC 4809 = Tcp J12545110+0239149", Central Bureau Electronic Telegrams **2962**, 1 (2011).

[336]V. Stanishev and T. Pursimo, "Supernova 2012A in NGC 3239 = PSN J10250739+1709146.", Central Bureau Electronic Telegrams **2974**, 3 (2012).

[337]B. Moore, J. Newton, and T. Puckett, "Supernova 2012A in NGC 3239 = Psn J10250739+1709146", Central Bureau Electronic Telegrams **2974**, 1 (2012).

[338]A. Dimai, F. Briganti, and J. Brimacombe, "Supernova 2012P in NGC 5806 = PSN J14595904+0153251.", Central Bureau Electronic Telegrams **2993**, 1 (2012).

[339]S. Howerton, A. J. Drake, S. G. Djorgovski, A. Mahabal, M. J. Graham, R. Williams, R. Roy, V. Mohan, J. L. Prieto, M. Catelan, E. C. Beshore, S. M. Larson, E. Christensen, L. Elenin, I. Molotov, R. A. Koff, J. M. Silverman, S. B. Cenko, A. A. Miller, P. E. Nugent, and A. V. Filippenko, "Supernova 2012au in NGC 4790 = Psn J12545218-1014502", Central Bureau Electronic Telegrams **3052**, 1 (2012).

[340]U. Munari, A. Henden, R. Belligoli, F. Castellani, G. Cherini, G. L. Righetti, and A. Vagnozzi, "BVRI lightcurves of supernovae SN 2011fe in M101, SN 2012aw in M95, and SN 2012cg in NGC 4424", New Astronomy **20**, 30–37 (2013).

[341]U. Quadri, L. Strabla, R. Girelli, A. Quadri, R. Itoh, T. Ui, A. Siviero, L. Tomasella, A. Pastorello, S. Benetti, U. Munari, M. Ergon, J. Sollerman, F. Taddia, and G. Barisevicius, "Supernova 2012aw in M95 = Psn J10435372+1140177", Central Bureau Electronic Telegrams **3054**, 1 (2012).

[342]S. B. Cenko, M. Kandrashoff, W. Li, A. V. Filippenko, J. Brimacombe, G. H. Marion, D. Milisavljevic, and J. Irwin, "Supernova 2012cc in NGC 4419 = Psn J12265681+1502455", Central Bureau Electronic Telegrams **3105**, 1 (2012).

[343]K. Itagaki, T. Noguchi, S. Nakano, T. Yusa, X. .-. Wang, Q. Liu, J. .-. Zhang, and T. .-. Zhang, "Supernova 2012cw in NGC 3166 = Psn J10134795+0326026", Central Bureau Electronic Telegrams **3148**, 1 (2012).

[344]G. Bock, A. Klotz, J. T. Parrent, and D. A. Howell, "Supernova 2012dj in NGC 7531 = Psn J23144798-4336223", Central Bureau Electronic Telegrams **3167**, 1 (2012).

[345]L. A. G. Monard, M. Childress, R. Scalzo, F. Yuan, and B. Schmidt, "Supernova 2012ec in NGC 1084 = Psn J02455988-0734270", Central Bureau Electronic Telegrams **3201**, 1 (2012).

[346]J. R. Maund, M. Fraser, S. J. Smartt, M. T. Botticella, C. Barbarino, M. Childress, A. Gal-Yam, C. Inserra, G. Pignata, D. Reichart, B. Schmidt, J. Sollerman, F. Taddia, L. Tomasella, S. Valenti, and O. Yaron, "Supernova 2012ec: identification of the progenitor and early monitoring with PESSTO.", Monthly Notices of the RAS **431**, L102–L106 (2013).

[347]S. Nakano, T. Yusa, K. Yoshimoto, L. Tomasella, M. Turatto, A. Pastorello, P. Ochner, E. Cappellaro, K. Takaki, R. Itoh, I. Ueno, T. Urano, Y. Moritani, H. Akitaya, K. S. Kawabata, and M. Yamanaka, "Supernova 2012fh in NGC 3344 = Psn J10433405+2453290", Central Bureau Electronic Telegrams **3263**, 1 (2012).

[348]G. Pignata, M. Cifuentes, Y. Apostolovski, J. Maza, M. Hamuy, R. Antezana, L. Gonzalez, R. Cartier, F. Forster, S. Silva, F. Carrasco, P. Sanchez, C. Hervias, R. Ramirez, F. Aros, B. Conuel, G. Folatelli, D. Reichart, K. Ivarsen, J. Haislip, A. Crain, D. Foster, M. Nysewander, A. LaCluyze, F. Bufano, S. Gonzalez-Gaitan, S. Marchi, J. Anderson, C. Gutierrez, S. Taubenberger, S. Valenti, A. Pastorello, S. Benetti, S. J. Smartt, K. Smith, D. Young, C. Inserra, M. Sullivan, A. Gal-Yam, and O. Yaron, "Supernova 2012hb in ESO 90-15 = Psn J09020546-6454197", Central Bureau Electronic Telegrams **3322**, 1 (2012).

[349] M. Cifuentes, G. Pignata, Y. Apostolovski, J. Maza, M. Hamuy, R. Antezana, L. Gonzalez, R. Cartier, F. Forster, S. Silva, F. Carrasco, P. Sanchez, C. Hervias, R. Ramirez, F. Aros, B. Conuel, G. Folatelli, D. Reichart, K. Ivarsen, J. Haislip, A. Crain, D. Foster, M. Nysewander, A. LaCluyze, F. Bufano, S. Gonzalez-Gaitan, S. Marchi, J. Anderson, C. Gutierrez, S. Taubenberger, S. Valenti, A. Pastorello, S. Benetti, S. J. Smartt, K. Smith, D. Young, C. Inserra, M. Sullivan, A. Gal-Yam, and O. Yaron, “Supernova 2012hc in NGC 986A (ESO 299-6) = Psn J02324096-3917562”, Central Bureau Electronic Telegrams **3323**, 1 (2012).

[350] S. Howerton, A. J. Drake, S. G. Djorgovski, A. Mahabal, M. J. Graham, R. Williams, J. L. Prieto, M. Catelan, R. H. McNaught, E. C. Beshore, S. M. Larson, E. Christensen, S. Benitez-Herrera, S. Taubenberger, S. Valenti, S. Benetti, A. Pastorello, S. J. Smartt, D. Young, K. Smith, M. Sullivan, I. Arcavi, A. Gal-Yam, and O. Yaron, “Supernova 2012hn in NGC 2272 = Psn J06424255-2726498”, Central Bureau Electronic Telegrams **3337**, 1 (2012).

[351] M. Cifuentes, G. Pignata, Y. Apostolovski, P. Sanchez, M. Hamuy, R. Antezana, L. Gonzalez, R. Cartier, F. Forster, S. Silva, F. Carrasco, C. Hervias, R. Ramirez, F. Aros, B. Conuel, G. Folatelli, D. Reichart, K. Ivarsen, J. Haislip, A. Crain, D. Foster, M. Nysewander, A. LaCluyze, D. Milisavljevic, R. Fesen, T. Pickering, D. Buckley, A. Soderberg, and R. Margutti, “Supernova 2012hs in ESO 213-2 = Psn J09491471-4754456”, Central Bureau Electronic Telegrams **3347**, 1 (2012).

[352] S. Howerton, A. J. Drake, S. G. Djorgovski, A. Mahabal, M. J. Graham, R. Williams, J. L. Prieto, M. Catelan, R. H. McNaught, E. Christensen, S. M. Larson, N. Elias-Rosa, A. Pastorello, S. Benetti, M. Stritzinger, N. Morrell, C. Contreras, and E. Y. Hsiao, “Supernova 2013F in IC 5325 = Psn J23284503-4119562”, Central Bureau Electronic Telegrams **3380**, 1 (2013).

[353] S. Parker, F. Taddia, J. Sollerman, G. Leloudas, M. Ergon, S. Benetti, A. Pastorello, S. Valenti, S. Taubenberger, S. J. Smartt, K. Smith, D. Young, M. Fraser, M. Sullivan, A. Gal-Yam, and O. Yaron, “Supernova 2013K in ESO 9-G10 = Psn J17393154-8518381”, Central Bureau Electronic Telegrams **3391**, 1 (2013).

[354] P. Blanchard, W. Zheng, S. B. Cenko, W. Li, A. V. Filippenko, J. Brimacombe, M. Martignoni, A. Cucchiara, S. Valenti, D. Sand, J. T. Parrent, M. L. Graham, and D. A. Howell, “Supernova 2013ab in NGC 5669 = Psn J14324449+0953123”, Central Bureau Electronic Telegrams **3422**, 1 (2013).

[355] F. Carrasco, M. Hamuy, R. Antezana, L. Gonzalez, R. Cartier, F. Forster, S. Silva, P. Sanchez, C. Hervias, R. Ramirez, G. Pignata, S. Varela, Y. Apostolovski, F. Aros, B. Conuel, G. Folatelli, D. Reichart, K. Ivarsen, J. Haislip, A. Crain, D. Foster, M. Nysewander, A. LaCluyze, D. Milisavljevic, R. Fesen, T. Pickering, A. Kniazev, and J. Parrent, “Supernova 2013ak in ESO 430-20 = Psn J08070669-2803101”, Central Bureau Electronic Telegrams **3437**, 1 (2013).

[356] L. Tomasella, E. Cappellaro, M. L. Pumo, A. Jerkstrand, S. Benetti, N. Elias-Rosa, M. Fraser, C. Inserra, A. Pastorello, M. Turatto, J. P. Anderson, L. Galbany, C. P. Gutiérrez, E. Kankare, G. Pignata, G. Terreran, S. Valenti, C. Barbarino, F. E. Bauer, M. T. Botticella, T. .-. Chen, A. Gal-Yam, A. Harutyunyan, D. A. Howell, K. Maguire, A. Morales Garoffolo, P. Ochner, S. J. Smartt, S. Schulze, D. R. Young, and L. Zampieri, “SNe 2013K and 2013am: observed and physical properties of two slow, normal Type IIP events”, Monthly Notices of the RAS **475**, 1937–1959 (2018).

[357] S. Nakano, M. Sugano, K. Kadota, S. Benetti, L. Tomasella, A. Pastorello, E. Cappellaro, M. Turatto, and P. Ochner, “Supernova 2013am in M65 = Psn J11185695+1303494”, Central Bureau Electronic Telegrams **3440**, 1 (2013).

[358] K. Itagaki, T. Noguchi, S. Nakano, L. Elenin, I. Molotov, Y. Moritani, K. Takaki, K. S. Kawabata, H. Akitaya, N. Ebisuda, K. Kawaguchi, K. Mori, Y. Ohashi, I. Ueno, M. Sasada, M. Yamanaka, P. Ochner, L. Tomasella, A. Pastorello, S. Benetti, E. Cappellaro, and M. Turatto, “Supernova 2013bu in NGC 7331 = Psn J22370217+3424052”, Central Bureau Electronic Telegrams **3498**, 1 (2013).

[359] S. Parker, S. Kiyota, N. Morrell, E. Hsiao, C. Contreras, C. Gonzalez, A. Campillay, M. Gromadzki, M. T. Ruiz, D. Milisavljevic, R. Fesen, T. Pickering, P. Vaisanen, G. H. Marion, J. Parrent, R. Margutti, and A. Soderberg, "Supernova 2013by in ESO 138-G10 = Psn J16590243-6011418", Central Bureau Electronic Telegrams **3506**, 1 (2013).

[360] S. Valenti, D. Sand, M. Stritzinger, D. A. Howell, I. Arcavi, C. McCully, M. J. Childress, E. Y. Hsiao, C. Contreras, N. Morrell, M. M. Phillips, M. Gromadzki, R. P. Kirshner, and G. H. Marion, "Supernova 2013by: a Type IIL supernova with a IIP-like light-curve drop", Monthly Notices of the RAS **448**, 2608–2616 (2015).

[361] F. Ciabattari, E. Mazzoni, S. Donati, G. Petroni, S. Foglia, G. Galli, S. B. Cenko, K. I. Clubb, W. Zheng, P. L. Kelly, A. V. Filippenko, and S. D. Van Dyk, "Supernova 2013df in NGC 4414 = Psn J12262933+3113383", Central Bureau Electronic Telegrams **3557**, 1 (2013).

[362] F. Carrasco, M. Hamuy, R. Antezana, L. Gonzalez, R. Cartier, F. Forster, S. Silva, R. Ramirez, G. Pignata, Y. Apostolovski, E. Paillas, S. Varela, F. Aros, B. Conuel, G. Folatelli, D. E. Reichart, J. B. Haislip, J. P. Moore, A. P. LaCluyze, A. Harutyunyan, S. Benetti, A. Pastorello, E. Cappellaro, L. Tomasella, P. Ochner, M. Turatto, J. Vinko, G. H. Marion, J. M. Silverman, J. C. Wheeler, T. Szalai, and R. Quimby, "Supernova 2013dk in NGC 4038 = Psn J12015272-1852183", Central Bureau Electronic Telegrams **3566**, 2 (2013).

[363] G. Cortini, J. Brimacombe, L. Tomasella, P. Ochner, A. Pastorello, S. Benetti, E. Cappellaro, M. Turatto, J. Farinato, T. Pursimo, and M. Dennefeld, "Supernova 2013ee in NGC 3079 = Psn J10015683+5541440", Central Bureau Electronic Telegrams **3597**, 1 (2013).

[364] F. Huang, X. Wang, J. Zhang, P. J. Brown, L. Zampieri, M. L. Pumo, T. Zhang, J. Chen, J. Mo, and X. Zhao, "SN 2013ej in M74: A Luminous and Fast-declining Type II-P Supernova", Astrophysical Journal **807**, 59, 59 (2015).

[365] P. b. D. C. Leonard, G. Pignata, L. Dessart, D. Hillier, H. G. Khandrika, A. A. Rachubo, R. D. Fahad, S. J. Hadden, and L. Gonzalez, "SN 2013ej is a Highly Polarized Type II-Plateau Supernova", The Astronomer's Telegram **5275**, 1 (2013).

[366] M. Kim, W. Zheng, W. Li, A. V. Filippenko, S. B. Cenko, M. W. Richmond, A. Amorim, D. D. Balam, M. L. Graham, and E. Y. Hsiao, "Supernova 2013ej in M74 = Psn J01364816+1545310", Central Bureau Electronic Telegrams **3606**, 1 (2013).

[367] J. Brimacombe, S. Zaggia, M. Barbieri, A. Silvestri, V. Ronzani, S. Benetti, A. Pastorello, E. Cappellaro, L. Tomasella, P. Ochner, M. Turatto, and S. Valenti, "Supernova 2013ff in NGC 2748 = Psn J09133888+7628108", Central Bureau Electronic Telegrams **3647**, 1 (2013).

[368] R. Antezana, M. Hamuy, L. Gonzalez, R. Cartier, F. Forster, F. Carrasco, G. Pignata, Y. Apostolovski, E. Paillas, S. Varela, F. Bufano, F. Olivares, K. Takats, F. Aros, B. Conuel, G. Folatelli, D. E. Reichart, J. B. Haislip, J. P. Moore, A. P. LaCluyze, and N. Morrell, "Supernova 2013gc in ESO 430-20 = Psn J08071188-2803263", Central Bureau Electronic Telegrams **3699**, 1 (2013).

[369] A. Reguitti, "Signatures of an eruptive phase before SN 2013gc", American Institute of Physics Conference Series **2032**, 030001, 030001 (2018).

[370] M. R. Drout, D. Milisavljevic, J. Parrent, R. Margutti, A. Kamble, A. M. Soderberg, P. Challis, R. Chornock, W. Fong, S. Frank, N. Gehrels, M. L. Graham, E. Hsiao, K. Itagaki, M. Kasliwal, R. P. Kirshner, D. Macomb, G. H. Marion, J. Norris, and M. M. Phillips, "The Double-peaked SN 2013ge: A Type Ib/c SN with an Asymmetric Mass Ejection or an Extended Progenitor Envelope", Astrophysical Journal **821**, 57, 57 (2016).

[371] S. Nakano, S. Kiyota, G. Masi, F. Nocentini, P. Schmeer, J. .-. Zhang, and X. .-. Wang, "Supernova 2013ge in NGC 3287 = Psn J10344846+2139419", Central Bureau Electronic Telegrams **3701**, 1 (2013).

[372] H. Kim, W. Zheng, W. Li, A. V. Filippenko, S. B. Cenko, L. Le Guillou, M. Fleury, S. Baumont, P. .-. Leget, C. Inserra, S. Smartt, K. Smith, D. Young, M. Sullivan, S. Taubenberger, S. Valenti, M. Fraser, O. Yaron, I. Manulis, A. Gal-Yam, C. Knapic, R. Smareglia, M. Molinaro, E. Y. Hsiao, and J. L. Prieto, "Supernova 2014A in NGC 5054 = Psn J13165936-1637570", Central Bureau Electronic Telegrams **3771**, 1 (2014).

[373] M. Kim, W. Zheng, W. Li, A. V. Filippenko, S. B. Cenko, R. Arbour, G. Masi, F. Nocentini, P. Schmeer, J. Zhang, X. Want, L. Tartaglia, A. Pastorello, S. Benetti, E. Cappellaro, L. Tomasella, P. Ochner, N. Elias-Rosa, and M. Turatto, "Supernova 2014C in NGC 7331 = Psn J22370560+3424319", Central Bureau Electronic Telegrams **3777**, 1 (2014).

[374] D. Denisenko, V. Lipunov, E. Gorbovskoy, P. Lake, T. Yusa, K. Kadota, R. Itoh, Y. Moritani, K. S. Kawabata, M. Yamanaka, P. Ochner, A. Siviero, L. Tomasella, S. Benetti, E. Cappellaro, N. Elias-Rosa, A. Pastorello, L. Tartaglia, G. Terreran, M. Turatto, and S. Nakano, "Supernova 2014G in NGC 3448 = Psn J10543413+5417569", Central Bureau Electronic Telegrams **3787**, 2 (2014).

[375] S. Nakano, "Supernova 2014G in NGC 3448 = Psn J10543413+5417569", Central Bureau Electronic Telegrams **3787**, 1 (2014).

[376] S. J. Smartt, K. W. Smith, D. Wright, D. R. Young, R. Kotak, M. Nicholl, J. Polshaw, C. Inserra, T. .-. Chen, G. Terreran, E. Gall, M. Fraser, M. McCrum, S. Valenti, R. Foley, A. Lawrence, S. Gezari, W. Burgett, K. Chambers, M. Huber, R. P. Kudritzki, E. Magnier, J. Morgan, J. Tonry, W. Sweeney, R. Wainscoat, C. Waters, C. Stubbs, R. Kirshner, N. Metcalfe, P. Draper, and A. Rest, "Supernova 2014bc in M106 = Psn J12185771+4718113", Central Bureau Electronic Telegrams **3876**, 1 (2014).

[377] G. Cortini, G. Masi, F. Nocentini, P. Schmeer, P. Ochner, S. Benetti, L. Tomasella, A. Pastorello, N. Elias-Rosa, E. Cappellaro, M. Turatto, and G. Terraran, "Supernova 2014bc in M106 = Psn J12185771+4718113", Central Bureau Electronic Telegrams **3876**, 2 (2014).

[378] S. Kumar, W. Zheng, A. V. Filippenko, G. Masi, J. .-. Zhang, and X. .-. Wang, "Supernova 2014bi in NGC 4096 = Psn J12060299+4729335", Central Bureau Electronic Telegrams **3892**, 1 (2014).

[379] L. Gonzalez, M. Hamuy, R. Antezana, R. Cartier, F. Forster, F. Carrasco, G. Pignata, Y. Apostolovski, E. Paillas, S. Varela, F. Bufano, F. Olivares, K. Takats, T. Catalan, C. Rivas, L. Gutierrez, C. Flores, F. Aros, B. Conuel, G. Folatelli, S. Montufar, D. E. Reichart, J. B. Haislip, J. P. Moore, and A. P. LaCluyze, "Supernova 2014cl in IC 217 = Psn J02160910-1156026", Central Bureau Electronic Telegrams **3950**, 1 (2014).

[380] S. Nakano, K. Itagaki, T. Yusa, S. Howerton, N. Elias-Rosa, L. Tartaglia, E. Cappellaro, A. Pastorello, M. T. Botticella, C. Inserra, K. Maguire, S. Smartt, K. W. Smith, M. Sullivan, S. Valenti, O. Yaron, D. Young, and I. Manulis, "Supernova 2014cx in NGC 337 = Psn J00594783-0734186", Central Bureau Electronic Telegrams **3963**, 1 (2014).

[381] S. Kiyota, J. Brimacombe, T. Yusa, N. Morrell, M. M. Phillips, C. Contreras, G. H. Marion, E. Y. Hsiao, C. Gall, M. D. Stritzinger, and R. P. Kirshner, "Supernova 2014cy in NGC 7742 = Psn J23441603+1046125", Central Bureau Electronic Telegrams **3964**, 2 (2014).

[382] K. Nishimura, "Supernova 2014cy in NGC 7742 = Psn J23441603+1046125", Central Bureau Electronic Telegrams **3964**, 1 (2014).

[383] L. A. G. Monard, R. Kneip, J. Brimacombe, H. Sato, M. Childress, G. Zhou, R. Scalzo, F. Yuan, B. Zhang, A. Ruiter, I. Seitenzahl, B. Schmidt, and B. Tucker, "Supernova 2014df in NGC 1448 = Psn J03442399-4440081", Central Bureau Electronic Telegrams **3977**, 1 (2014).

[384] S. Parker, J. Maza, J. Brimacombe, M. Childress, R. Scalzo, F. Yuan, B. Zhang, A. Ruiter, I. Seitenzahl, B. Schmidt, and B. Tucker, "Supernova 2014do in ESO 431-G2 = Psn J08174339-3007211", Central Bureau Electronic Telegrams **4000**, 1 (2014).

[385] G. Bock, P. Challis, and P. Berlind, "Supernova 2014dq in ESO 467-G51 = Psn J22231609-2858318", Central Bureau Electronic Telegrams **4008**, 1 (2014).

[386] S. Parker, I. Arcavi, G. Hosseinzadeh, S. Valenti, D. A. Howell, C. McCully, T. Diamond, M. M. Phillips, C. Contreras, and E. Y. Hsiao, "Supernova 2014dw in NGC 3568 = Psn J11104841-3727022", Central Bureau Electronic Telegrams **4047**, 1 (2015).

[387] A. Pastorello and G. Terreran, "Padova-Asiago Transient Classification Report for 2021-07-12", Transient Name Server Classification Report **2021-2418**, 1–2418 (2021).

[388] O. Gress, V. Lipunov, E. Gorbovskoy, V. Kornilov, N. Tyurina, P. Balanutsa, A. Kuznetsov, F. Balakin, V. Vladimirov, D. Vlasenko, I. Gorbunov, D. Zimnukhov, V. Senik, T. Pogrosheva, D. Kuvshinov, R. Podesta, C. Lopez, F. Podesta, C. Francile, H. Levato, R. Rebolo, M. Serra, D. Buckley, N. M. Budnev, O. Ershova, A. Tlatov, D. Dormidontov, V. Yurkov, A. Gabovich, and Y. Sergienko, "MASTER Transient Discovery Report for 2019-08-19", Transient Name Server Discovery Report **2019-1539**, 1 (2019).

[389] T. Yusa, D. Buczynski, T. Noguchi, S. Nakano, S. Kiyota, G. Masi, K. Ayani, R. J. Foley, W. Zheng, A. V. Filippenko, and S. D. Van Dyk, "Supernova 2015G in NGC 6951 = Psn J20372558+6607115", Central Bureau Electronic Telegrams **4087**, 1 (2015).

[390] R. Dastidar, K. Misra, S. Valenti, J. Burke, G. Hosseinzadeh, A. Gangopadhyay, D. A. Howell, M. Singh, I. Arcavi, B. Kumar, C. McCully, P. Sanwal, and S. B. Pandey, "SN 2015an: a normal luminosity type II supernova with low expansion velocity at early phases", Monthly Notices of the RAS **490**, 1605–1619 (2019).

[391] A. Delgado, D. Harrison, S. Hodgkin, M. V. Leeuwen, G. Rixon, and A. Yoldas, "GaiaAlerts Transient Discovery Report for 2016-07-22", Transient Name Server Discovery Report **2016-481**, 1 (2016).

[392] A. Gangopadhyay, K. Misra, A. Pastorello, D. K. Sahu, L. Tomasella, L. Tartaglia, M. Singh, R. Dastidar, S. Srivastav, P. Ochner, P. J. Brown, G. C. Anupama, S. Benetti, E. Cappellaro, B. Kumar, B. Kumar, and S. B. Pandey, "SN 2015as: a low-luminosity Type IIb supernova without an early light-curve peak", Monthly Notices of the RAS **476**, 3611–3630 (2018).

[393] T. Nakaoka, K. S. Kawabata, M. Yamanaka, K. Takaki, and M. Kawabata, "Transient Classification Report for 2016-01-10", Transient Name Server Classification Report **2016-11**, 1 (2016).

[394] Stanek, Brown, Holoien, Kochanek, Godoy-rivera, Basu, Shappee, Prieto, Bersier, Dong, Chen, and Brimacombe, "ASAS-SN Transient Discovery Report for 2016-01-03", Transient Name Server Discovery Report **2016-3**, 1 (2016).

[395] D. K. Sahu, G. C. Anupama, S. Srivastav, and N. K. Chakradhari, "Transient Classification Report for 2016-01-09", Transient Name Server Classification Report **2016-9**, 1 (2016).

[396] M. Aoki, "Transient Discovery Report for 2016-01-04", Transient Name Server Discovery Report **2016-4**, 1 (2016).

[397] J. Zhang and X. Wang, "Transient Classification Report for 2016-01-11", Transient Name Server Classification Report **2016-12**, 1 (2016).

[398] J. Grzegorzek, "Transient Discovery Report for 2016-01-09", Transient Name Server Discovery Report **2016-8**, 1 (2016).

[399] S. Bose, S. Dong, N. Elias-Rosa, B. J. Shappee, D. Bersier, S. Benetti, M. D. Stritzinger, D. Grupe, C. S. Kochanek, J. L. Prieto, P. Chen, H. Kuncarayakti, S. Mattila, A. Morales-Garoffolo, N. Morrell, F. Onori, T. M. Reynolds, A. Siviero, A. Somero, K. Z. Stanek, G. Terreran, T. A. Thompson, L. Tomasella, C. Ashall, C. Gall, M. Gromadzki, and T. W. .-. Holoien, "Strongly Bipolar Inner Ejecta of the Normal Type IIP Supernova ASASSN-16at", Astrophysical Journal, Letters **873**, L3, L3 (2019).

[400] Stanek, Bock, Shappee, Brown, Holoien, Kochanek, Godoy-rivera, Basu, Prieto, Bersier, Dong, Chen, and Brimacombe, "ASAS-SN Transient Discovery Report for 2016-01-20", Transient Name Server Discovery Report **2016-38**, 1 (2016).

[401] M. Stritzinger, E. Y. Hsiao, N. Morrell, M. M. Phillips, C. Contreras, S. Castellon, and A. Clocchiatti, "Transient Classification Report for 2016-02-09", Transient Name Server Classification Report **2016-1117**, 1 (2016).

[402] P. Marples and G. Bock, "BOSS Transient Discovery Report for 2016-02-08", Transient Name Server Discovery Report **2016-94**, 1 (2016).

[403] S. Jha, "Transient Classification Report for 2016-02-28", Transient Name Server Classification Report **2016-1119**, 1 (2016).

[404] S. Benetti, E. Cappellaro, N. Elias-rosa, A. Pastorello, and L. Tomasella, "Padova-Asiago Transient Classification Report for 2016-03-16", Transient Name Server Classification Report **2016-224**, 1 (2016).

[405] R. Arbour, "Transient Discovery Report for 2016-03-14", Transient Name Server Discovery Report **2016-215**, 1 (2016).

[406] T. Nakaoka, K. S. Kawabata, K. Maeda, M. Tanaka, M. Yamanaka, T. J. Moriya, N. Tominaga, T. Morokuma, K. Takaki, M. Kawabata, N. Kawahara, R. Itoh, K. Shiki, H. Mori, J. Hirochi, T. Abe, M. Uemura, M. Yoshida, H. Akitaya, Y. Moritani, I. Ueno, T. Urano, M. Isogai, H. Hanayama, and T. Nagayama, "The Low-luminosity Type IIP Supernova 2016bkv with Early-phase Circumstellar Interaction", Astrophysical Journal **859**, 78, 78 (2018).

[407] G. Hosseinzadeh, D. A. Howell, I. Arcavi, C. Mccully, and S. Valenti, "LCOGT SN-KP Transient Classification Report for 2016-03-23", Transient Name Server Classification Report **2016-239**, 1 (2016).

[408] K. Itagaki, "Transient Discovery Report for 2016-03-22", Transient Name Server Discovery Report **2016-234**, 1 (2016).

[409] B. Kumar, A. Singh, S. Srivastav, D. K. Sahu, and G. C. Anupama, "ASASSN-16fp (SN 2016coi): a transitional supernova between Type Ic and broad-lined Ic", Monthly Notices of the RAS **473**, 3776–3788 (2018).

[410] K. Z. Stanek, "ASAS-SN Transient Discovery Report for 2016-05-27", Transient Name Server Discovery Report **2016-379**, 1 (2016).

[411] G. Bock, S. Dong, C. S. Kochanek, K. Z. Stanek, J. S. Brown, T. W. .-. Holoien, D. Godoy-Rivera, U. Basu, B. J. Shappee, J. L. Prieto, D. Bersier, P. Chen, and J. Brimacombe, "ASASSN-16fq: Discovery of A Probable Supernova in M66", The Astronomer's Telegram **9091**, 1 (2016).

[412] J. Zhang, X. Zheng, X. Wang, and L. Rui, "Transient Classification Report for 2016-05-31", Transient Name Server Classification Report **2016-391**, 1 (2016).

[413] J. Neill, "iPTF Transient Classification Report for 2016-06-12", Transient Name Server Classification Report **2016-1123**, 1 (2016).

[414] G. Bock and S. Dong, "ASAS-SN Transient Discovery Report for 2016-05-28", Transient Name Server Discovery Report **2016-382**, 1 (2016).

[415] S. D. Van Dyk, W. Zheng, I. Shivvers, A. V. Filippenko, B. E. Tucker, D. A. Perley, and N. Smith, "Further Classification of SN 2016gkg as a Probable Type IIb Supernova", The Astronomer's Telegram **9573**, 1 (2016).

[416] S. Otero and V. Buso, "Transient Discovery Report for 2016-09-21", Transient Name Server Discovery Report **2016-695**, 1 (2016).

[417] S. Jha, "Transient Classification Report for 2016-11-13", Transient Name Server Classification Report **2016-1135**, 1 (2016).

[418] J. Tonry, L. Denneau, B. Stalder, A. Heinze, A. Sherstyuk, A. Rest, K. W. Smith, and S. J. Smartt, "ATLAS Transient Discovery Report for 2016-11-12", Transient Name Server Discovery Report **2016-909**, 1 (2016).

[419] C. Barbarino, A. Nyholm, F. Taddia, J. Sollerman, C. Fremling, and O. Yaron, "PESSTO Transient Classification Report for 2017-03-07", Transient Name Server Classification Report **2017-281**, 1 (2017).

[420] N. Morrell, "Transient Classification Report for 2017-07-04", Transient Name Server Classification Report **2017-736**, 1 (2017).

[421] S. Parker, "BOSS Transient Discovery Report for 2017-03-07", Transient Name Server Discovery Report **2017-279**, 1 (2017).

[422] R. J. Buta and W. C. Keel, "BVRI photometry of the classic Type II-P supernova 2017eaw in NGC 6946: d 3 to d 594", Monthly Notices of the RAS **487**, 832–844 (2019).

[423] C. Kilpatrick, "Transient Classification Report for 2018-06-04", Transient Name Server Classification Report **2018-2102**, 1 (2018).

[424] P. Wiggins, "Psn J20344424+6011359 = Supernova 2017eaw in NGC 6946", Central Bureau Electronic Telegrams **4390**, 1 (2017).

[425] D. Xiang, L. Rui, X. Wang, H. Song, F. Xiao, T. Zhang, and J. Zhang, "Transient Classification Report for 2017-05-26", Transient Name Server Classification Report **2017-599**, 1 (2017).

[426] R. Arbour, "Transient Discovery Report for 2017-05-25", Transient Name Server Discovery Report **2017-588**, 1 (2017).

[427] S. Valenti, D. J. Sand, and L. Tartaglia, "DLT40 Transient Discovery Report for 2017-08-14", Transient Name Server Discovery Report **2017-866**, 1 (2017).

[428] S. W. Jha, Y. Camacho, K. Dettman, D. Sand, S. Wyatt, L. Tartaglia, S. Valenti, and B. Miszalski, "SALT spectroscopic classification of DLT17ch (= SN 2017gax) as a type-Ib/c supernova before maximum light", The Astronomer's Telegram **10640**, 1 (2017).

[429] S. Jha, "Transient Classification Report for 2017-08-15", Transient Name Server Classification Report **2017-870**, 1 (2017).

[430] F. Onori, "NUTS Transient Classification Report for 2017-09-03", Transient Name Server Classification Report **2017-964**, 1 (2017).

[431] K. Itagaki, "Transient Discovery Report for 2017-08-31", Transient Name Server Discovery Report **2017-940**, 1 (2017).

[432] N. Elias-Rosa, "Transient Classification Report for 2017-09-18", Transient Name Server Classification Report **2017-1015**, 1 (2017).

[433] S. Valenti, D. J. Sand, and L. Tartaglia, "DLT40 Transient Discovery Report for 2017-09-04", Transient Name Server Discovery Report **2017-966**, 1 (2017).

[434] D. O'neill, M. Magee, O. Yaron, and N. Knezevic, "ePESSTO Transient Classification Report for 2017-10-30", Transient Name Server Classification Report **2017-1191**, 1 (2017).

[435] K. Z. Stanek, "ASAS-SN Transient Discovery Report for 2017-10-26", Transient Name Server Discovery Report **2017-1169**, 1 (2017).

[436] B. Kumar, A. Singh, D. K. Sahu, and G. C. Anupama, "Investigating the Observational Properties of Type Ib Supernova SN 2017iro", Astrophysical Journal **927**, 61, 61 (2022).

[437] P. Wiggins, "Transient Discovery Report for 2017-11-30", Transient Name Server Discovery Report **2017-1354**, 1 (2017).

[438] D. O. Jones, G. Dimitriadis, Y. C. Pan, and R. J. Foley, "Transient Classification Report for 2017-12-23", Transient Name Server Classification Report **2017-1464**, 1 (2017).

[439] J. Tonry, B. Stalder, L. Denneau, A. Heinze, H. Weiland, A. Rest, K. W. Smith, S. J. Smartt, M. Fulton, and O. Mcbrien, "ATLAS Transient Discovery Report for 2017-12-11", Transient Name Server Discovery Report **2017-1395**, 1 (2017).

[440] N. Morrell, B. J. Shappee, and M. Drout, "Transient Classification Report for 2017-12-27", Transient Name Server Classification Report **2017-1483**, 1 (2017).

[441] A. Delgado, D. Harrison, S. Hodgkin, M. V. Leeuwen, G. Rixon, and A. Yoldas, "GaiaAlerts Transient Discovery Report for 2017-12-19", Transient Name Server Discovery Report **2017-1441**, 1 (2017).

[442] S. Bose, S. Dong, A. Pastorello, Y. Cai, E. A. Barsukova, V. P. Goranskij, K. Z. Stanek, J. Shield, R. Post, and Y. H. E. Al, "ASAS-SN Transient Classification Report for 2018-01-11", Transient Name Server Classification Report **2018-42**, 1 (2018).

[443] R. Gagliano, R. Post, E. Weinberg, J. Newton, and T. Puckett, "POSS Transient Discovery Report for 2017-12-31", Transient Name Server Discovery Report **2017-1505**, 1 (2017).

[444] D. Y. Tsvetkov, N. N. Pavlyuk, O. V. Vozyakova, N. I. Shatsky, A. M. Tatarnikov, A. A. Nikiforova, P. V. Baklanov, S. I. Blinnikov, M. G. Ushakova, E. G. Larionova, and G. A. Borman, "Type II-P Supernova SN 2018aoq in NGC 4151: Light Curves, Models, and Distance", Astronomy Letters **47**, 291–306 (2021).

[445] M. Yamanaka, "Transient Classification Report for 2018-04-02", Transient Name Server Classification Report **2018-432**, 1 (2018).

[446] C. Soler, W. Zheng, and A. V. Filippenko, "LOSS Transient Discovery Report for 2018-04-01", Transient Name Server Discovery Report **2018-426**, 1 (2018).

[447] S. Prentice, "Transient Classification Report for 2018-09-12", Transient Name Server Classification Report **2018-1369**, 1 (2018).

[448] J. Brimacombe and K. Z. Stanek, "ASAS-SN Transient Discovery Report for 2018-09-11", Transient Name Server Discovery Report **2018-1351**, 1 (2018).

[449] C. Kilpatrick, "Transient Classification Report for 2018-01-15", Transient Name Server Classification Report **2018-2075**, 1 (2018).

[450] P. Wiggins, "Transient Discovery Report for 2018-01-14", Transient Name Server Discovery Report **2018-53**, 1 (2018).

[451] E. Paraskeva, A. Z. Bonanos, A. Liakos, Z. T. Spetsieri, and J. R. Maund, "First systematic high-precision survey of bright supernovae. I. Methodology for identifying early bumps", Astronomy and Astrophysics **643**, A35, A35 (2020).

[452] M. Kawabata, "Transient Classification Report for 2018-10-29", Transient Name Server Classification Report **2018-2159**, 1 (2018).

[453] K. Itagaki, "Transient Discovery Report for 2018-10-22", Transient Name Server Discovery Report **2018-1614**, 1 (2018).

[454] K. Itagaki, "Transient Discovery Report for 2018-11-14", Transient Name Server Discovery Report **2018-1766**, 1 (2018).

[455] M. Yamanaka, "Transient Classification Report for 2018-11-15", Transient Name Server Classification Report **2018-2035**, 1 (2018).

[456] S. Valenti, D. J. Sand, and S. Wyatt, "DLT40 Transient Discovery Report for 2018-01-20", Transient Name Server Discovery Report **2018-92**, 1 (2018).

[457] D. Sand, S. Valenti, J. Andrews, J. Strader, and L. Chomiuk, "DLT40 Transient Classification Report for 2018-01-22", Transient Name Server Classification Report **2018-103**, 1 (2018).

[458] M. Yamanaka, "Transient Classification Report for 2018-11-24", Transient Name Server Classification Report **2018-1818**, 1 (2018).

[459] S. Valenti, D. J. Sand, and S. Wyatt, "DLT40 Transient Discovery Report for 2018-11-24", Transient Name Server Discovery Report **2018-1816**, 1 (2018).

[460] M. A. Tucker, M. E. Huber, J. Strader, K. Z. Stakek, and B. J. Shappee, "SCAT Transient Classification Report for 2019-01-09", Transient Name Server Classification Report **2019-62**, 1 (2019).

[461] K. Z. Stanek, "ASAS-SN Transient Discovery Report for 2018-12-31", Transient Name Server Discovery Report **2018-2010**, 1 (2018).

[462] J. Zhang, X. Wang, V. József, Q. Zhai, T. Zhang, A. V. Filippenko, T. G. Brink, W. Zheng, Ł. Wyrzykowski, P. Mikołajczyk, F. Huang, L. Rui, J. Mo, H. Sai, X. Zhang, H. Wang, J. M. DerKacy, E. Baron, K. Sárneczky, A. Bódi, G. Csörnyei, O. Hanyecz, B. Ignácz, C. Kalup, L. Kriskovics, R. Könyves-Tóth, A. Ordasi, A. Pál, Á. Sódor, R. Szakáts, K. Vida, and G. Zsidi, "SN 2018zd: an unusual stellar explosion as part of the diverse Type II Supernova landscape", Monthly Notices of the RAS **498**, 84–100 (2020).

[463] K. Itagaki, "Transient Discovery Report for 2018-03-02", Transient Name Server Discovery Report **2018-285**, 1 (2018).

[464] O. Rodriguez, G. Pignata, M. Gromadzki, and O. Yaron, "ePESSTO Transient Classification Report for 2019-01-08", Transient Name Server Classification Report **2019-49**, 1 (2019).

[465] J. Tonry, L. Denneau, A. Heinze, H. Weiland, H. Flewelling, B. Stalder, A. Rest, C. Stubbs, K. W. Smith, S. J. Smartt, D. R. Young, K. Maguire, S. J. Prentice, O. McBrien, D. O'Neill, P. Clark, M. Magee, M. Fulton, A. Mccormack, and D. E. Wright, "ATLAS Transient Discovery Report for 2019-01-04", Transient Name Server Discovery Report **2019-21**, 1 (2019).

[466] D. Hiramatsu, J. Burke, I. Arcavi, D. A. Howell, C. McCully, and S. Valenti, "Global SN Project Transient Classification Report for 2019-04-28", Transient Name Server Classification Report **2019-659**, 1 (2019).

[467] K. Z. Stanek, "ASAS-SN Transient Discovery Report for 2019-04-27", Transient Name Server Discovery Report **2019-643**, 1 (2019).

[468] G. Dimitriadis, M. R. Siebert, C. D. Kilpatrick, C. Rojas-Bravo, R. J. Foley, and M. Rich, "Transient Classification Report for 2019-04-30", Transient Name Server Classification Report **2019-675**, 1 (2019).

[469] L. Tomasella, S. Benetti, E. Cappellaro, and M. Turatto, "Asiago spectroscopic observation of ASASSN-19ku and SN 2019ehk", The Astronomer's Telegram **12714**, 1 (2019).

[470] K. De, U. C. Fremling, A. Gal-Yam, O. Yaron, M. M. Kasliwal, and S. R. Kulkarni, "The Peculiar Ca-rich SN2019ehk: Evidence for a Type IIb Core-collapse Supernova from a Low-mass Stripped Progenitor", Astrophysical Journal, Letters **907**, L18, L18 (2021).

[471] J. Grzegorzek, "PSH Transient Discovery Report for 2019-04-29", Transient Name Server Discovery Report **2019-666**, 1 (2019).

[472] M. Nicholl, P. Short, E. Swann, C. R. Angus, M. Smith, and O. Yaron, "ePESSTO+ Transient Classification Report for 2019-05-03", Transient Name Server Classification Report **2019-700**, 1 (2019).

[473] J. Tonry, L. Denneau, A. Heinze, H. Weiland, H. Flewelling, B. Stalder, A. Rest, C. Stubbs, K. W. Smith, S. J. Smartt, D. R. Young, S. Srivastav, O. McBrien, D. O'Neill, P. Clark, M. Fulton, J. Gillanders, A. McCormack, and D. E. Wright, "ATLAS Transient Discovery Report for 2019-05-02", Transient Name Server Discovery Report **2019-687**, 1 (2019).

[474] D. Hiramatsu, J. Burke, I. Arcavi, D. A. Howell, C. McCully, and S. Valenti, "Global SN Project Transient Classification Report for 2019-05-09", Transient Name Server Classification Report **2019-738**, 1 (2019).

[475] D. Sand, S. Valenti, R. Amaro, M. Lundquist, S. Wyatt, J. Andrews, and Y. Dong, "DLT40 Transient Discovery Report for 2019-05-06", Transient Name Server Discovery Report **2019-717**, 1 (2019).

[476] J. Brimacombe, K. Z. Stanek, P. Vallely, C. S. Kochanek, J. Shields, T. A. Thompson, B. J. Shappee, T. W. .-. Holoien, J. L. Prieto, D. Bersier, S. Dong, S. Bose, P. Chen, M. Stritzinger, and S. Holmbo, "ASASSN-19ml: Discovery of A Probable Supernova in ESO 430-G 020 (d 17 Mpc)", The Astronomer's Telegram **12754**, 1 (2019).

[477] M. Nicholl, P. Short, C. Angus, T. Muller, M. Pursiainen, C. Barbarino, M. Dennefeld, S. C. Williams, A. Pastorello, M. Smith, S. Benetti, R. Cartier, J. Anderson, T. W. Chen, C. Inserra, D. R. Young, O. Y. I. Manulis, J. Tonry, L. Denneau, A. Heinze, H. Weiland, B. Stalder, A. Rest, K. W. Smith, S. J. Smartt, O. McBrien, and S. Srivastav, "ePESSTO+ spectroscopic classification of optical transients", Transient Name Server AstroNote **14**, 1 (2019).

[478] K. Z. Stanek, D. Bersier, and C. S. Kochanek, "ASAS-SN Transient Discovery Report for 2019-05-13", Transient Name Server Discovery Report **2019-766**, 1 (2019).

[479] T. M. Bravo, J. Antilen, P. Wiseman, M. Grayling, M. Smith, C. Frohmaier, T. W. Chen, R. Cartier, R. Carini, J. Anderson, M. Gromadzki, C. Inserra, E. Kankare, M. Nicholl, O. Yaron, D. Young, I. Manulis, J. Tonry, L. Denneau, A. Heinze, H. Weiland, H. Flewelling, B. Stalder, A. Rest, K. W. Smith, S. J. Smartt, O. McBrien, S. Srivastav, K. C. Chambers, T. D. Boer, J. Bulger, J. Fairlamb, M. Huber, C. C. Lin, T. Lowe, E. Magnier, . Schultz, R. J. Wainscoat, and M. Willman, "ePESSTO+ spectroscopic classification of optical transients", Transient Name Server AstroNote **162**, 1 (2019).

[480] G. Dimitriadis, "UCSC Transient Classification Report for 2019-12-29", Transient Name Server Classification Report **2019-2736**, 1 (2019).

[481] J. Tonry, L. Denneau, A. Heinze, H. Weiland, H. Flewelling, B. Stalder, A. Rest, C. Stubbs, K. W. Smith, S. J. Smartt, D. R. Young, S. Srivastav, O. McBrien, D. O'Neill, P. Clark, M. Fulton, J. Gillanders, M. Dobson, T. W. Chen, D. E. Wright, and J. Anderson, "ATLAS Transient Discovery Report for 2019-12-29", Transient Name Server Discovery Report **2019-2726**, 1 (2019).

[482] R. Leadbeater, "Transient Classification Report for 2020-03-25", Transient Name Server Classification Report **2020-1512**, 1 (2020).

[483] P. Wiggins, "Transient Discovery Report for 2020-02-27", Transient Name Server Discovery Report **2020-653**, 1 (2020).

[484] J. Zhang, A. Gal-Yam, L. Wang, X. Wang, L. Xing, Y. Yang, and S. Schulze, "Transient Classification Report for 2020-04-12", Transient Name Server Classification Report **2020-1516**, 1 (2020).

[485] F. Forster, F. E. Bauer, G. Pignata, J. Arredondo, G. Cabrera-Vives, R. Carrasco-Davis, P. A. Estevez, P. Huijse, E. Reyes, I. Reyes, P. Sanchez-Saez, C. Valenzuela, E. Castillo, D. Ruz-Mieres, D. Rodriguez-Mancini, F. E. Bauer, M. Catelan, S. Eyheramendy, and M. J. Graham, "ALeRCE/ZTF Transient Discovery Report for 2020-03-31", Transient Name Server Discovery Report **2020-914**, 1 (2020).

[486] J. Burke, D. Hiramatsu, D. A. Howell, C. McCully, E. P. Gonzalez, and C. Pellegrino, "Global SN Project Transient Classification Report for 2020-04-25", Transient Name Server Classification Report **2020-1129**, 1 (2020).

[487] J. Tonry, L. Denneau, A. Heinze, H. Weiland, H. Flewelling, B. Stalder, A. Rest, C. Stubbs, K. W. Smith, S. J. Smartt, D. R. Young, S. Srivastav, O. McBrien, D. O'Neill, P. Clark, M. Fulton, J. Gillanders, M. Dobson, T. W. Chen, D. E. Wright, and J. Anderson, "ATLAS Transient Discovery Report for 2020-04-22", Transient Name Server Discovery Report **2020-1094**, 1 (2020).

[488] R. S. Teja, A. Singh, D. K. Sahu, G. C. Anupama, B. Kumar, and N. A. J., "SN 2020jfo: A Short-plateau Type II Supernova from a Low-mass Progenitor", Astrophysical Journal **930**, 34, 34 (2022).

[489] R. S. Teja, A. Singh, D. K. Sahu, G. C. Anupama, B. Kumar, and N. A. J., "SN 2020jfo: A Short-plateau Type II Supernova from a Low-mass Progenitor", Astrophysical Journal **930**, 34, 34 (2022).

[490] J. Sollerman, S. Yang, S. Schulze, N. L. Strotjohann, A. Jerkstrand, S. D. Van Dyk, E. C. Kool, C. Barbarino, T. G. Brink, R. Bruch, K. De, A. V. Filippenko, C. Fremling, K. C. Patra, D. Perley, L. Yan, Y. Yang, I. Andreoni, R. Campbell, M. Coughlin, M. Kasliwal, Y. .-. Kim, M. Rigault, K. Shin, A. Tzanidakis, M. C. B. Ashley, A. M. Moore, and T. Travouillon, "The Type II supernova SN 2020jfo in M 61, implications for progenitor system, and explosion dynamics", Astronomy and Astrophysics **655**, A105, A105 (2021).

[491] J. Nordin, V. Brinnel, M. Giomi, J. V. Santen, A. Gal-Yam, O. Yaron, and S. Schulze, "ZTF Transient Discovery Report for 2020-05-06", Transient Name Server Discovery Report **2020-1248**, 1 (2020).

[492] D. Hiramatsu, J. Burke, I. Arcavi, D. A. Howell, C. McCully, C. Pellegrino, and S. Valenti, "Global SN Project Transient Classification Report for 2020-06-13", Transient Name Server Classification Report **2020-1789**, 1 (2020).

[493] K. De, "ZTF Transient Discovery Report for 2020-06-12", Transient Name Server Discovery Report **2020-1770**, 1 (2020).

[494] C. Balcon, "Transient Classification Report for 2020-06-22", Transient Name Server Classification Report **2020-1887**, 1 (2020).

[495] F. Forster, F. E. Bauer, L. Galbany, G. Pignata, E. Camacho, J. Silva-Farfan, J. Arredondo, G. Cabrera-Vives, R. Carrasco-Davis, P. A. Estevez, P. Huijse, E. Reyes, I. Reyes, P. Sanchez-Saez, C. Valenzuela, E. Castillo, D. Ruz-Mieres, D. Rodriguez-Mancini, F. E. Bauer, M. Catelan, S. Eyheramendy, and M. J. Graham, "ALeRCE/ZTF Transient Discovery Report for 2020-06-13", Transient Name Server Discovery Report **2020-1774**, 1 (2020).

[496] R. Cartier, C. Corco, and C. Briceno, "Transient Classification Report for 2020-10-09", Transient Name Server Classification Report **2020-3072**, 1 (2020).

[497] S. T. Hodgkin, E. Breedt, A. Delgado, D. L. Harrison, M. V. Leeuwen, G. Rixon, T. Wevers, A. Yoldas, N. Ihanec, K. Kruszyńska, K. A. Rybicki, Ł. Wyrzykowski, Z. Kostrzewa-Rutkowska, D. Eappachen, and G. Marton, "GaiaAlerts Transient Discovery Report for 2020-07-08", Transient Name Server Discovery Report **2020-2061**, 1 (2020).

[498] A. Dahiwale and C. Fremling, "ZTF Transient Classification Report for 2020-01-14", Transient Name Server Classification Report **2020-1482**, 1 (2020).

[499]F. Forster, G. Pignata, F. E. Bauer, J. Arredondo, G. Cabrera-Vives, R. Carrasco-Davis, P. A. Estevez, P. Huijse, E. Reyes, I. Reyes, P. Sanchez-Saez, C. Valenzuela, E. Castillo, D. Ruz-Mieres, D. Rodriguez-Mancini, F. E. Bauer, M. Catelan, S. Eyheramendy, and M. J. Graham, "ALeRCE/ZTF Transient Discovery Report for 2020-01-07", Transient Name Server Discovery Report **2020-67**, 1 (2020).

[500]T. Nakaoka, "Transient Classification Report for 2020-07-31", Transient Name Server Classification Report **2020-2351**, 1 (2020).

[501]K. De and M. Hankins, "Gattini Transient Discovery Report for 2020-07-30", Transient Name Server Discovery Report **2020-2334**, 1 (2020).

[502]S. Schulze, I. Irani, E. Zimmerman, R. Bruch, and O. Yaron, "ePESSTO+ Transient Classification Report for 2020-01-16", Transient Name Server Classification Report **2020-160**, 1 (2020).

[503]F. Forster, G. Pignata, F. E. Bauer, J. Arredondo, G. Cabrera-Vives, R. Carrasco-Davis, P. A. Estevez, P. Huijse, E. Reyes, I. Reyes, P. Sanchez-Saez, C. Valenzuela, E. Castillo, D. Ruz-Mieres, D. Rodriguez-Mancini, F. E. Bauer, M. Catelan, S. Eyheramendy, and M. J. Graham, "ALeRCE/ZTF Transient Discovery Report for 2020-01-13", Transient Name Server Discovery Report **2020-115**, 1 (2020).

[504]R. Amaro, M. Lundquist, J. Andrews, Y. Dong, S. Valenti, D. Sand, A. Bostroem, and S. Wyatt, "DLT40 Transient Classification Report for 2020-11-11", Transient Name Server Classification Report **2020-3422**, 1 (2020).

[505]S. Valenti, D. J. Sand, S. Wyatt, M. Lundquist, R. Amaro, J. Andrews, J. Jencson, and Y. Dong, "DLT40 Transient Discovery Report for 2020-11-10", Transient Name Server Discovery Report **2020-3404**, 1 (2020).

[506]A. Dahiwale and C. Fremling, "ZTF Transient Classification Report for 2021-01-18", Transient Name Server Classification Report **2021-193**, 1–193 (2021).

[507]A. Munoz-Arancibia, A. Mourao, F. Forster, F. E. Bauer, L. Hernandez-Garcia, G. Pignata, L. Galbany, E. Camacho, J. Silva-Farfan, J. Arredondo, G. Cabrera-Vives, R. Carrasco-Davis, P. A. Estevez, P. Huijse, E. Reyes, I. Reyes, P. Sanchez-Saez, C. Valenzuela, E. Castillo, D. Ruz-Mieres, D. Rodriguez-Mancini, M. Catelan, S. Eyheramendy, and M. J. Graham, "ALeRCE/ZTF Transient Discovery Report for 2021-01-12", Transient Name Server Discovery Report **2021-112**, 1–112 (2021).

[508]M. Chu, A. Dahiwale, and C. Fremling, "ZTF Transient Classification Report for 2021-11-23", Transient Name Server Classification Report **2021-4007**, 1–4007 (2021).

[509]C. Fremling, "ZTF Transient Discovery Report for 2021-10-30", Transient Name Server Discovery Report **2021-3692**, 1–3692 (2021).

[510]S. Benetti, L. Tartaglia, R. Carini, F. Ragosta, A. Pastorello, and S. Smartt, "ePESSTO+ Transient Classification Report for 2021-11-11", Transient Name Server Classification Report **2021-3872**, 1–3872 (2021).

[511]J. Tonry, L. Denneau, A. Heinze, H. Weiland, B. Stalder, A. Rest, C. Stubbs, K. W. Smith, S. J. Smartt, D. R. Young, S. Srivastav, M. Fulton, J. Gillanders, T. Moore, C. Richman, L. Cai, T. W. Chen, D. E. Wright, and J. Anderson, "ATLAS Transient Discovery Report for 2021-11-01", Transient Name Server Discovery Report **2021-3717**, 1–3717 (2021).

[512]K. Atapin, A. Dodin, A. Tatarnikov, D. Tsvetkov, N. Shatski, A. Belinski, L. Galbany, A. Munoz-Arancibia, F. Forster, F. E. Bauer, L. Hernandez-Garcia, G. Pignata, E. Camacho, J. Silva-Farfan, A. Mourao, J. Arredondo, G. Cabrera-Vives, R. Carrasco-Davis, P. A. Estevez, P. Huijse, E. Reyes, I. Reyes, P. Sanchez-Saez, C. Valenzuela, E. Castillo, D. Ruz-Mieres, D. Rodriguez-Mancini, M. Catelan, S. Eyheramendy, and M. J. Graham, "ALeRCE Transient Classification Report for 2021-11-09", Transient Name Server Classification Report **2021-3842**, 1–3842 (2021).

[513]A. Munoz-Arancibia, F. Forster, F. E. Bauer, G. Pignata, A. Mourao, L. Hernandez-Garcia, L. Galbany, E. Camacho, J. Silva-Farfan, J. Arredondo, G. Cabrera-Vives, R. Carrasco-Davis, P. A.

Estevez, P. Huijse, E. Reyes, I. Reyes, P. Sanchez-Saez, C. Valenzuela, E. Castillo, D. Ruz-Mieres, D. Rodriguez-Mancini, M. Catelan, S. Eyheramendy, and M. J. Graham, "ALeRCE/ZTF Transient Discovery Report for 2021-11-05", Transient Name Server Discovery Report **2021-3767**, 1–3767 (2021).

[514] I. Seitenzahl, J. P. Anderson, L. Galbany, and R. J. Bruch, "ePESSTO+ Transient Classification Report for 2021-12-04", Transient Name Server Classification Report **2021-4093**, 1–4093 (2021).

[515] K. De, "ZTF Transient Discovery Report for 2021-11-14", Transient Name Server Discovery Report **2021-3913**, 1–3913 (2021).

[516] S. Ciroi, G. Pignata, S. Benetti, E. Cappellaro, A. Pastorello, A. Reguitti, and L. Tomasella, "Padova-Asiago Transient Classification Report for 2021-03-21", Transient Name Server Classification Report **2021-864**, 1–864 (2021).

[517] S. Valenti, D. J. Sand, S. Wyatt, M. Lundquist, R. Amaro, J. Andrews, J. Jencson, Y. Dong, S. Davis, and D. Janzen, "DLT40 Transient Discovery Report for 2021-03-20", Transient Name Server Discovery Report **2021-837**, 1–837 (2021).

[518] E. Zimmerman, S. Schulze, J. Johansson, Y. Yang, D. Perley, R. Bruch, and A. Gal-Yam, "ZTF early discovery and rapid follow-up of two very nearby infant SNe: ZTF21aaqhhfu / 2021gno and ZTF21aaqgmjt / 2021gmj", Transient Name Server AstroNote **91**, 1–91 (2021).

[519] D. Perley, "ZTF Transient Classification Report for 2021-04-02", Transient Name Server Classification Report **2021-1009**, 1–1009 (2021).

[520] R. Bruch, E. Zimmerman, and J. Johansson, "ZTF Transient Discovery Report for 2021-03-20", Transient Name Server Discovery Report **2021-843**, 1–843 (2021).

[521] J. Tonry, L. Denneau, A. Heinze, H. Weiland, B. Stalder, A. Rest, C. Stubbs, K. W. Smith, S. J. Smartt, D. R. Young, S. Srivastav, O. McBrien, M. Fulton, J. Gillanders, C. Webb, T. W. Chen, D. E. Wright, and J. Anderson, "ATLAS Transient Discovery Report for 2021-05-21", Transient Name Server Discovery Report **2021-1743**, 1–1743 (2021).

[522] M. R. Siebert, K. Davis, S. Tinyanont, R. J. Foley, and E. Strasburger, "UCSC Transient Classification Report for 2021-07-09", Transient Name Server Classification Report **2021-2383**, 1–2383 (2021).

[523] C. Fremling, "ZTF Transient Discovery Report for 2021-07-07", Transient Name Server Discovery Report **2021-2352**, 1–2352 (2021).

[524] J. Tonry, L. Denneau, A. Heinze, H. Weiland, B. Stalder, A. Rest, C. Stubbs, K. W. Smith, S. J. Smartt, D. R. Young, S. Srivastav, O. McBrien, M. Fulton, J. Gillanders, C. Webb, T. W. Chen, D. E. Wright, and J. Anderson, "ATLAS Transient Discovery Report for 2021-07-09", Transient Name Server Discovery Report **2021-2372**, 1–2372 (2021).

[525] M. Williamson, M. Modjaz, C. Pellegrino, G. Hosseinzadeh, J. Burke, D. Hiramatsu, D. A. Howell, C. McCully, M. Newsome, E. P. Gonzalez, and A. Filippenko, "Transient Classification Report for 2021-09-10", Transient Name Server Classification Report **2021-3130**, 1–3130 (2021).

[526] J. Tonry, L. Denneau, A. Heinze, H. Weiland, B. Stalder, A. Rest, C. Stubbs, K. W. Smith, S. J. Smartt, D. R. Young, S. Srivastav, M. Fulton, J. Gillanders, C. Richman, T. W. Chen, D. E. Wright, and J. Anderson, "ATLAS Transient Discovery Report for 2021-09-08", Transient Name Server Discovery Report **2021-3093**, 1–3093 (2021).

[527] M. M. Kasliwal, N. Degenaar, and D. Polishook, "FIRE Classification of iPTF13bvn", The Astronomer's Telegram **5151**, 1 (2013).

[528] Y. Cao, E. Gorbikov, I. Arcavi, E. Ofek, A. Gal-Yam, P. Nugent, and M. Kasliwal, "iPTF discovery of a young SN candidate at z=0.00449", The Astronomer's Telegram **5137**, 1 (2013).

Appendix A: Host Galaxy Tables

Supernova	Host galaxy name	Host galaxy distance (Mpc)	Distance error	Method	Host galaxy extinction (Av)	MW extinction (Av)	Host galaxy inclination (deg)
SN2000db	NGC 3949	15.66	1.12	Virgo infall			56
SN2000ds	NGC 2768	22.39	2.62	SBF [36]			90
SN2000ew	NGC 3810	10.85	3.50	Virgo infall	0.15 [37]	0.121	48.2
SN2001B	IC 391	25.8	1.8	Virgo infall			18.1
SN2001X	NGC 5921	24.3	1.7	Virgo infall			49.5
SN2001du	NGC 1365	17.22	0.40	Cepheids [38]			62.6
SN2001fv	NGC 3512	25.3	1.82	Virgo infall			31.7
SN2001fz	NGC 2280	25.48	1.79	Virgo infall			66.2
SN2001gd	NGC 5033	15.28	0.65	Sosie [39]		0.032	64.6
SN2001hg	NGC 4162	26.79	3.55	Sosie [39]			55.1
SN2001ig	NGC 7424	12.91	0.9	Virgo infall	0.06 [40]	0.029	59
SN2002E	NGC 4129	18.72	1.35	Virgo infall		0.196	90
SN2002ao	UGC 9299	25.1	1.8	Virgo infall			69.6
SN2002ap	NGC 0628	10.09	0.14	TRGB [41]	0.06 [42]	0.192	19.8
SN2002bu	NGC 4242	8.82	0.62	Virgo infall	0.012 [43]	0.033	51.5
SN2002hc	NGC 2559	16.52	2.02	Sosie [39]		0.599	63.5
SN2002hh	NGC 6946	5.41	1	EPM [44]	5 [45]	0.938	18.3
SN2002ji	NGC 3655	23.99	2.93	Sosie [39]			47.5
SN2002jz	UGC 02984	22.93	1.61	Virgo infall		1.546	60
SN2003B	NGC 1097A	16.7	1.2	Virgo infall		0.075	90
SN2003J	NGC 4157	15.47	1.1	Virgo infall		0.058	90
SN2003Z	NGC 2742	23.65	1.67	Virgo infall			60.7
SN2003am	ESO 576-040	29.31	0.52	SN Ia [46]			78

Supernova	Host galaxy name	Host galaxy distance (Mpc)	Distance error	Method	Host galaxy extinction (Av)	MW extinction (Av)	Host galaxy inclination (deg)
SN2003bg	ESO 420- G 009	16.4	1.1	Virgo infall	0.073 [47]	0.062	41.7
SN2003bk	NGC 4316	14.12	1	Virgo infall			82
SN2003ci	NGC 3079	21.02	1.49	Virgo infall		0.031	90
SN2003ed	NGC 5303	27.15	1.94	Virgo infall			62.4
SN2003gd	NGC 0628	10.09	0.14	TRGB [41]	0.238 [48]	0.192	19.8
SN2003hl	NGC 0772	17.7		EPM [49]			59.6
SN2003hn	NGC 1448	16.60	0.26	SN Ia [50]	0.043 [51]	0.039	86.4
SN2003ie	NGC 4051	12.71	0.9	Virgo infall		0.036	48.7
SN2003iq	NGC 0772	17.7		EPM [49]			59.6
SN2003jg	NGC 2997	14.2	1.01	Virgo infall	4 [52]	0.296	53.7
SN2004A	NGC 6207	18.29	1.3	Virgo infall	0.598 [53]	0.042	64.7
SN2004C	NGC 3683	28.2	2	Virgo infall			69
SN2004G	NGC 5668	25.9	1.8	Virgo infall			33
SN2004am	NGC 3034	3.27	0.20	SN Ia [54]	5 [55]	0.429	76.9
SN2004ao	UGC 10862	29	2.04	Virgo infall			53.4
SN2004bm	NGC 3437	23.37	1.69	Virgo infall			72.8
SN2004cc	NGC 4568	19.68	1.02	Sosie [39]			67.5
SN2004cm	NGC 5486	24.4	1.7	Virgo infall			61.1
SN2004cz	ESO 407-009	21.98	1.54	Virgo infall			69.7
SN2004dg	NGC 5806	21.38	0.80	Sosie [39]			60.4
SN2004dj	NGC 2403	3.13	0.15	Cepheids [56]	0.42 [48]	0.11	61.3
SN2004dk	NGC 6118	26.77	1.89	Virgo infall			68.7
SN2004ep	IC 2152	23.5	1.6	Virgo Infall			49.5

Supernova	Host galaxy name	Host galaxy distance (Mpc)	Distance error	Method	Host galaxy extinction (Av)	MW extinction (Av)	Host galaxy inclination (deg)
SN2004et	NGC 6946	5.41	1	EPM [44]	0.217 [53]	0.938	18.3
SN2004fc	NGC 701	21.28	1.63	Sosie [39]			62.5
SN2004gn	NGC 4527	13.95	0.85	Cepheids [57]		0.06	81.2
SN2004gq	NGC 1832	14.19	2.95	Sosie [39]		0.2	71.8
SN2004gt	NGC 4038	24.33	0.56	SN Ia [46]			51.9
SN2005V	NGC 2146	18.21	1.28	Virgo infall			37.4
SN2005ad	NGC 0941	23.14	1.62	Virgo infall			45.7
SN2005ae	ESO 209-009	13.7	0.97	Virgo infall		0.708	90
SN2005af	NGC 4945	3.47	0.04	TRGB [58]	0.083 [59]	0.484	90
SN2005at	NGC 6744	9.33	0.44	Sosie [39]	1.8 [60]	0.118	53.5
SN2005av	NGC 6943	28.71	1.77	Sosie [39]			54.6
SN2005ay	NGC 3938	15.28	1.09	Virgo infall	0.252 [61]	0.058	17.6
SN2005cs	NGC 5194	8.9	0.63	Virgo infall	0.43 [48]	0.096	32.6
SN2005cz	NGC 4589	20.4		SBF [62]			56.2
SN2005kl	NGC 4369	20.28	1.46	Virgo infall			18.6
SN2006bc	NGC 2397	16.94	1.2	Virgo infall			80.5
SN2006bp	NGC 3953	18.82	1.04	EPM [44]			62.3
SN2006jc	UGC 04904	26.2	1.9	Virgo infall			52.2
SN2006my	NGC 4651	23.55	1.92	Sosie [39]			49.5
SN2006ov	NGC 4303	14.51	1.38	EPM [44]	0.02 [63]	0.061	18.1
SN2007C	NGC 4981	22.28	2.60	Sosie [39]			44.7
SN2007Y	NGC 1187	19.41	1.87	Sosie [39]			44.1
SN2007aa	NGC 4030	26.93	1.97	Virgo infall			47

Supernova	Host galaxy name	Host galaxy distance (Mpc)	Distance error	Method	Host galaxy extinction (Av)	MW extinction (Av)	Host galaxy inclination (deg)
SN2007av	NGC 3279	23.88	1.72	Virgo infall			90
SN2007gr	NGC 1058	10.6	1.9	EPM [44]	0.093 [64]	0.17	58.5
SN2007it	NGC 5530	17.36	1.23	Virgo infall	0.39 [65]	0.316	66.3
SN2007od	UGC 12846	27.63	1.94	Virgo infall			25.7
SN2008S	NGC 6946	5.41	1	EPM [44]		0.938	18.3
SN2008ax	NGC 4490	9.55	6.74	Sosie [39]	1.674 [66]	0.06	90
SN2008bk	NGC 7793	3.21	0.23	Virgo infall	0 [67]	0.053	63.5
SN2008bo	NGC 6643	27.72	1.95	Virgo infall			62.7
SN2008fb	UGC 02813	25.05	1.76	Virgo infall		1.353	76.6
SN2008gz	NGC 3672	21.09	3.461	SN Ia [68]			56.2
SN2008ij	NGC 6643	27.72	1.95	Virgo infall			62.7
SN2008in	NGC 4303	14.51	1.38	EPM [44]		0.061	18.1
SN2008iz	NGC 3034	3.27	0.20	SN Ia [54]	10 [55]	0.429	76.9
SN2008jb	ESO 302- G 014	10.4	0.73	Virgo infall	0.186 [69]	0.024	73.6
SN2009G	IC 4441	28.74	2.02	Virgo infall			65.1
SN2009H	NGC 1084	15.49	1.81	Sosie [39]		0.073	49.9
SN2009N	NGC 4487	14.04	0.99	Virgo infall	0.113 [70]	0.058	58.2
SN2009at	NGC 5301	28.29	2.01	Virgo infall			90
SN2009bw	UGC 02890	15.93	0.32	EPM [44]	0.332 [71]	0.629	90
SN2009dd	NGC 4088	15.35	0.50	Sosie [39]	1.33 [72]	0.054	71.3
SN2009dq	IC 2554	25.59	4.34	Sosie [39]			70.8
SN2009em	NGC 0157	29.11	2.66	Sosie [39]			61.8
SN2009gj	NGC 0134	21.76	1.53	Virgo infall		0.05	90

Supernova	Host galaxy name	Host galaxy distance (Mpc)	Distance error	Method	Host galaxy extinction (Av)	MW extinction (Av)	Host galaxy inclination (deg)
SN2009hd	NGC 3627	11.00	0.43	Cepheids [57]	3.8 [73]	0.091	67.5
SN2009ib	NGC 1559	16	2	EPM [74]	0.4061 [75]	0.082	59.9
SN2009ip	NGC 7259	25.91	1.82	Virgo infall			40.4
SN2009js	NGC 0918	23.23	1.63	Virgo Infall	0.18 [76]	0.968	57.6
SN2009kr	NGC 1832	14.19	2.95	Sosie [39]	0.048	0.2	71.8
SN2009ls	NGC 3423	14.19	1	Virgo infall		0.082	32.1
SN2009md	NGC 3389	23.29	1.96	EPM [44]			66.2
SN2009mk	ESO 293-034	20.53	1.44	Virgo infall			74.6
SN2010br	NGC 4051	12.71	0.9	Virgo infall		0.036	48.7
SN2010gi	IC 4660	24.41	1.71	Virgo infall		0.103	87
SN2011am	NGC 4219	28.51	2.01	Virgo infall			76.1
SN2011aq	NGC 1056	24.39	1.71	Virgo infall			46.7
SN2011dh	NGC 5194	7.49	0.14	EPM [44]	0.15 [77]	0.096	32.6
SN2011dq	NGC 0337	24.03	1.69	Virgo infall			50.6
SN2011hp	NGC 4219	28.51	2.01	Virgo infall			76.1
SN2011hs	IC 5267	23.78	1.67	Virgo infall			47.8
SN2011ht	UGC 05460	20.69	1.47	Virgo infall			39.7
SN2011jm	NGC 4810	7.09	0.66	Virgo infall		0.093	72.4
SN2012A	NGC 3239	8.76	0.61	Virgo infall	[78]	0.088	46.8
SN2012P	NGC 5806	21.38	0.80	Sosie [39]			60.4
SN2012au	NGC 4790	22.7		TF [79]			58.8
SN2012aw	NGC 3351	9.75	0.41	Cepheids [57]	0.157 [80]	0.076	54.6

Supernova	Host galaxy name	Host galaxy distance (Mpc)	Distance error	Method	Host galaxy extinction (Av)	MW extinction (Av)	Host galaxy inclination (deg)
SN2012cc	NGC 4419	13.49	1.65	SBF [81]		0.091	84.7
SN2012cw	NGC 3166	18.62	1.33	Virgo infall			56.2
SN2012dj	NGC 7531	21.99	1.54	Virgo infall			68.9
SN2012ec	NGC 1084	15.49	1.81	Sosie [39]	0.268[82]	0.073	49.9
SN2012fh	NGC 3344	9.82	1.27	TRGB [58]	0 [83]	0.091	18.7
SN2012hb	ESO 090-015	20.3	1.4	Virgo infall			64.4
SN2012hc	NGC 0986A	18.64	1.31	Virgo infall			90
SN2012hn	NGC 2272	28.85	2.03	Virgo infall			57.4
SN2012hs	ESO 213- G 002	26.22	1.85	Virgo infall			29.6
SN2013F	IC 5325	19.2	1.4	Virgo infall			25.3
SN2013K	ESO 009-010	28.05	1.46	Sosie [39]			51
SN2013ab	NGC 5669	25.35	1.82	Virgo infall	0.0614[84]	0.075	56.8
SN2013ak	ESO 430- G 020	12	0.8	Virgo infall		1.253	70.3
SN2013am	NGC 3623	7.81	0.57	Virgo infall	1.705 [85]	0.068	90
SN2013bu	NGC 7331	14.85	0.58	Cepheids [57]		0.25	70
SN2013by	ESO 138- G 010	15.89	1.12	Virgo infall	0 [86]	0.603	49.2
SN2013df	NGC 4414	17.41	0.42	Cepheids [57]	0.226 [87]	0.053	56.6
SN2013dk	NGC 4039	13.31	1.08	TRGB [88]	0.617 [89]	0.127	71.2
SN2013ee	NGC 3079	21.02	1.49	Virgo infall		0.031	90
SN2013ej	NGC 628	10.09	0.14	TRGB [41]	0 [86]	0.192	19.8
SN2013ff	NGC 2748	26.91	1.89	Virgo infall			68.1
SN2013gc	ESO 430- G 020	12	0.8	Virgo infall	0	1.253[90]	70.3
SN2013ge	NGC 3287	23.51	1.69	Virgo infall	0.1457 [91]	0.063	75.3

Supernova	Host galaxy name	Host galaxy distance (Mpc)	Distance error	Method	Host galaxy extinction (Av)	MW extinction (Av)	Host galaxy inclination (deg)
SN2014A	NGC 5054	14.72	1.65	Sosie [39]		0.226	56.9
SN2014C	NGC 7331	14.85	0.58	Cepheids [92]	1.86 [93]	0.25	70
SN2014G	NGC 3448	25.05	1.78	Virgo infall			79.2
SN2014bc	NGC 4258	7.59	0.21	Cepheids [57]	0.0434 [94]	0.045	68.3
SN2014bi	NGC 4096	10.36	0.73	Virgo infall		0.05	80.6
SN2014cl	IC 0217	26.62	1.87	Virgo infall			82.6
SN2014cx	NGC 0337	24.03	1.69	Virgo infall			50.6
SN2014cy	NGC 7742	26.12	1.83	Virgo infall			16.8
SN2014df	NGC 1448	20.36	0.74	SNIa [95]			86.4
SN2014do	ESO 431-G2	22.45	1.58	Virgo infall			47.4
SN2014dq	ESO 467- G 051	26.28	1.84	Virgo infall			90
SN2014ge	NGC 3344	9.82	1.27	TRGB [96]		0.091	18.7
SN2015G	NGC 6951	22.09	1.16	SN Ia [95]			50.8
SN2015V	UGC 11000	25.78	1.81	Virgo infall			69.7
SN2015an	IC 2367	25.00	4.10	Sosie [39]			61.3
SN2015aq	UGC 05015	27.6	1.95	Virgo infall			20.5
SN2015as	UGC 05460	20.69	1.47	Virgo infall			39.7
SN2016B	CGCG 012-116	25.61	1.9	Virgo infall			52.5
SN2016C	NGC 5247	22.31	1.6	Virgo infall			38.5
SN2016G	NGC 1171	27.67	5.90	Sosie [39]			64.9
SN2016X	UGC 08041	26.51	1.96	Virgo infall	0.05[97]	0.061	54
SN2016adj	NGC 5128	3.42	0.33	Cepheids [98]	1.542 [99]	0.315	45.3
SN2016aqf	NGC 2101	14.68	1.03	Virgo infall	0.096 [100]	0.151	69.1

Supernova	Host galaxy name	Host galaxy distance (Mpc)	Distance error	Method	Host galaxy extinction (Av)	MW extinction (Av)	Host galaxy inclination (deg)
SN2016bau	NGC 3631	22.36	1.59	Virgo infall			34.7
SN2016bkv	NGC 3184	9.77	0.69	Virgo infall	0 [101]	0.046	14.4
SN2016coi	UGC 11868	19.46	1.36	Virgo infall			25.5
SN2016cok	NGC 3627	11.00	0.43	Cepheids [57]	1.459[102]	0.091	67.5
SN2016gkg	NGC 0613	20.05	1.41	Virgo infall			35.7
SN2016iae	NGC 1532	12.91	0.91	Virgo infall			83
SN2017aym	NGC 5690	29.94	2.12	Virgo infall			75.9
SN2017bzb	NGC 7424	12.91	0.91	Virgo infall		0.029	59
SN2017eaw	NGC 6946	6.73	0.16	TRGB [103]	0 [85]	0.938	18.3
SN2017ein	NGC 3938	15.28	1.09	Virgo infall	1.26 [104]	0.058	17.6
SN2017gax	NGC 1672	16.45	1.15	Virgo infall		0.064	28.9
SN2017gkk	NGC 2748	26.91	1.89	Virgo infall			68.1
SN2017gmr	NGC 0988	16.00	1.79	Sosie [39]	1.066 [105]	0.074	69.1
SN2017hpi	AM 0813-284	23.11	1.63	Virgo infall			90
SN2017iro	NGC 5480	20.2		Sosie [106]			41.5
SN2017ivh	NGC 5254	29.24	1.52	Sosie [39]			67.2
SN2017izl	ESO 269-085	20.51	1.57	Sosie [39]			58.9
SN2017jmk	NGC 7541	24.77	4.33	SN Ia [68]			74.8
SN2018aoq	NGC 4151	19.67	1.42	Virgo infall	0.05 [107]	0.074	42
SN2018get	UGC 03912	18.25	1.29	Virgo infall			37.6
SN2018gj	NGC 6217	25.95	1.82	Virgo infall			44.8
SN2018hna	UGC 07534	15.34	1.09	Virgo infall	1.425 [108]	0.032	41.4
SN2018imf	VCC 1931	14.12	1	Virgo infall		0.071	52.1

Supernova	Host galaxy name	Host galaxy distance (Mpc)	Distance error	Method	Host galaxy extinction (Av)	MW extinction (Av)	Host galaxy inclination (deg)
SN2018is	NGC 5054	14.72	1.65	Sosie [39]		0.226	56.9
SN2018ivc	NGC 1068	16.48	1.16	Virgo infall	1.147 [109]	0.091	34.7
SN2018lei	NGC 0986	26.36	1.85	Virgo infall			40
SN2018zd	NGC 2146	18.21	1.28	Virgo infall			37.4
SN2019ci	MCG -01-25-033	26.5	1.9	Virgo infall			72.4
SN2019edo	NGC 4162	26.79	3.55	Sosie [39]			55.1
SN2019ehk	NGC 4321	14.92	0.47	Cepheids [98]	1.05 [110]	0.072	24
SN2019ejj	ESO 430- G 020	12.91	0.91	Virgo infall	0[111]	1.253	70.3
SN2019esa	ESO 035-018	22.97	1.61	Virgo infall			82.6
SN2019fcn	ESO 430- G 020	12.91	0.91	Virgo infall	0[111]	1.253	70.3
SN2019yvr	NGC 4666	28.16	2.05	Virgo infall	2.332 [112]	0.068	69.6
SN2020dpw	NGC 6951	22.09	1.16	SN Ia [95]			50.8
SN2020fqv	NGC 4568	19.68	1.02	Sosie [39]			67.5
SN2020hvp	NGC 6118	26.77	1.89	Virgo infall			68.7
SN2020jfo	NGC 4303	12.31	0.59	EPM [44]		0.061	18.1
SN2020mjm	UGC 09299	26.99	1.92	Virgo infall			69.6
SN2020mmz	NGC 2814	28.19	1.98	Virgo infall			90
SN2020ocz	UGCA 103	11.89	0.83	Virgo infall		0.034	27.1
SN2020oi	NGC 4321	14.2		Cepheids [57]	0 [113]	0.072	24
SN2020qmp	UGC 07125	21.31	1.54	Virgo infall			90
SN2020vg	NGC 3915	28.13	2.02	Virgo infall			62.9
SN2020zbv	NGC 1448	14.42	1.01	Virgo infall		0.039	86.4
SN2021aai	NGC 2268	29.38	3.28	Sosie [39]			67.6

Supernova	Host galaxy name	Host galaxy distance (Mpc)	Distance error	Method	Host galaxy extinction (Av)	MW extinction (Av)	Host galaxy inclination (deg)
SN2021acna	NGC 3972	20.8		Cepheids [114]			81.1
SN2021aczp	NGC 2935	24.89	3.69	SN Ia [68]			42.8
SN2021adlw	NGC 3813	27.26	1.95	Virgo infall			57.6
SN2021aess	NGC 1359	26.97	1.89	Virgo infall			37.7
SN2021gmj	NGC 3310	19.37	1.38	Virgo infall			16.1
SN2021gno	NGC 4165	14.12	1.29	Virgo infall	0 [115]	0.097	61.8
SN2021mwj	NGC 2935	24.89	3.69	SN Ia [68]			42.8
SN2021sjt	NGC 6951	22.09	1.12	SN Ia [95]			50.8
SN2021suk	MRK 1039	29.64	2.08	Virgo infall			75.6
SN2021yja	NGC 1325	21.41	1.5	Virgo infall			74.4
iPTF13bvn	NGC 5806	21.38	0.80	Sosie [39]			60.4

Appendix B: Core-Collapse Supernova Tables

Supernova	Apparent magnitude	Absolute magnitude	Absolute magnitude limits (upper, lower)	Filter	Age at time of discovery	Type	Amateur or no
SN2000db						II [116]	yes [117]
SN2000ds						Ib [118]	yes [119]
SN2000ew	14.9 [120]	-15.48	-16.09, -14.63	unfiltered	14 days past max [120]	Ic [118]	yes [120]
SN2001B						Ib [121]	no [122]
SN2001X						II P [123]	no [124]
SN2001du						II P [125]	yes [126]
SN2001fv						II [127]	no [128]
SN2001fz						II [129]	no [130]
SN2001gd	16.2 [131]			unfiltered	-	II b [132]	yes [131]
SN2001hg						II [133]	yes [134]
SN2001ig	12.3 [135]	-18.34	-18.49, -18.19	V	7 days after explosion [40]	II b [136]	yes [137]
SN2002E	16.8 [138]			unfiltered	Past max [139]	II [139]	no [139]
SN2002ao						II b [140]	no [141]
SN2002ap	12.38 [142]	-17.89	-17.92, -17.86	V	7 days before peak [142]	Ic [143]	yes [144]
SN2002bu	15.23 [145]	-14.54	-14.69, -14.38	V	5 days before peak [146]	Gap [146]	yes [147]
SN2002hc	17 [148]			unfiltered	-	II [148]	no [148]
SN2002hh	12.3 [45]	-18.04	-18.41, -17.60	J	21 after explosion [45]	II [149]	no [150]
SN2002ji						Ib/c [151]	no [152]
SN2002jz	15.9 [153]			unfiltered	-	Ic [154]	yes [153]
SN2003B	15[155]			V	14 days after peak [155]	II [156]	yes [155]
SN2003J	16.7 [157]			unfiltered	several days before peak [157]	II [158]	yes [157]
SN2003Z						II [159]	no [160]
SN2003am						II [161]	no [162]

Supernova	Apparent magnitude	Absolute magnitude	Absolute magnitude limits (upper, lower)	Filter	Age at time of discovery	Type	Amateur or no
SN2003bg	15 [163]	-16.18	-16.32, -16.02	unfiltered	14 after explosion [164]	Ic-pec [165]	yes [163]
SN2003bk						II [166]	no [167]
SN2003ci	17.5 [168]			unfiltered	21 days after explosion [169]	II [169]	no [168]
SN2003ed						II [170]	yes [171]
SN2003gd	13.2 [172]	-17.25	-17.28, -17.22	V	Roughly 2 months after explosion [173]	II [174]	yes [172]
SN2003hl						II [175]	no [176]
SN2003hn	14.1 [177]	-17.08	-17.12, -17.05	V	2 weeks after explosion [178]	II [178]	yes [177]
SN2003ie	15.18 [179]			V	-	II P [180]	yes [179]
SN2003iq						II [181]	yes [182]
SN2003jg	17 [183]	-16.99	-17.14, -16.83	unfiltered	several weeks past max [184]	Ib/c [184]	no [183]
SN2004A	15.5 [185]	-16.45	-16.60, -16.29	V	Few days before max [185]	II [186]	yes [187]
SN2004C						Ic [188]	no [189]
SN2004G						II [190]	yes [191]
SN2004am	12 [192]	-16.19	-16.32, -16.05	K_s		II [193]	no [194]
SN2004ao						Ib [195]	no [196]
SN2004bm						Ic [197]	no [198]
SN2004cc						Ic [199]	no [200]
SN2004cm						II [201]	no [201]
SN2004cz						II P [202]	no [203]
SN2004dg						II P [204]	yes [205]
SN2004dj	11.99 [206]	-16.02	-16.12, -15.91	V	36 days after explosion [206]	II P [207]	yes [208]
SN2004dk						Ic [209]	no [210]
SN2004ep						II [211]	no [212]

Supernova	Apparent magnitude	Absolute magnitude	Absolute magnitude limits (upper, lower)	Filter	Age at time of discovery	Type	Amateur or no
SN2004et	12.2 [213]	-17.33	-17.70, -16.89	R	-	II [214]	no [215]
SN2004fc						II [216]	no [217]
SN2004gn	16.6 [218]			unfiltered	-	Ic [219]	no [218]
SN2004gq	15.4 [220]			unfiltered	4 days before max [220]	Ib [221]	no [220]
SN2004gt						Ib/c [222]	yes [223]
SN2005V						Ib/c [224]	no [225]
SN2005ad						II [226]	yes [227]
SN2005ae	15.9 [228]			V	-	II b [229]	yes [228]
SN2005af	12.6 [230]	-15.67	-15.69, -15.64	V	1 month after explosion [231]	II [231]	no [231]
SN2005at	14.3 [60]	-17.47	-17.57, -17.36	V	2 weeks past max [232]	Ic [60]	yes [60]
SN2005av						II n [233]	yes [234]
SN2005ay	15.2 [61]	-16.03	-16.18, -15.87	V	8-10 days after explosion [61]	II [235]	yes [236]
SN2005cs	14.45 [61]	-15.82	-15.97, -15.66	V	3 days after explosion [61]	II [237]	no [238]
SN2005cz						Ib [239]	yes [240]
SN2005kl						Ic [241]	yes [242]
SN2006bc						II [243]	yes [244]
SN2006bp						II [245]	yes [246]
SN2006jc						Ib/c [247]	no [247]
SN2006my						II [248]	yes [249]
SN2006ov	15.2 [250]	-15.67	-15.87, -15.45	unfiltered	several months after explosion [250]	II [251]	yes [252]
SN2007C						Ib [253]	yes [254]
SN2007Y						Ib/c [255]	yes [256]
SN2007aa						II [257]	yes [258]

Supernova	Apparent magnitude	Absolute magnitude	Absolute magnitude limits (upper, lower)	Filter	Age at time of discovery	Type	Amateur or no
SN2007av						II [259]	yes [260]
SN2007gr	12.91 [64]	-17.48	-17.84, -17.05	V	soon after explosion [64]	Ib/c [261]	no [262]
SN2007it	13.5 [65]	-18.40	-18.55, -18.24	V	7 days after explosion [65]	II [263]	no [263]
SN2007od						II [264]	no [265]
SN2008S	16.87 [266]			V	shortly after explosion [266]	II n [267]	yes [268]
SN2008ax	13.55 [269]	-18.08	-19.24, -15.43	V	-	II b [270]	no [271]
SN2008bk	12.94 [67]	-14.65	-14.80, -14.48	V	1 day after explosion [67]	II [272]	yes [273]
SN2008bo						Ib [274]	no [275]
SN2008fb	16.9 [276]			R	several weeks past max [276]	II [276]	no [277]
SN2008gz						II P [278]	yes [279]
SN2008ij						II [280]	yes [281]
SN2008in	15.07 [282]			V	1-2 weeks after core-collapse [282]	II [283]	yes [284]
SN2008iz	16 [55]	-19.40	-19.53, -19.26	unfiltered	2 weeks after explosion [55]	II [285]	no [285]
SN2008jb	13.6 [69]	-16.70	-16.84, -16.54	V	shortly after explosion [69]	II [286]	no [286]
SN2009G						II P [287]	no [288]
SN2009H	16.8 [289]			unfiltered	1 week after explosion [289]	II [289]	no [290]
SN2009N	16.27 [70]	-14.64	-14.79, -14.48	V	few days after peak [70]	II P [291]	yes [292]
SN2009at						II [293]	yes [294]
SN2009bw	14.88 [71]	-17.09	-17.14, -17.05	V	soon after explosion [295]	II [295]	no [296]
SN2009dd	14.76 [72]	-17.55	-17.62, -17.48	V	several days after explosion [297]	II [297]	no [298]
SN2009dq						II b [299]	no [300]
SN2009em						Ic [301]	yes [302]
SN2009gj	15.9 [303]			unfiltered	three weeks after explosion [304]	II b [304]	yes [303]
SN2009hd	16.73 [73]	-17.37	-17.45, -17.28	V	20 days after discovery [73]	II L [73]	yes [305]
SN2009ib	15.81 [75]	-15.70	-15.95, -15.41	V	around explosion [75]	II P [306]	no [306]
SN2009ip						II n [307]	no [308]

Supernova	Apparent magnitude	Absolute magnitude	Absolute magnitude limits (upper,lower)	Filter	Age at time of discovery	Type	Amateur or no
SN2009js	17.28 [76]	-15.70	-15.85, -15.54	V	2 days after explosion [76]	II [309]	yes [310]
SN2009kr	15.6 [311]	-15.35	-15.76, -14.84	unfiltered	young [312]	II [313]	yes [311]
SN2009ls	15.1 [314]			unfiltered	young [315]	II [315]	yes [314]
SN2009md						II [316]	yes [317]
SN2009mk						II b [318]	yes [319]
SN2010br	17.7 [320]			V	-	Ib/c [321]	yes [320]
SN2010gi	15.8 [322]			R	week before peak [323]	II b [323]	no [324]
SN2011am						Ib [325]	yes [325]
SN2011aq						II [326]	no [327]
SN2011dh	15.19 [328]	-14.43	-14.47, -14.39	V	3 days after explosion [328]	II P [329]	yes [329]
SN2011dq						II [330]	yes [330]
SN2011hp						Ic [331]	yes [331]
SN2011hs						II b [332]	yes [332]
SN2011ht						II n [333]	no [334]
SN2011jm	14.8 [335]			unfiltered	2-4 months after peak [335]	Ic [335]	no [335]
SN2012A	14.02 [336]			V	soon after explosion [336]	II [337]	yes [337]
SN2012P						Ib/c [338]	yes [338]
SN2012au						Ib [339]	no [339]
SN2012aw	13.3 [340]	-16.88	-16.97, -16.78	V	Week before peak [340]	II P [341]	yes [341]
SN2012cc	14.9 [342]			unfiltered	Near peak [342]	II [342]	no [342]
SN2012cw						Ic [343]	yes [343]
SN2012dj						Ib/c [344]	yes [344]
SN2012ec	14.8 [345]	-16.31	-16.55, -16.04	Infrared >700 nm	2 days after explosion [53]	II P [346]	yes [345]
SN2012fh	14.7 [347]	-15.35	-15.62, -15.05	V	more than hundred days after explosion [347]	Ib/c [347]	yes [347]
SN2012hb						II [348]	no [348]
SN2012hc						II [349]	no [349]

Supernova	Apparent magnitude	Absolute magnitude	Absolute magnitude limits (upper,lower)	Filter	Age at time of discovery	Type	Amateur or no
SN2012hn						Ic-pec [350]	no [350]
SN2012hs						II [351]	no [351]
SN2013F						Ib/c [352]	no [352]
SN2013K						II P [353]	yes [353]
SN2013ab	14.7 [84]	-17.46	-17.61, -17.29	V	2 days after explosion [84]	II [354]	no [354]
SN2013ak	13.5 [355]			unfiltered	close after explosion [355]	II [355]	no [355]
SN2013am	16.34 [356]	-14.90	-15.05, -14.73	V	1 day after explosion [356]	II [357]	yes [357]
SN2013bu	16.3 [86]			V	2 days after explosion [86]	II [358]	yes [358]
SN2013by	13.69 [359]	-17.92	-18.07, -17.76	V	young [359]	II L [360]	yes [359]
SN2013df	14 [361]	-17.41	-17.47, -17.36	unfiltered	young [361]	II [361]	no [361]
SN2013dk	15.5 [362]	-15.68	-15.85, -15.49	unfiltered	few days before peak [362]	Ic [362]	no [362]
SN2013ee	15.5 [363]			unfiltered	well past peak[363]	II [363]	no [363]
SN2013ej	12.5 [364]	-17.71	-17.74, -17.68	V	young [364]	II P [365]	no [366]
SN2013ff						Ic [367]	yes [367]
SN2013gc	16.7 [368]	-14.64	-14.78, -14.49	unfiltered	2 months after explosion [368]	II n [369]	no [368]
SN2013ge	14.52 [370]	-17.54	-17.70, -17.38	V	13 days before maximum light [370]	Ic [371]	yes [371]
SN2014A	16.4 [372]			unfiltered	1-2 weeks past explosion [372]	II P [372]	no [372]
SN2014C	14.5 [373]	-17.94	-18.03, -17.86	unfiltered	around maximum light [373]	Ib [373]	no [373]
SN2014G						II [374]	yes [375]
SN2014bc	14.8 [376]	-14.64	-14.70, -14.58	z	-	II [377]	no [376]
SN2014bi	18.2 [378]			unfiltered	2 weeks after maximum light[378]	II P [378]	no [378]
SN2014cl						II b [379]	no [379]
SN2014cx						II [380]	yes [380]

Supernova	Apparent magnitude	Absolute magnitude	Absolute magnitude limits (upper, lower)	Filter	Age at time of discovery	Type	Amateur or no
SN2014cy						II [381]	no [382]
SN2014df						Ib [383]	yes [383]
SN2014do						II [384]	yes [384]
SN2014dq						II [385]	yes [385]
SN2014ge	13.9 [386]			unfiltered	2-3 weeks after maximum light [386]	Ib [387]	no [388]
SN2015G						Ibn [389]	yes [389]
SN2015V						Ib/c [219]	-
SN2015an						II [390]	no [391]
SN2015aq						II P [219]	no
SN2015as						II b [392]	no
SN2016B						II P [393]	no [394]
SN2016C						II P [395]	yes [396]
SN2016G						Ic BL [397]	yes [398]
SN2016X	14 [97]	-18.23	-18.38, -18.06	V	2 days after explosion [97]	II P [399]	no [400]
SN2016adj	14 [99]	-15.53	-15.73, -15.31	V	around maximum light [99]	II [401]	yes [402]
SN2016aqf	15.8 [100]	-15.28	-15.43, -15.12	V	5 days after explosion [100]	II [403]	no
SN2016bau						Ib [404]	yes [405]
SN2016bkv	14.68 [406]	-15.32	-15.46, -15.16	V	3 days before V peak [406]	II [407]	yes [408]
SN2016coi						Ic BL [409]	no [410]
SN2016cok	16.7 [411]	-15.06	-15.14, -14.97	V	few days before maximum light [412]	II P [413]	no [414]
SN2016gkg						II b [415]	yes [416]
SN2016iae						Ic [417]	no [418]
SN2017aym						II P [419]	no [419]

Supernova	Apparent magnitude	Absolute magnitude	Absolute magnitude limits (upper, lower)	Filter	Age at time of discovery	Type	Amateur or no
SN2017bzb	13 [420]			unfiltered		II [420]	yes [421]
SN2017eaw	12.8 [422]	-17.28	-17.33, -17.23	V	3 days after explosion [422]	II P [423]	yes [424]
SN2017ein	15.3 [104]	-16.94	-17.09, -16.78	V	Week before V peak [104]	Ic [425]	yes [426]
SN2017gax	14.12 [427]			G-Gaia	9 days before maximum light [428]	Ib/c [429]	no [427]
SN2017gkk						II b [430]	yes [431]
SN2017gmr	14.26 [105]	-17.90	-18.13, -17.64	V	around explosion [105]	II [432]	no [433]
SN2017hpi						II [434]	no [435]
SN2017iro						Ib [436]	yes [437]
SN2017ivh						II [438]	no [439]
SN2017izl						II [440]	no [441]
SN2017jmk						II [442]	no [443]
SN2018aoq	15.38 [444]	-16.21	-16.36, -16.05	V	young [445]	II [445]	no [446]
SN2018get						II [447]	no [448]
SN2018gj						II b [449]	yes [450]
SN2018hna	14.2 [451]	-18.19	-18.33, -18.03	V	76 days before maximum [451] light	II [452]	yes [453]
SN2018imf	15.8 [454]			unfiltered	60 days after explosion [454]	II P [455]	yes [454]
SN2018is	18 [456]			unfiltered	1-2 weeks after explosion [456]	II [457]	no [456]
SN2018ivc	14.8 [109]	-17.52	-17.67, -17.36	V	soon after explosion [109]	II [458]	no [459]
SN2018lei						Ic [460]	no [461]
SN2018zd						II [462]	yes [463]
SN2019ci						II [464]	no [465]
SN2019edo						II [466]	no [467]
SN2019ehk	15.8 [468]	-15.91	-15.98, -15.84	r_ZTF	young [469]	II b [470]	yes [471]
SN2019ejj	17.41 [472]	-14.09	-14.23, -13.93	G-Gaia	-	II [472]	no [473]
SN2019esa						II n [474]	no [475]

Supernova	Apparent magnitude	Absolute magnitude	Absolute magnitude limits (upper, lower)	Filter	Age at time of discovery	Type	Amateur or no
SN2019fcn	15.2 [476]	-17.03	-17.18, -16.87	g	-	II [477]	no [478]
SN2019yvr	15.3 [479]	-18.75	-18.90, -18.59	r_ZTF	-	Ib [480]	no [481]
SN2020dpw						II [482]	yes [483]
SN2020fqv						Ib/c [484]	no [485]
SN2020hvp						Ib [486]	no [487]
SN2020jfo	14.57 [488]			V	3 days after explosion[489]	II P [490]	no [491]
SN2020mjm						II [492]	no [493]
SN2020mmz						II [494]	no [495]
SN2020ocz	15.3 [496]			orange-ATLAS	About 100 after explosion [496]	II [496]	no [497]
SN2020oi	13.81 [113]	-17.02	-17.02, -17.02	V	About 7 days before maximum light [113]	Ic [498]	no [499]
SN2020qmp						II [500]	no [501]
SN2020vg						II [502]	no [503]
SN2020zbv	18.83 [504]			unfiltered	About 60 days after explosion [504]	II P [504]	no [505]
SN2021aai						II [506]	no [507]
SN2021acna						II [508]	no [509]
SN2021aczp						II [510]	no [511]
SN2021adlw						II [512]	no [513]
SN2021aess						II n pec [514]	no [515]
SN2021gmj						II [516]	no [517]
SN2021gno	18 [518]	-12.82	-13.01, -12.61	orange-ATLAS	-	Ib [519]	no [520]
SN2021mwj						II [521]	no [521]
SN2021sjt						II b [522]	no [523]
SN2021suk						II [524]	no [524]
SN2021yja						II [525]	no [526]
iPTF13bvn						Ib [527]	no [528]